CHALMERS

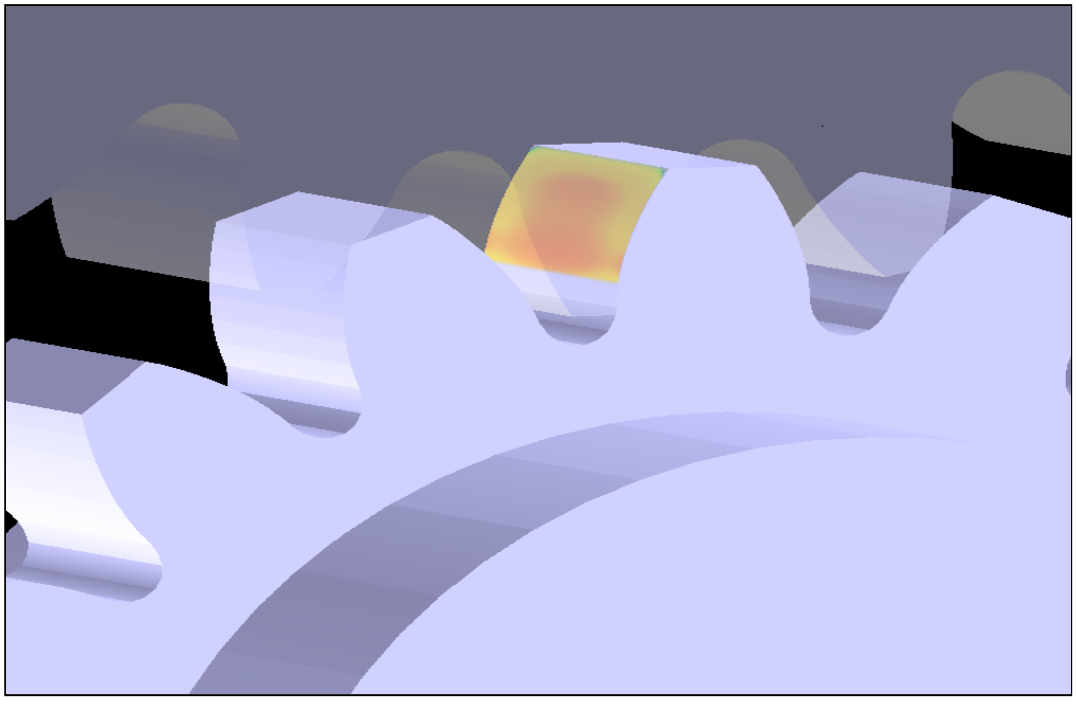

# Contact Mechanics in Gears

## A Computer-Aided Approach for Analyzing Contacts in Spur and Helical Gears

*Master's Thesis in Product Development*

MARCUS SLOGÉN

Department of Product and Production Development
*Division of Product Development*
CHALMERS UNIVERSITY OF TECHNOLOGY
Gothenburg, Sweden, 2013

MASTER'S THESIS IN PRODUCT DEVELOPMENT

# Contact Mechanics in Gears

A Computer-Aided Approach for Analyzing Contacts in Spur and Helical Gears

Marcus Slogén

Department of Product and Production Development
*Division of Product Development*

CHALMERS UNIVERSITY OF TECHNOLOGY

Göteborg, Sweden 2013

Contact Mechanics in Gear
A Computer-Aided Approach for Analyzing Contacts in Spur and Helical Gears
MARCUS SLOGÉN



Department of Product and Production Development
Division of Product Development
Chalmers University of Technology
SE-412 96 Göteborg
Sweden
Telephone: + 46 (0)31-772 1000

Cover:
The picture on the cover page shows the contact stress distribution over a crowned spur gear tooth.

Department of Product and Production Development
Göteborg, Sweden 2013

Contact Mechanics in Gears
A Computer-Aided Approach for Analyzing Contacts in Spur and Helical Gears
Master's Thesis in *Product Development*
MARCUS SLOGÉN
Department of Product and Production Development
Division of Product Development
Chalmers University of Technology

ABSTRACT
Computer Aided Engineering, CAE, is becoming more and more vital in today's product development. By using reliable and efficient computer based tools it is possible to replace initial physical testing. This will result in cost savings, but it will also reduce the development time and material waste, since the demand of physical prototypes decreases. This thesis shows how a computer program for analyzing contact mechanics in spur and helical gears has been developed at the request of Vicura AB. The stakeholder has addressed a desire of acquiring more knowledge of contact mechanics and thereby also a request of obtaining a reliable computer based procedure for analyzing this phenomenon. A mechanical standard and a computational program have been used in order to evaluate the performance of the computer program that has been developed. The results indicate that the computer program behaves correctly, but also requires further evaluation with help of physical testing in order to completely verify the reliability of the program. In addition to the development of a computer program, the focus of the thesis has also been to investigate how gears can be designed in order to improve the contact durability. A study on how the micro geometry of a gear tooth influences the contact durability has therefore been carried out. The developed computer program has been used as an analytical tool for this study. The results from the analysis show that contact stresses in gears may be reduced by performing modifications in the lead and profile directions of a gear tooth.

Key words: Computer Aided Engineering, contact mechanics, spur and helical gears

# Acknowledgements

First of all, I would like to thank my supervisor Peter Hall for mentoring and constant support during the work with the thesis. I would also like to thank the rest of the staff at Vicura AB for encouragement and for having contributed with their knowledge within the field of mechanical engineering. I am also very grateful for the help that Sandeep Vijayakar at ANSOL has contributed with in order to solve different issues with the FE program. Finally, I would like to thank Göran Brännare for taken on the role as examiner for the project.

Marcus Slogén, Trollhättan 12/6-2013

# Table of Contents

# Abbreviations

| | |
|---|---|
| AGMA | American Gear Manufacturers Association |
| AISI | American Iron and Steel Institute |
| ANSI | American National Standards Institute |
| ANSOL | Advanced Numerical Solutions |
| CAE | Computer-Aided Engineering |
| DIN | Deutches Institute für Normung |
| EHD | Elastohydrodynamic |
| FE | Finite Element |
| FZG | Forschungsstelle für Zahnräder und Getriebebau |
| GUI | Graphical User Interface |
| ISO | International Organization for Standardization |
| LACR | Low Axial Contact Ratio |
| LDP | Load Distribution Program |
| LOA | Line of Action |
| RCF | Rolling Contact Fatigue |
| SAE | Society of Automotive Engineers |
| SMS | Svensk Maskinstandard |

# Notations

| | |
|---|---|
| $a$ | Center distance, i.e. shaft distance, of two meshing gears or the contact area of two contacting spheres |
| $A_V$ | Transmission accuracy number |
| $b$ | The width of a gear tooth or the half width of the contact band of two cylinders in contact |
| $B$ | Width of the contact band of a gear tooth |
| $c_f$ | Specific heat constant |
| $C_\psi$ | Helical overlap factor |
| $d$ | Pitch diameter of a gear |
| $d_a$ | Tip radius of a gear |
| $d_f$ | Root radius of a gear |
| $d_l$ | Limit diameter of a gear |
| $d_{w1}$ | Operating pitch diameter of the driving wheel |
| $E$ | Young's modulus of elasticity |
| $E_r$ | Reduced modulus of elasticity |
| $f$ | Friction coefficient |
| $F$ | Contact force |
| $F_e$ | Face width in contact |
| $F_{calc}$ | Calculated load on a gear tooth |
| $F_t$ | Tangential transmitted load |
| $h_{min}$ | Minimum lubricant film thickness |
| $i$ | Speed ratio |
| $K_0$ | Overload factor |
| $K_H$ | Load distribution factor |
| $K_I$ | Load coefficient |
| $K_v$ | Dynamic load coefficient |
| $K_s$ | Size factor |

| | |
|---|---|
| $L$ | Length of the contact line |
| $L_{min}$ | Minimum length of the contact line |
| $m$ | Module |
| $m_N$ | Load sharing ratio |
| $M$ | Torque |
| $N$ | Contact force |
| $p_b$ | Base pitch |
| $p_{max}$ | Maximal pressure |
| $P$ | Contact load |
| $r$ | Pitch radius of a gear |
| $r_b$ | Base radius of a gear |
| $r_k$ | Radius of curvature of the contacting surface on a gear tooth |
| $R$ | Radius of curvature of a cylinder or a sphere |
| $s_b$ | Base circular thickness |
| $s_t$ | Transverse circular thickness of a tooth |
| $S_H$ | Safety factor for pitting |
| $T$ | Torque |
| $T_b$ | Bulk temperature of the gear |
| $T_f$ | Flash temperature |
| $T_s$ | Scuffing temperature |
| $u$ | Speed ratio |
| $v$ | Rolling velocity |
| $v_t$ | Pitch line velocity at the operating pitch diameter |
| $V_e$ | Entraining velocity of the lubricant |
| $V_r$ | Rolling velocity of a gear |
| $w_{Nr}$ | Normal unit load |
| $W_{Nr}$ | Normal operating load |
| $W_t$ | Tangential load |
| $x$ | Addendum modification coefficient |
| $X_w$ | Welding factor of gear materials |
| $X_\Gamma$ | Load sharing factor |
| $z$ | Number of teeth |
| $Z_E$ | Elastic coefficient |
| $Z_H$ | Stress cycle factor for pitting resistance |
| $Z_I$ | Geometry factor for pitting resistance |
| $Z_N$ | Stress cycle factor for pitting |
| $Z_R$ | Surface condition factor |
| $Z_W$ | Hardness ratio factor for pitting resistance |
| $Y_z$ | Reliability factor |
| $Y_\theta$ | Temperature factor |
| | |
| $\alpha$ | Pressure-viscosity coefficient |
| $\alpha_0$ | Pressure angle of a gear |
| $\alpha_n$ | Pressure angle defined in the normal plane |
| $\alpha_t$ | Pressure angle defined in the transversal plane |
| $\beta_b$ | Helix angle at the base circle of a gear |
| $\lambda$ | Specific film thickness of the lubricant |
| $\mu_0$ | Absolute Viscosity |
| $\nu$ | Poisson's ratio |

| | |
|---|---|
| $\rho$ | Transverse radius of curvature of a gear |
| $\rho_n$ | Normal relative radius of curvature of a gear |
| $\sigma$ | Surface roughness of a gear |
| $\sigma_H$ | Hertzian contact stress |
| $\sigma_{HP}$ | Allowable Hertzian contact stress |
| $\Phi_t$ | Transverse pressure angle |
| $\Phi_r$ | Operating pressure angle |
| $\psi_b$ | Base helix angle |
| $\omega$ | Angular velocity |

# 1. Introduction

Computer-Aided Engineering, CAE, is becoming more and more vital in today's product development. By using reliable computer based tools it is possible to replace initial physical testing. This will result in cost savings, but it will also reduce the development time and material waste, since the demand of physical prototypes decreases (Siemens, 2013). This thesis gives an introduction to contact mechanics and shows how a computer based tool has been developed for analyzing the contact durability in gears.

## 1.1 Background

The initiative to this project derives from a summer internship which was performed at Vicura AB, former Saab Automobile and GM Powertrain, in Trollhättan. The project concerned the integration of already existing computer based tools that were used for gear design, i.e. terminal programs which perform gear calculations according to Deutches Institute für Normung, DIN, standards, into a single program in order to simplify the usage of the computer based tools. The next step then became to develop a computer based tool that could be used for analyzing contact mechanics in a gear pair.

Contact mechanics has been analyzed in industry for a long time. In the end of the 19th century Hertz presented a formula for calculating the contact stresses in two infinite elastic half spaces (Mägi and Melkersson, 2009), which became the general praxis for analyzing contacts and is still used in mechanical standards (AGMA, 2004). The tools which are used for analyzing contacts have evolved during time; from theoretical methods, e.g. mechanical standards, to finite element, FE, programs (Bergseth, 2012). The same thing has happened to the way of analyzing contact fatigue. Before the 1970's it was thought that all materials had a specific endurance limit regarding contact fatigue, but after the 1970's it was shown that no endurance limit exists for contact fatigue and that contact fatigue is affected by the lubrication conditions (Dudley, 1994).

The reason for why Vicura AB has an interest in contact mechanics is due to the fact that the company has discovered an increase in contact related problems, e.g. pitting and scuffing, in gear pairs which are used in various applications. These problems may result in even worse conditions, such as rough running gears and contamination of the gear lubricant caused by loose particles, which in its turn may lead to a gearbox failure (Davis, 2005). Of that reason, follows a demand of developing a computer based tool for analyzing contact mechanics in gears.

Vicura AB is an engineering company that delivers products which are used in different mechanical transmission systems and electrical drivelines. The company was founded in 2011 and is majority owned by Fouriertransform AB (Vicura, 2013).

## 1.2 Problem Statement

The purpose of the study was to acquire knowledge in contact mechanics with a focus on gears and the different failure modes that relate to this area. The expected outcome of the project was to create a computer program which generates a model of a gear pair and then performs a contact analysis on it by using an external FE program.

In addition to delivering a computer based tool for analyzing contact mechanics in gears the project has also attempted to answer the following questions:

- What kinds of failures relate to contact mechanics?
- What kinds of methodologies are available today for analyzing contact failures?
- How can gears be designed in order to reduce the risk of contact failure?

## 1.3 Scope and Limitations

External cylindrical gears, i.e. spur and helical, have only been studied in this study in order to delimitate the literature study. Other types of gears such as bevel gears and hypoid gears have not been taken into consideration even though some of the findings may be applicable for these kinds of gears.

Contact mechanics and failures related to this phenomenon have been the primary focus for the literature study since the stakeholder, i.e. Vicura AB, was interested of getting more knowledge in this area. Mägi and Melkersson (2009) define four factors which should be taken into consideration in gear design the bending stress, contact fatigue, adhesive wear and abrasive wear. The first factor, bending stress, has not been prioritized within this study since the company has well developed methods for analyzing this phenomenon while the latter three have been examined further in the literature study.

Another limitation that had to be done concerned the computer based tool that was to be developed. Due to the limited amount of time and the resources available it was decided to only focus on developing a function for analyzing contact stresses in gears. Analysis of the lubrication related factors, e.g. minimum lubricant thickness and lubricant temperature, were therefore disregarded in the methodological work even though it is shown in the theory section that these factors have an influence on the contact mechanics.

# 2. Theory Chapter

This chapter presents relevant literature that has been reviewed in order to establish a theoretical foundation for the study. The intention with the chapter is to give an introduction to gear design with a focus on the nomenclature and the general equations that are used for defining a gear. A presentation of the different failure modes that relate to contact mechanics is also given together with the procedures, i.e. analytical and physical methods, which are used for predicting the risk of contact failure.

## 2.1 Gear Design

Gears can be arranged in different ways depending on which kind of transmission that is taken into consideration, e.g. if it is a linear manual or a planetary transmission. Examples of different gears that may occur in such transmissions are spur gears, helical gears, ring gears and bevel gears.

The two types of gears which are considered in this study are external spur and helical gears. The section will begin by describing the design of a spur gear and thereafter will complementary information be given regarding the design of a helical gear. Simplified models of a spur and a helical gear are shown in Figure 1.

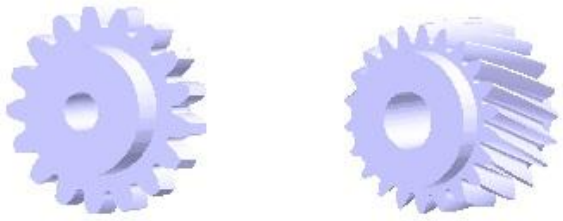

**Figure 1: The picture shows examples of a spur and a helical gear.**

### 2.1.1 Spur Gear

An approach that may be used for generating the shape of a gear tooth is to consider an involute profile. The involute curve can be thought of as a curve created by a point on a straight line which rolls on a circle without sliding. The advantage of using such a profile is primarily the fact that it fulfills the requirement of a constant speed ratio (Mägi and Melkersson, 2009). An example of an involute curve is shown in Figure 2.

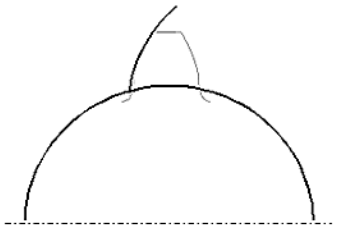

**Figure 2: Illustration of the involute profile of a spur gear tooth.**

Figure 3 is used in order to illustrate different diametric sections which are used for defining the gear's geometry. The tip and root diameters define the highest and lowest parts of a gear tooth respectively, while the base diameter is the part where the involute profile begins (Dudley, 1994). The pitch is defined as the rolling circle of a gear, i.e. the gears can be thought of as two rolling cylinders in contact with diameters equal to the pitch diameters of the gears (Mägi and Melkersson, 2009).

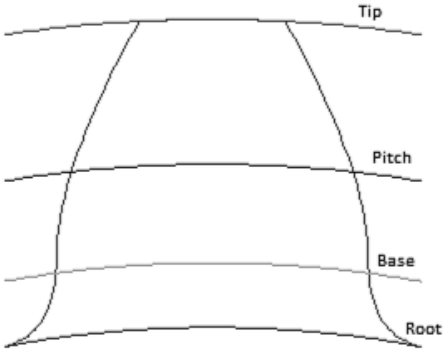


**Figure 3: Picture that shows the terminology that is used for the diametric sections of a gear tooth.**

An expression for calculating the pitch diameter, $d$, is given by Mägi and Melkersson (2009) and is shown in eq 1. Mägi and Melkersson (2009) mention that this equation can be used used for defining the module, $m$, which is a measure that characterizes the size of a gear tooth (Dudley, 1994).

$$d = mz \quad (1)$$

The geometry of a gear can be divided into two different groups of parameters, i.e. primary and secondary units. Primary units are used for describing the gear's function while secondary units are used as complementary data for generating the shape of a gear (Mägi and Melkersson, 2009).

Mägi and Melkersson (2009) differ between two different systems of primary units, i.e. the natural system and the modular system, and according to the authors it is sufficient to use one system in order to unambiguously determine the shape of a tooth flank. The units which are used within the natural system are the number of teeth, $z$, the base pitch, $p_b$, and the base circular thickness, $s_b$. The units within the modular system are the number of teeth, $z$, module, $m$, pressure angle, $\alpha_0$, and the addendum modification coefficient, $x$.

A parameter that occurs in both systems is the number of teeth, $z$, which determines the speed ratio, $i$, of a gear pair (Mägi and Melkersson, 2009). This ratio defines the relation between the torques of the gears, $T$, or the relation between the angular velocity of the gears, $\omega$. The ratio is shown in eq 2.

$$i = \frac{z_2}{z_1} = \frac{T_2}{T_1} = \frac{\omega_1}{\omega_2} \quad (2)$$

The base pitch, $p_b$, is used in order to ensure that two gears can work together in a gear pair, i.e. if the operating wheels have the same base pitch then they will be able to transfer power (Mägi and Melkersson, 2009). The parameter is defined as the distance from a point that is positioned at the base circle on one tooth to the corresponding point on the next tooth, see Figure 4. The mathematical expression for the base pitch is shown in eq 3, where $r_b$ is the radius of the base circle (Coy, Townsend and Zaretsky, 1986).

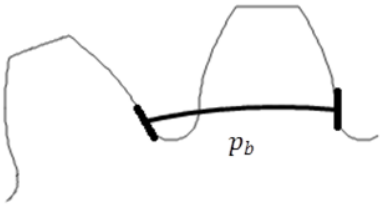


**Figure 4: Illustration that shows the base pitch.**

$$p_b = \frac{2\pi r_b}{z} \quad (3)$$

The pressure angle, $\alpha_0$, is defined as the angle between the line that is perpendicular to the line of action, LOA, and the shared centerline of the two gears (Coy, Townsend and Zaretsky, 1986). LOA is an imagined line that the contact point travels along during the time when a pair of teeth is in action. A standard value of the pressure angle is given as 20 degrees (Mägi and Melkersson, 2009), but other values can be used depending on application (Coy, Townsend and Zaretsky, 1986). The pressure angle is shown in Figure 5.

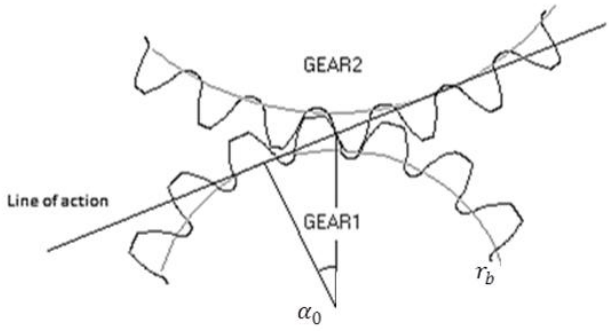


**Figure 5: The definition of the pressure angle.**

The addendum modification coefficient, $x$, is a dimensionless factor which is used in order to improve the performance of a gear. The modification is achieved by modifying the involute shape such that the contact of two mating gears will be changed compared to the standard case when no modification has been applied. The reason for adding an addendum modification may be due to a demand of higher tooth root durability, reduced contact stresses and sliding (Karlebo Handbok, 1992).

The base circular thickness, $s_b$, of a tooth is the thickness of a tooth measured along the base circle. The mathematical expression for the base circular thickness is shown in eq 4, where $inv\ \alpha$ is the involute function. The involute function is given by eq 5 (Mägi and Melkersson, 2009).

$$s_b = \left(\frac{\pi}{2} + 2x\ tan\alpha_0 + z\ inv\ \alpha_0\right) m\ cos\alpha_0 \quad (4)$$

$$inv\ \alpha_0 = tan\alpha_0 - \alpha_0 \quad (5)$$

Mägi and Melkersson (2009) mention that the proportions of a tooth flank are limited by the root circle, the tip circle and the gear width. The root and tip diameters, i.e. $d_f$ and $d_a$, are the lower and upper boundaries in the profile direction whilst the gear width, $b$, limits the axial size of a gear. The size of the gear width can be estimated by

considering tooth bending equations, while the root circle is defined by the geometry of the tool, e.g. a hob, which is used for generating the gear. The size of the tip circle is limited by the size of the raw material which the gear is generated from before it undergoes any manufacturing process (Mägi and Melkersson, 2009).

### 2.1.2 Helical Gear

The involute profile of a helical gear tooth is generated by a plane, that is cut with a skewed angle $\beta_b$. The plane is then rolled off from a cylinder, which is illustrated in Figure 6 (Mägi and Melkerson, 2009). The other half of the tooth is generated by rolling of a plane in the opposite direction such that the two planes will intersect each other and thus create a complete helical gear tooth.

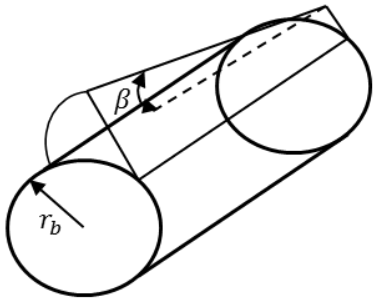


**Figure 6: Illustration that shows how an involute profile is generated for a helical gear.**

The parameters which define the geometry of a helical gear are given in two different planes, i.e. the transversal plane and the normal plane (Mägi and Melkersson, 2009). A picture is used in order to illustrate the relation between the normal plane and the transversal plane, see Figure 7. According to Mägi and Melkersson (2009) the primary units in the transversal plane are defined in the same way as for spur gears. The primary units, defined in the normal plane, are then obtained by rotating the parameters defined in the transversal plane with the helix angle.

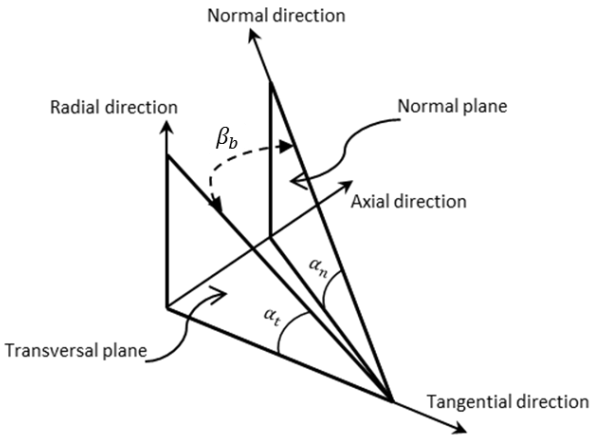


**Figure 7: The relation between the normal and transversal plane based on a definition given by Mägi and Melkersson (2007). The angles which are shown in the picture are the helix angle, $\beta_b$, defined at the base circle, the pressure angle, $\alpha_t$, defined in the transversal plane and the pressure angle, $\alpha_n$, defined in the normal plane.**

A gear's helix angle can be defined in different directions depending on a left or right handed helical gear is used, i.e. two mating helical gears need to have different hand of helix if they should be able to work in a gear pair. According to Mägi and Melkersson (2009), the sign of the helix angle is negative for a left-handed gear and

positive for a right-handed gear. Figure 8 illustrates the difference between a left and a right handed helical gear.

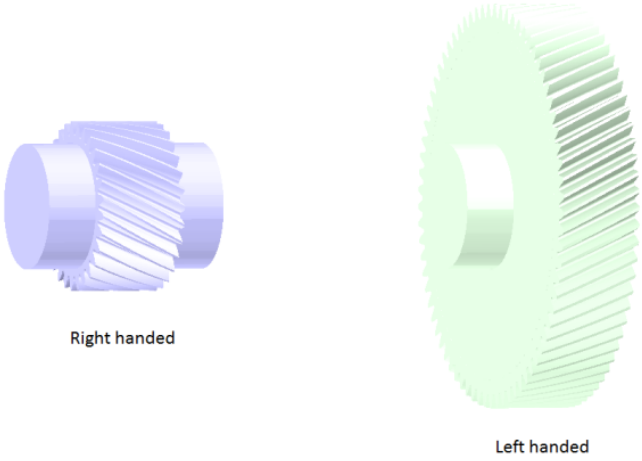


**Figure 8: Picture showing examples of left and right handed helical gears.**

### 2.1.3 Micro Geometry

Misalignments of gear shafts and manufacturing errors may result in unfavorable loading conditions which sometimes might require a change of the tooth flank in order to improve the gear performance (Dudley, 1994). Profile modification, e.g. tip or root relief, is used for modifying the involute shape of a gear tooth in order to achieve smoother entrance in the gear mesh or to eliminate severe stresses in the root and tip regions (Dudley, 1994). Another type of modification is lead modification, e.g. crowning or end relief, which is used in order to prevent axial misalignments of the gears (Houser, Harianto & Talbot, 2006).

Tip relief is defined as a design attribute that is used, in both spur and helical gears, in order to achieve a smooth entrance in the mesh cycle, i.e. the time when a gear pair is active (Mägi and Melkersson, 2009). A tip relief is generated by removing material from the edge of a tooth tip. This is illustrated in Figure 9 where the tip reliefs are indicated by the dashed lines. The corresponding easement for the root section is known as root relief (Mägi and Melkersson, 2009).

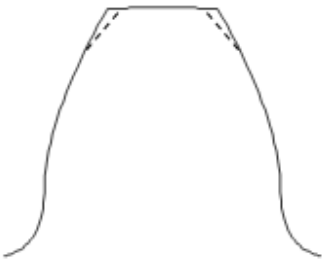

**Figure 9: Example of a gear tooth with tip reliefs.**

Crowning of a gear tooth is made in order to secure that the entire load is carried by the center of the tooth flank even though the gears may be displaced from their ideal positions, e.g. due to axial misalignments or other distortions (Dudley, 1994). Crowning is characterized by a curved tooth flank. An example of a crowned tooth can be seen in Figure 10.

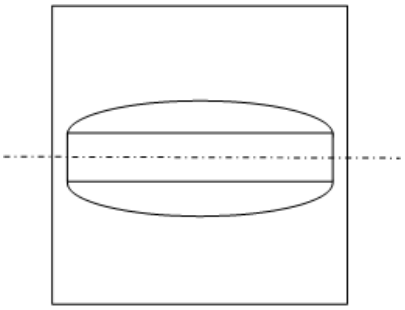

**Figure 10: Crowned gear tooth seen from above.**

End reliefs are used in order to prevent misalignments and to avoid stress concentrations which may occur at the edges of a gear tooth (Dudley, 1994). The end relief is achieved by removing material from the edge of the tooth face in order to obtain a tapered shape of the face. Dudley (1994) mentions that end reliefs are used on wider gears, e.g. helical gears, while crowning is made on narrower gears, e.g. spur gears.

## 2.2 Contact Failures

Different modes of failure may occur on a gear surface, and sometimes may different failure modes occur in combination which might make it hard to determine which type of failure that originally caused the damage (Dudley, 1994). This section will address some different types of failures that might occur on the surface of a gear tooth.

Davis (2005) divides gear failures into different categories, i.e. non lubrication-related failures and lubrication-related failures. Non lubrication-related failures are then divided into failures caused by overload and bending fatigue, while the lubrication-related failures are divided into Hertzian fatigue, wear, and scuffing (Davis, 2005). Dudley (1994) is critical to that kind of categorization and states that in many cases is the lubricant mistakenly accused for gear failures while it actually is the mechanical design that is the real cause of the failure. True lubrication failures are instead related to the lubricant properties, e.g. lack of the right additives or not sufficient cooling performance, rather than to a specific gear failure (Dudley, 1994).

Different nomenclatures are used for characterizing the modes of failure depending on which kind of literature, e.g. American or European, that is used. American authors tend to use the word scoring for adhesive wear whilst European authors use the word scuffing for adhesive wear and scoring for abrasive wear (Davis, 2005). The European nomenclature is used in this section in order to make the classification of failures unambiguous.

### 2.2.1 Contact Fatigue

Glaeser and Shaffer (1996) describe contact fatigue as a phenomenon that differs from structural fatigue, e.g. bending and torsional fatigue, in the sense that it arises from a contact or Hertzian stress state. The contact is defined as a localized stress which occurs when two curved surfaces, in a rolling motion, are in contact under a normal load. The contact geometry and the motion of the rolling elements create an alternating subsurface shear stress which in its turn produces a subsurface plastic deformation that increases with repeating cycles (Glaeser and Shaffer, 1996). Finally, the plastic deformation initiates a crack which grows into a pit if the fracture

continues. Glaeser and Schaffer (1996) mention bearings, cams and gears as examples of applications where contact fatigue may occur.

Contact fatigue life, in gears, can be improved by introducing compressive stresses on the tooth surface, e.g. by considering shot peening or burnishing (Glaeser and Shaffer, 1996). Townsend and Zaretsky (1982) showed in a study that shot-peened gears had pitting fatigue lives of 1.6 times the life length of standard gears that were not shot-peened. The longer life length of the gear was due to the compressive stresses in the tooth surfaces (Townsend and Zaretsky, 1982).

In another study Townsend, Chevalier and Zaretsky (1973) showed that a nitrided material with a soft ductile core, i.e. Super Nitralloy, was less sensitive to fatigue fracture when a spall had been formed in comparison with a through hardened material, i.e. AISI M-50 steel, which suffered from catastrophic failure, i.e. tooth fracture. On the other hand, the gears made of the through hardened AISI M-50 steel showed longer lives than the surface hardened gears (Townsend, Chevalier and Zaretsky, 1973).

International Organization for Standardization, ISO, 10825 (2009) describes surface fatigue as a material damage that is caused by repeated surface stresses and subsurface stresses. The ISO standard divides the different surface fatigue failures into different categories, e.g. pitting, flake pitting, spalling and case crushing (ISO 10825, 2009). Flake pitting and spalling refer to pitting on a macro level, i.e. several pits have grown together into larger pits (Davis, 2005), and of that reason will they not be further described in this section. The focus will instead be directed at the origin of the fatigue failures, i.e. pitting and case crushing.

### *Pitting*

Pitting is caused by rolling contact or a mixed condition of rolling and sliding contact (ISO 10825, 2009). Pitting is, according to the ISO standard, characterized by small scattered holes, i.e. pits, which occur on the surface area.

The size of the pits depends on the gear material (Davis, 2005). Large pits of millimeter sizes may occur on a soft gear tooth that is of through hardened material while surface hardened gears, e.g. carburized or nitrided gears, receive smaller pits in micrometer sizes (Davis, 2005).

According to Davis (2005) the pitting process starts with a fatigue crack that initiates either at the surface or at a small depth just below the surface. When the crack grows the surface loses a piece of material which results in a pit. A spall may then be formed if several small pits grow together into one single pit (Davis, 2005).

### *Case Crushing*

Another type of contact fatigue is case crushing, which occurs in case-hardened gears when a crack propagates in the interface between the case material and the core material (ISO 10825, 2009). The crack initiates when subsurface stresses exceed the material strength of the subsurface material. The crack then propagates along the interface between the case and the core until material is lost and a spall is formed. Case crushing can be avoided by increasing the case depth of the gear (Shipley, 1967).

According to Lawcock (2006) there is a distinction between rolling contact fatigue, e.g. pitting, and subcase fatigue, e.g. case crushing, in that sense that rolling contact

fatigue durability is reduced by the presence of sliding forces. Subcase fatigue, on the other hand, is not significantly affected by sliding forces (Lawcock, 2006).

### 2.2.2 Wear

Shipley (1967) defines wear as the process when layers of metal are removed from the surfaces that are in contact. This section will primarily focus on wear that relates to Hertzian contact stresses and elastohydrodynamic, EHD, lubrication, e.g. abrasive wear and adhesive wear (Gopinath and Mayuram, 2013). Other types of wear exist, e.g. corrosive wear and wear which is caused by erosion (ISO 10825, 2009), but these will not be given further attention since they are caused by actions, e.g. chemical reactions, which are out of the scope for this study.

Shipley (1967) divides normal wear into different categories depending on how severe the wear is. The mildest form of wear is defined as polishing and is characterized by a slow wear-in process where fine pieces of material are worn off until a smooth surface is created. The second category is defined as moderate wear and is characterized by the loss of material in the tip and root areas of the tooth. Moderate wear is caused by the selection of a too thin layer of the lubricant which cannot withstand the load that it is subjected to. The third category is defined as excessive wear and is characterized by the removal of a considerable amount of material. Rough running gears and a destroyed involute profile are described as results of excessive wear (Shipley, 1967).

#### *Abrasive Wear*

Abrasive wear in gears is caused by hard particles which act as contaminants in the gear lubricant (Davis, 2005). These particles have either been added externally or internally depending on the source of origin. If the contaminants have been added externally it might have been due to contamination from manufacturing or assembly while internal contaminants may originate from pitting or wear, i.e. material that has been removed from the gear due to a surface failure (Davis, 2005). The abrasive wear is characterized by the removal of surface material, e.g. radial scratch marks that are formed due to the loss of material, which is caused by the wear process (ISO 10825, 2009).

In order to avoid abrasive wear, Davis (2005) recommend a cleaning procedure of the lubricant, i.e. draining and flushing the lubricant, which is performed before the gearbox is started for the first time. This procedure is made in order to remove contamination that is built-in into the gearbox. For gearboxes that are using a circulating oil system Davis (2005) recommends fine filtration in order to remove contaminants while for oil bath gearboxes a recommendation follows on frequent shift of the lubricant in order to remove the contamination.

#### *Adhesive Wear*

Adhesive wear, e.g. scuffing, is the process that occurs when the surfaces of two contacting bodies are joined by localized welding and then pulled apart (Frazer, Shaw, Palmer & Fish, 2010). A material transfer occurs between the two contacting surfaces due to high metal-to-metal contact and hence produces a weld (Davis, 2005). The high metal-to-metal contact is the result of a local failure of the gear lubricant which has been caused by frictional heating due to high sliding speed and high surface pressure (Davis, 2005). Dudley (1994) define this type of scuffing as hot scuffing, i.e. hot scoring according to the American definition, and mention that this type of scuffing primarily relates to the flash temperature of the gear lubricant.

Another scenario which also may cause scuffing occurs when the gears are running at slow speeds and are subjected to high loads. The surfaces of the teeth might then not be completely lubricated which may cause metal-to-metal contact which in its turn may initiate scuffing (Mägi and Melkersson, 2009). The reason for why the lubricant does not cover the entire tooth is due to the fact that the EHD film thickness, i.e. the thickness of the lubricant, is small in comparison to the surface roughness of the tooth (Dudley, 1994).

According to the American Gear Manufacturers Association, AGMA, 1010-E95 (1995) it is stated that scuffing differs from other gear failures, e.g. fatigue, in that sense that scuffing may initiate at any time in a gear's life while the other kinds appear after a number of life cycles. Davis (2005) recommends a running-in period of a new gearbox in order to smooth the surfaces of the teeth since rough surfaces may lead to high frictional loads which favor scuffing.

Scuffing can be prevented by avoiding high sliding velocities and lowering the Hertzian contact stresses. The sliding velocity can be reduced by considering a tip and root relief of the gear profile, since the sliding velocity has its maximum value at these positions (Davis, 2005). Other recommendations presented by Davis (2005) are to use high viscosity lubricants with antiscuff additives and considering nitrided steels as gear materials since they have been proved to have good scuffing resistance. An improved surface finish of the teeth may also be considered in order to avoid scuffing (Dudley, 1994).

### 2.2.3 Plastic Deformation of the Tooth Surface

ISO 10825 (1995) describe plastic deformation as the residual deformation that is left after a load has been removed. Furthermore, it is stated by the ISO standard that surface materials may be plastically deformed due to rolling or sliding caused by overloads and friction.

Ognjanovic (2004) describe the tooth failure known as teeth squeezing as a gear failure which is characterized by plastic deformation. Teeth squeezing is the result of a combined load of contact stresses and high shear stresses which causes the gear tooth to plastically deform. Teeth squeezing may be found in gears that are subjected to high surface stresses and show low hardness (Ognjanovic, 2004). A gear tooth that has suffered from teeth squeezing may be characterized by a neck in the middle of the tooth flank if squeezing has occurred at that position or by an elevated edge in the addendum area if squeezing has taken place in the upper region of the tooth (Ognjanovic, 2004).

## 2.3 Methods used for Predicting Contact Failures

Before 1970 it was thought that there was an endurance limit for surface durability at ten million cycles, e.g. for case carburized gears which were fully hardened the endurance limit was assumed to be 1724 $N/mm^2$ (Dudley, 1994). After 1970 two facts, based on discoveries made in the 1960's, were presented regarding surface durability. The first one was that pitting in gears is affected by the lubrication conditions and the second was that there exists no endurance limit against pitting (Dudley, 1994). This section will show how contact stresses and lubrication related factors can be estimated with help of different methods.

### 2.3.1 Contact Stress

The procedure of calculating contact stresses in gears is based on an assumption of simplifying two teeth in contact by two rolling cylinders (Karlebo Handbok, 1992). An illustration of the analogy is shown in Figure 11.

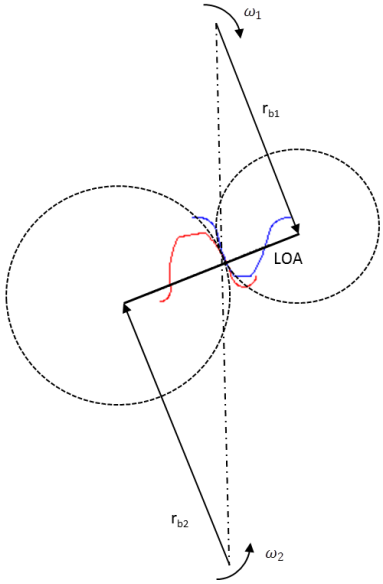


**Figure 11: Simplified definition of Hertzian contact based on a definition obtained from Karlebo Handbok (1992).**

*Hertzian Contact*

Contact stresses appears when two bodies with curved surfaces, e.g. spheres or cylinders, are in contact or when one body with a curved surface is in contact with a plate, i.e. a plate can be thought of as a sphere with an infinite radius. If two spheres were in contact the theoretical contact area would be a point and the theoretical contact area between two cylinders would result in a line. The theoretical contact stresses in both cases would thus be infinite due to the minimal contact area and thereby initiate immediate yielding. This is not the case in reality since the contact areas of the bodies are elastically deformed which implies that the stresses are limited. These stresses are known as Hertz stresses (University of Utah – ME EN 7960, 2006).

According to Sundström (2008) the Hertzian contact areas of the bodies which are in contact need to be small in relation to their total sizes and their curvatures in the contact point. Furthermore, it is mentioned that friction forces are neglected in the Hertzian theory (Sundström, 2008).

When two spherical bodies are in contact the contact area receives a circular shape. Equation 6 shows the radius, $a$, of the contact area. The factors which occur in the equation are the contact load, $P$, the radiuses of curvature of the contacting parts, $R_1$ and $R_2$, and the material properties which are defined by the expression given in eq 7. The parameters which are used in eq 7 are Poisson's ratio,$\nu$, and Young's modulus of elasticity, $E$, of the respective materials. The maximal pressure, $p_{max}$, is then given by eq 8 which includes the same parameters as the radius of the contact area (Sundström, 2008).

$$a = \left( \frac{3P\left(1 - \nu_{eff}^2\right)}{2E_{eff}\left(\frac{1}{R_1} + \frac{1}{R_2}\right)} \right)^{\frac{1}{3}} \quad (6)$$

$$\frac{(1 - \nu_{eff}^2)}{E_{eff}} = \frac{1}{2}\left(\frac{1 - \nu_1^2}{E_1} + \frac{1 - \nu_2^2}{E_2}\right) \quad (7)$$

$$p_{max} = \frac{1}{\pi}\left( \frac{3PE_{eff}^2}{2\left(1 - \nu_{eff}^2\right)^2} \left(\frac{R_1 + R_2}{R_1 R_2}\right)^2 \right)^{\frac{1}{3}} \quad (8)$$

The contact area receives a rectangular shape when two cylinders are in contact. The equations for the half width of the contact band, $b$, and the maximal pressure, $p_{max}$, are shown in eq 9 and eq 10. The equations include similar factors as were described for the case with spherical contact, but with exception for the contact load which is defined as the force, $F$, divided by the length of the line of contact, $L$ (University of Utah – ME EN 7960, 2006).

$$b = \sqrt{\frac{4F\left(\frac{1 - \nu_1^2}{E_1} + \frac{1 - \nu_2^2}{E_2}\right)}{\pi L\left(\frac{1}{R_1} + \frac{1}{R_2}\right)}} \quad (9)$$

$$p_{max} = \frac{2F}{\pi b L} \quad (10)$$

### *Contact Stresses in Spur and Helical Gears*

External cylindrical spur gears can be thought of as two parallel cylinders in contact with radiuses of curvature $r_{k1}$ and $r_{k2}$. This relation has been shown in Figure 11 where the two circles indicate the cylinders. The maximal contact stress is then given by eq 11 which origins from the Hertzian theory of contact. The other parameters that occur in the equation are the contact force, $N$, material constants, $k_i$, which are given by eq 12 and the length of the line of contact, $L$, which in this case is equal to the width of the gear tooth, $b$ (Mägi and Melkersson, 2009).

$$\sigma_H = \sqrt{\frac{N}{\pi(k_1 + k_2)L}\left(\frac{1}{r_{k1}} + \frac{1}{r_{k2}}\right)} \quad (11)$$

$$k_i = \frac{1 - \nu_i^2}{E_i} \quad (12)$$

For a helical gear pair, with the same material used in both gears, the contact stress is given by eq 13. The contact load, $N$, is defined in the normal direction of the gears, see eq 14, and the line of contact, $L$, which is defined by eq 15 and the radiuses of curvature $r_{kn1,2}$ given in the normal plane (Mägi and Melkersson, 2009).

$$\sigma_H = \sqrt{\frac{NE}{2\pi(1-\nu^2)L}\left(\frac{1}{r_{kn1}}+\frac{1}{r_{kn2}}\right)} \quad (13)$$

$$N = \frac{F_{calc}}{\cos\alpha_t \cos\beta_b} \quad (14)$$

$$L = \frac{b}{\cos\beta_b} \quad (15)$$

The calculated load, $F_{calc}$, that is given by eq 16 is defined by the torque, $M_1$, divided by the pitch radius, $r_1$, and multiplied with the load factors $K_I$ and $K_v$. These factors are known as the load coefficient and the dynamic load coefficient which can be found in the Svensk Maskinstandard, SMS. The values on the coefficients are recommended to be larger than one (Mägi and Melkersson, 2009). The expression for the calculated load is shown in eq 16.

$$F_{calc} = K_I K_v \frac{M_1}{r_1} \quad (16)$$

Standard procedures for determining the contact stresses are given by ISO, AGMA, and DIN (Dudley, 1994). According to Dudley (1994) these standards need to be studied in depth before they can be used for stress rating calculations. As Dudley (1994, p. 3.142) expresses it:

> *"Standards are like legal documents. All the fine print must be read and followed before one can claim to be acting in accordance with the standard."* (Dudley, 1994)

Example of S-N curves which can be used for estimating the life length of gears versus the calculated contact stresses are given by Dudley (1994) and are shown in Figure 12. The S-N curves show example data for AGMA steel grade 1 and 2, where steel grade 1 is characterized by having good quality but not optimum and steel grade 2 has the best quality obtainable. The parameters $L_1$ and $L_{10}$ indicate the reliability level of the gears, e.g. $L_1$ indicates one failure out of hundred (Dudley, 1994).

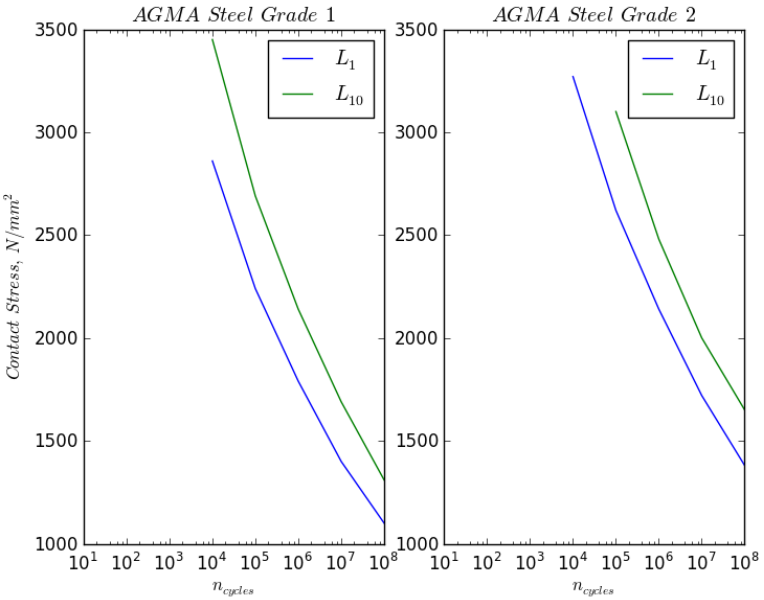


**Figure 12: S-N curves based on data given by Dudley (1994).**

### 2.3.2 Lubrication

According to Coy, Townsend and Zaretsky (1985) gear lubrication serves four functions which are providing a separating film between rolling and sliding contacting surfaces, acting as a cooling medium, protecting the gears from contaminants and preventing from corrosion of the gear surfaces. The first described function is of high interest, in this study, due to the fact that it may reduce or prevent contact related failures (Davis, 2005). Two different factors are investigated in order to evaluate the lubricant's properties, i.e. the film thickness and the flash temperature (Dudley, 1994).

*Film Thickness*

The lubricant pressure in highly loaded contacting elements, e.g. gear teeth and rolling bearings, can sometimes cause elastic deformation of the surfaces with the same magnitude as the lubricant film thickness (Davies, 2005). Elastrohydrodynamic lubrication is assumed to occur under such operating conditions (Davies, 2005) and is characterized by a very thin lubricant film that manages to separate two contacting surfaces such that there is no or little metallic contact (Dudley, 1994).

Dudley (1994) divides elastohydrodynamic lubrication into three different categories: EHD I, EHD II and EHD III. EHD I occurs when there is no appreciable film thickness of the lubricant. This may be found in highly loaded gears which are running at slow speeds. EHD II is the case when there is a partial lubricant film thickness between the teeth of the gears. According to Dudley (1994) EHD II cases can be found in gears which are used in road vehicles. The EHD III characterizes full film lubrication and can be found in applications that are using high speed gears, e.g. turbines, electric generators and turboprop drives in aviation (Dudley, 1994). Figure 13 shows a rough sketch of the three different cases, where the parameter $B$ is the width of the contact area and $h_{min}$ is the lubricant thickness.

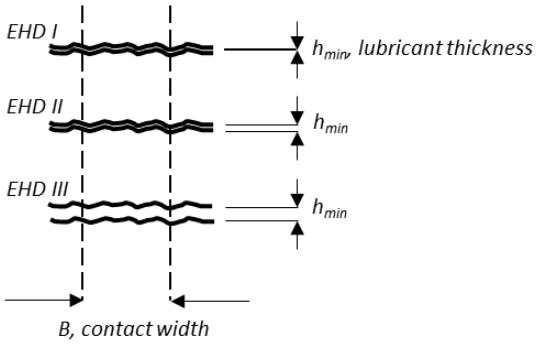


**Figure 13: EHD categorization based on a definition given by Dudley (1994).**

An expression for calculating the minimum lubricant film thickness, $h_{min}$, is given by Davis (2005), see eq 17. The parameters that are used in the equation are summarized in Table 1.

$$h_{min} = \frac{1.63\alpha^{0.54}(\mu_0 V_e)^{0.7}\rho_n^{0.43}}{(X_\Gamma w_{Nr})^{0.13}E_r^{0.03}} \quad (17)$$

**Table 1: Parameters used in the minimum lubricant film thickness equation**

| **Parameter:** | **Description:** |
|---|---|
| $\alpha$ | Pressure-viscosity coefficient [in$^2$/lbf] |
| $\mu_0$ | Absolute viscosity [lbf s/ n$^2$] |
| $V_e$ | Entraining velocity |
| $\rho_n$ | Normal relative radius of curvature |
| $X_\Gamma$ | Load sharing factor |
| $w_{Nr}$ | Normal unit load |
| $E_r$ | Reduced modulus of elasticity |

The entraining velocity, $V_e$, is given by the sum of the rolling velocities of the gears, $V_{r1}$ and $V_{r2}$ (Davis, 2005). An expression for the entraining velocity is given by eq 18 while eq 19 defines the rolling velocity which is given by the angular velocity of a gear multiplied with the transverse radius of curvature (Davis, 2005).

$$V_e = V_{r1} + V_{r2} \quad (18)$$

$$V_{ri} = \omega_i \rho_i, \;\; i = 1{,}2 \quad (19)$$

Davis (2005) gives an expression of the normal relative radius of curvature, $\rho_n$, which is shown in eq 20. The parameters $\rho_1$ and $\rho_2$ are the transverse radius of curvature of the driving wheel and the gear. The angle $\psi_b$ is defined as the base helix angle (Davis, 2005).

$$\rho_n = \frac{\rho_1 \rho_2}{(\rho_2 \pm \rho_1)\cos\psi_b} \quad (20)$$

The load sharing factor, $X_\Gamma$, ranges from zero to one and varies for different roll angles of the driving wheel. It is also dependent on whether if it is the smaller wheel that is the driving wheel or the larger wheel, and if the tooth profile is modified or unmodified (Davis, 2005).

The normal unit load, $w_{Nr}$, is given by eq 21. The factors that are used in the equation are defined as the normal operating load, $W_{Nr}$, and the minimum contact length, $L_{min}$ (Davis, 2005).

$$w_{Nr} = \frac{W_{Nr}}{L_{min}} \quad (21)$$

An expression for the reduced modulus of elasticity is given by eq 22. The factors that occur in the equation are the Young's modulus of elasticity and Poisson's ratio of the driving wheel and the gear (Davis, 2005).

$$E_r = 2\left(\frac{(1-\nu_1^2)}{E_1} + \frac{(1-\nu_2^2)}{E_2}\right)^{-1} \quad (22)$$

After the minimum film thickness has been determined a ratio called specific film thickness, $\lambda$, can be calculated (Davis, 2005). The ratio is given by eq 23 where $h_{min}$ is the minimum film thickness and $\sigma$ is the root mean square value of the surface roughness of the gear teeth which is given in eq 24 (Davis, 2005).

$$\lambda = \frac{h_{min}}{\sigma} \quad (23)$$

$$\sigma = (\sigma_1^2 + \sigma_2^2)^{\frac{1}{2}} \quad (24)$$

The specific film thickness can be used as an indicator of gear performance (Coy, Townsend and Zaretsky, 1985). Table 2 shows different ranges of the specific film thickness with examples of failures that may occur within the different ranges.

**Table 2: Failure characteristics for different ranges of the specific film thickness (Coy, Townsend and Zaretsky, 1985)**

| **Range:** | **Failure characteristics:** |
|---|---|
| $\lambda < 1$ | Surface scoring, smearing or deformation occurs on the gear surface and is followed by wear |
| $1 < \lambda < 1.5$ | Surface distress and pitting may occur |
| $1.5 < \lambda < 3$ | Surface glazing may occur and there is a risk of subsurface originated pitting |
| $3 \leq \lambda$ | Minimal wear and long life can be expected. Failure can eventually be caused by subsurface originated pitting |

### *Flash Temperature*

Another factor that needs to be determined in order to obtain proper lubrication of the gears is the flash temperature, $T_f$. This is described as the temperature that occurs when the temperature of the lubricant is hot enough to destroy the film layer and then initiates welding at the contact point (Dudley, 1994).

Dudley (1994) gives an expression for the flash temperature which is shown in eq 25. The parameters which occur in the expression are briefly described in Table 3.

$$T_f = T_b + \frac{c_f f W_t (v_1 - v_2)}{cos\phi_t \, F_e (\sqrt{v_1} + \sqrt{v_2}) \sqrt{\frac{B}{2}}} \quad (25)$$

**Table 3: Descriptions of the parameters which are included in the flash temperature equation**

| Parameter: | Description: |
|---|---|
| $T_b$ | The temperature of a blank surface in the contact zone, Dudley (1994) mentions that this can be given the same value as the temperature of the inlet oil |
| $c_f$ | A material constant for specific heat, conductivity and density of the material |
| $f$ | The friction coefficient |
| $W_t$ | The tangential load |
| $v_i$ | The rolling velocity at the point of contact, for the driving wheel and the gear |
| $\phi_t$ | The transverse pressure angle |
| $F_e$ | Face width in contact, i.e. the length of the contact zone |
| $B$ | The width of the band of contact |

Similar equations which can be used for determining the flash temperature can be found in Davis (2005) and AGMA 925-A03 (2003), but with the exception that they use the definition scuffing temperature instead of flash temperature. The latter one is instead used for defining the second part of the equation, see eq 26.

$$T_s = T_b + T_f \quad (26)$$

Davis (2005) presents a slightly modified expression given by Forschungsstelle für Zahnräder und Getriebebau, FZG, which is shown in eq 27. This formula includes parameters which are measured from tests, i.e. the bulk temperature of the test gears, $T_{btest}$, the maximum flash temperature of the test gears, $T_{ftest}$, and the welding factor, $X_w$. The welding factor is used in order to take variations in different gear steels and treatments, e.g. heat and surface treatments, into consideration (Davis, 2005). Example on values of the welding factor for different gear materials are shown in Table 4.

$$T_s = T_{btest} + X_w T_{ftest} \quad (27)$$

**Table 4: Example of welding factors that are used for different gear materials (Davis, 2005)**

| Gear material: | Welding factor: |
|---|---|
| *Through hardened steel* | 1 |
| *Nitrided steel* | 1.5 |
| *Carburized steel* | $0.85 < X_w < 1.15$<br>Depending on the austenite content, e.g. less amount of austenite results in a higher welding factor while an average content gives $X_w=1$ |
| *Stainless steel* | 0.45 |

### 2.3.3 Practical Testing

Gear testing is performed in order to evaluate the performance of a gear and to obtain an estimation of how long the gear will live before it suffers any damage. Allowable stresses, e.g. contact stress limits, can then be determined based on such tests (Davis,

2005). Examples of two different test routines, which are used in order to evaluate the performance of a gear, are Rolling Contact Fatigue, RCF, testing and FZG testing.

### *RCF Testing*

RCF testing is used for simulating the rolling and sliding action in meshing gears. The purpose of performing that kind of testing is to determine a material's pitting resistance, but it can also be used to simulate other tooth surface failures (Davis, 2005).

An advantage of performing RCF testing is that cylindrical test specimens are used instead of real gears in order to evaluate a possible gear material candidate. Due to the simple geometry of the test specimens, in comparison with real gears, the cost of the test is reduced. On the other hand, the precision of the test result may not be as good as the results obtained from testing of real gears. Of that reason are RCF tests used as a screening procedure which is performed before more detailed testing (Davis, 2005).

The RCF test rig comprises of two rolling discs mounted on parallel shafts, a gear section which transfers torque from one shaft to the other and an engine that drives the ingoing shaft (Davis, 2005). A schematic picture of the RCF test rig is shown in Figure 14.

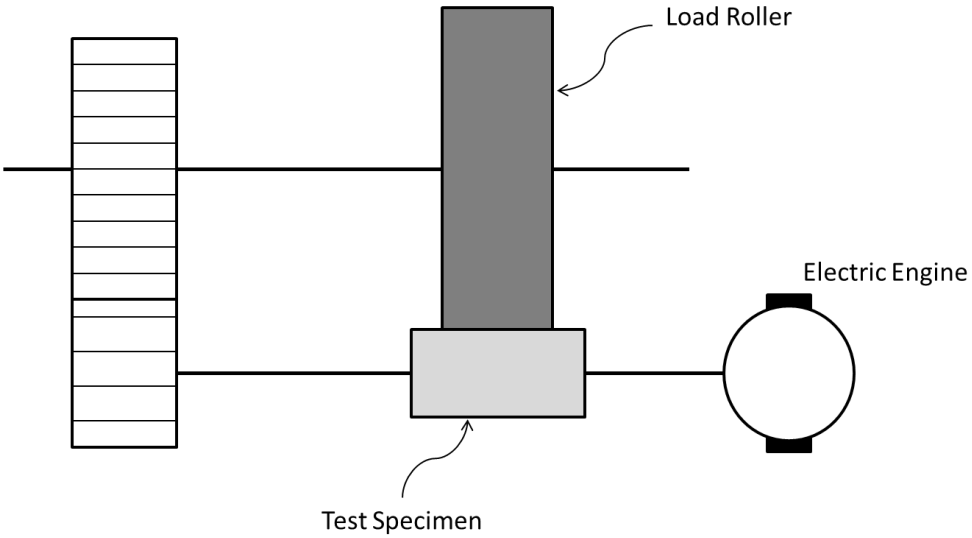


**Figure 14: Schematic illustration of the RCF test rig based on a definition given by Davis (2005).**

### *FZG Testing*

FZG tests are performed in order to evaluate the impact of different lubricants on gear failures, e.g. how scuffing, low-speed wear and pitting are affected by the choice of lubricant (ISO 14635-1, 2000). The scuffing test is conducted by letting two gears be subjected to a load that is stepwise increased until failure of the tooth surface occurs. In low-speed wear and pitting tests the gears are subjected to constant loads and the damages are measured at regular intervals (Intertek, 2013).

Two different types of spur gears are used in FZG tests, i.e. type A and type C. Type A gears are used in scuffing and low-speed wear tests while type C gears are used in pitting tests (Intertek, 2013). Both tests use involute gears, which do not have any modifications of the tooth flank. Table 5 shows some parameters which define the gear geometry of a Type A gear. Similar parameters which are used for defining the Type C geometry are shown in Table 6.

**Table 5: Example of Type A gear geometry given in mm and degrees (ISO14635, 2000)**

| **Parameter:** | **Driving wheel** | **Driven wheel** |
|---|---|---|
| *Center distance, a* | 91.5 | |
| *Effective tooth width, b* | 20 | |
| *Working pitch diameter, d* | 73.2 | 109.8 |
| *Tip diameter, $d_a$* | 88.7 | 112.5 |
| *Module, m* | 4.5 | |
| *Number of teeth, z* | 16 | 24 |
| *Addendum modification factor, x* | 0.853 | -0.5 |
| *Pressure angle, α* | 20 | |

**Table 6: Example of Type C geometry given in mm and degrees (DMGK, 2002)**

| **Parameter:** | **Driving wheel** | **Driven wheel** |
|---|---|---|
| *Center distance, a* | 91.5 | |
| *Effective tooth width, b* | 14 | |
| *Working pitch diameter, p* | 73.2 | 109.8 |
| *Tip diameter, $d_a$* | 82.46 | 118.36 |
| *Module, m* | 4.5 | |
| *Number of teeth, z* | 16 | 24 |
| *Addendum modification factor, x* | 0.1817 | 0.1715 |
| *Pressure angle, α* | 20 | |

The test rig that is used in FZG tests consists of two gear sections, i.e. one slave and one test section, a coupling for measuring the torque, a coupling for applying the load and an electric engine that drives the test rig (ISO 14635-1, 2000). The load coupling is attached to a loading arm, which may be loaded with different weights, and by that enables testing of different load stages. A schematic picture of the FZG test rig is illustrated in Figure 15.

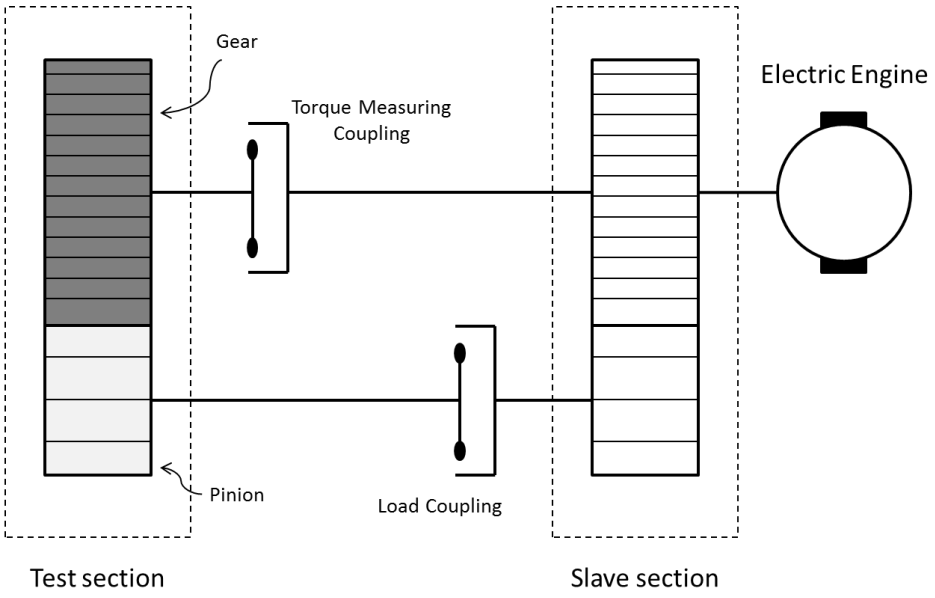


**Figure 15: Schematic illustration of the FZG rig based on ISO 14635-1 (ISO, 2000).**

### 2.3.4 Analyzing Contact Mechanics with Computer-Aided Tools

There exist a wide range of different computer based tools that can be used for analyzing contacts in gears. These tools are based on different analytical methods in order to analyze the contact mechanics, e.g. conventional FE solvers, and semi-analytical FE solvers and computational programs based on mechanical standards.

Gurumani and Shanmugam (2011) showed in a study how the conventional FE software ANSYS was used in order to investigate the impact of crowning on spur gears. The model that was used in the simulations consisted of three spur gear teeth which were mating with a contact surface that moved into the gear teeth in order to simulate the meshing process. A very fine FE mesh, i.e. a high number of elements, was used in the contact zone in order to obtain good accuracy of the contact stresses, while a coarser mesh was used for the rim structure (Gurumani and Shanmugam, 2011). According to Liu and Quek (2003) the calculation time increases with the number of elements, thereby occurs a risk of long computational times by using the method given by Gurumani and Shanmugam (2011).

Transmission3D is an FE program that uses a semi-analytical FE approach for analyzing gears (ANSOL, 2003). The advantage of using this approach is that it does not require any mesh of high precision in the contact zone, which conventional FE software would do. According to Advanced Numerical Solutions, ANSOL, (2003) conventional FE programs require a very fine mesh in the contact zone in order to properly reflect the contact conditions. If a coarse mesh then is used for the rest of the body then the gears need to be re-meshed for every time step of the calculation due to the rotational motion of the gears, i.e. the contact points move when the gears are rotating. An alternative approach is to use a fine mesh over the entire gear. Both these approaches result in long computational times (ANSOL, 2003).

ANSOL's method, on the other hand, solves the contact issue by using a linear FE method in order to calculate relative deformations and stresses which are located far away from the contact zone. A semi-analytical approach, based on the revised simplex method, is then used in order to calculate the relative deformations and stresses which are located within the contact zone (ANSOL, 2003). The revised simplex method is an updated version of the simplex method which is a mathematical procedure used in linear programming for finding an optimal solution to a problem. The method iterates between nearby extreme points until an optimal solution is found, which is achieved after a finite number of steps (Råde & Westergren, 2004).

Computational programs that are based on theoretical standards in combination with light FE techniques exist in addition to the FE programs. One example of such of a program is Load Distribution Program, LDP, which is a program that can be used for predicting the load distribution in gears (Harianto and Houser, 2002). LDP uses AGMA standards in combination with other techniques, e.g. simplex method and FE formulations, in order to perform the calculations. The advantage of using this approach is fast calculation times (Harianto and Houser, 2002). Assumptions regarding the gear geometry are required in order to use LDP's approach. One example is the assumption that the contacting surfaces have smooth shapes in order to simplify the contact conditions (Bergseth, 2012) and thus achieve faster calculations. The assumptions may, on the other hand, also lead to errors in the results (Bergseth, 2012).

# 3. Method

This chapter summarizes how the work with the thesis has been carried out. It starts by presenting the layout of the study, i.e. how the work was planned in order to reach the goals which were presented in the introductory chapter, and ends with the final analysis where the influence of the gear's micro geometry was investigated.

## 3.1 Layout of the Study

The study began with a thorough literature study that was conducted in order to acquire knowledge within the field of gear design and contact mechanics. The most important findings from the literature review have been summarized in the *Theory Chapter*, which has served as a theoretical foundation for the study.

After the literature study had been carried out it was decided to study gear standards more thoroughly. An intention of studying the gear standards was to learn the theory behind contact mechanics more in depth. The study was also made for establishing a theoretical procedure that could be used when the developed computer program was going to be evaluated.

A computational method was generated thereafter. This method was intended to be the included in computer program. The method was then evaluated with help of existing analytical methods, i.e. the gear standard and another gear program.

The final phases of the study consisted of further analysis of gear contact and the creation of the computer program for analyzing contact mechanics. The two parts were made simultaneously in order to test the computer program during the analysis and to improve the computational model used by the tool.

## 3.2 AGMA Procedure for Calculating Contact Stresses in Gears

A procedure for calculating the contact stresses in spur and helical gears was derived by using the American National Standards Institute-American Gear Manufacturers Association, ANSI/AGMA, 2101-D04 and AGMA 908-B89 standards which are briefly described in the following section. A more thorough description can be found in Appendix A: *Contact Stress Calculations according to AGMA*. The main reason for using the AGMA standard was due to the fact that it was used by most of the references which had been used in the literature study. More explicit descriptions of the included parameters in the gear standard could then be obtained by reviewing the references.

The equation that is used for calculating the contact stresses is given in eq 28 (AGMA, 2004). Descriptions of the included parameters which are used in the equation are given in Table 7.

$$\sigma_H = Z_E \sqrt{F_t K_0 K_V K_S \frac{K_H}{d_{W1} b} \frac{Z_R}{Z_I}} \quad (28)$$

**Table 7: Presentation of the parameters which are included in the contact stress equation**

| **Parameter:** | **Description:** |
|---|---|
| $Z_E$ | Elastic coefficient |
| $F_t$ | Tangential transmitted load [N] uniformly distributed along the face width |
| $K_0$ | Overload factor, see *Appendix A* |
| $K_v$ | Dynamic factor |
| $K_s$ | Size factor, see *Appendix A* |
| $K_H$ | Load distribution factor, see *Appendix A* |
| $d_{W1}$ | Operating pitch diameter of the driving wheel |
| $b$ | Face width of the narrower member in the gear pair |
| $Z_R$ | Surface condition factor, see *Appendix A* |
| $Z_I$ | Geometry factor for pitting resistance |

Many of the parameters which are included in Table 7 require experience within the field of application in order to be estimated (Budynas and Nisbett, 2008). Of that reason will only the parameters which involve general data concerning geometrical, material, and load characteristics be described. Descriptions of the overload, size, load distribution and surface condition factors are given in Appendix A: *Contact Stress Calculations according to AGMA.*

The elastic coefficient is given by eq 29. The equation includes the material properties of the gear, i.e. Young's modulus of elasticity and Poisson's coefficient.

$$Z_E = \sqrt{\frac{1}{\pi\left[\left(\frac{1-\nu_1^2}{E_1}\right)+\left(\frac{1-\nu_2^2}{E_2}\right)\right]}} \quad (29)$$

The operating pitch diameter is obtained by eq 30. The expression includes the shaft distance, a, and the speed ratio, u.

$$d_{W1} = \frac{2a}{u+1} \quad (30)$$

The tangential transmitted load is given by the expression shown in eq 31. The torque $T$ which occurs in the equation is the torque of the driving wheel (AGMA, 2004).

$$F_t = \frac{2000T}{d_{W1}} \quad (31)$$

The dynamic factor is given by eq 32 and is determined by the parameters C and B, which are given by eq 33 and 34 respectively, and the pitch line velocity at the operating pitch diameter, $v_t$, which can be seen in eq 35. The rotational speed, $\omega_1$, included in the expression for the pitch line velocity is the rotational speed of the driving wheel. The rotational speed should be defined in RPM (AGMA, 2004).

$$K_V = \left(\frac{C}{C+\sqrt{196.875v_t}}\right)^{-B} \quad (32)$$

$$C = 50 + 56(1-B) \;\; for \;\; 6 \leq A_V \leq 12 \quad (33)$$

$$B = 0.25(A_V - 5.0)^{0.667} \quad (34)$$

$$v_t = \frac{\pi \omega_1 d_{W1}}{60000} \quad (35)$$

The parameter $A_V$, which occurs in eq 33 and 34, is known as the transmission accuracy number. This number is used in order to define the quality of the gears. Higher transmission accuracy numbers indicate higher quality, while a lower number means less good quality. The AGMA standard states that equation for determining the dynamic factor is only valid for transmission accuracy numbers that ranges from six to twelve (AGMA, 2004).

The shape factor, $Z_I$, is given by the AGMA 908-B89 standard and is shown in eq 36 (AGMA, 1999). The nomenclatures of the included parameters are given in Table 8 and the equations for the different parameters are shown in Appendix A: *Contact Stress Calculations according to AGMA.*

$$Z_I = \frac{\cos \Phi_r C_\psi^2}{\left(\frac{1}{\rho_1} + \frac{1}{\rho_2}\right) d_{W1} m_N} \quad (36)$$

**Table 8: Presentation of the parameters which are included in the shape factor equation**

| **Factor:** | **Definition:** |
|---|---|
| $\Phi_r$ | Operating pressure angle |
| $C_\psi$ | Helical overlap factor |
| $\rho_1$ | Radius of curvature of the driving wheel |
| $\rho_2$ | Radius of curvature of the gear |
| $d_{W1}$ | Operating pitch diameter |
| $m_N$ | Load sharing ratio |

When the contact stress has been calculated it should be compared with the allowable contact stress number, $\sigma_{HP}$, which is seen in eq 37. Values of the allowable contact stress number for different materials can be found in the ANSI/AGMA 2101-D04 standard (AGMA, 2004). The other parameters which are used in the equation are defined in Table 9.

$$\sigma_{HP} \leq \frac{\sigma_{HP}}{S_H} \frac{Z_N}{Y_\theta} \frac{Z_W}{Y_z} \quad (37)$$

**Table 9: The factors used in the allowable contact stress equation**

| **Factor:** | **Definition:** |
|---|---|
| $S_H$ | Safety factor for pitting |
| $Z_N$ | Stress cycle factor for pitting resistance |
| $Z_W$ | Hardness ratio factor for pitting resistance |
| $Y_\theta$ | Temperature factor |
| $Y_z$ | Reliability factor |

According to Budynas and Nisbett (2008) the equation above is used when the allowable contact stress number, $\sigma_{HP}$, is given for a specific load case and a certain number of cycles and with a specific percentage of reliability. The other parameters are then used for modifying the allowable contact stress such that it will represent other scenarios, e.g. using the stress cycle factor in order to calculate stresses for other number of lives such that a stress rating curve can be established. The factors can be derived by using the ANSI/AGMA 2101-D04 standard (AGMA, 2004).

### 3.2.1 Deviations and Assumptions

The described AGMA procedure differs from the standard in that sense that the equations for the helical gear only considers helical gears of conventional type. The decision to only consider conventional helical gears in the procedure was due to the fact that it was assumed that the helical gears which were to be simulated had an axial contact ratio larger than one. According to the AGMA 908-B89 standard this condition is only fulfilled by conventional helical gears, since spur and low axial contact ratio, LACR, helical gears have axial contact ratios which are less than one (AGMA, 1999).

The allowable stress equation has not been used in the Validation process or the developed gear application. The S-N curves, which were shown in the *Theory Chapter*, have instead been used for contact stress rating.

The AGMA standards include parameters that need to be estimated by the mechanical designer. According to Budynas and Nisbett (2008) these estimations require experience within the specific field of application. The values of the experience-based parameters were therefore chosen according to recommendations given by Budynas and Nisbett (2008) and Childs (2005), and by assuming ideal manufacturing and assembly conditions. The assumed values which have been used in the calculations are shown in Appendix A: *Contact Stress Calculations according to AGMA*.

## 3.3 Computational Method

A computer-based calculation method was created before the development of the computer program for analyzing contact mechanics began. The computational method consisted of a generalized model of a gear pair that was analyzed in an FE solver. This process was then embedded into the computer program.

### 3.3.1 The FE Software

An external FE based program, i.e. Transmission3D, was used for analyzing the contact mechanics of the gears. Different kinds of three-dimensional transmissions, e.g. planetary systems and differentials, can be simulated in Transmission3D but in this study has the software been used for simulating the contact mechanics in a single gear pair.

One motivation for using this software was based on the fact that the software could be run as a sub process without needing to access the software's own graphical user interface. This was a desirable property since the software was intended to be embedded into the computer program that was to be developed. Another motivation for using Transmission3D was the post processing options that the software offered, since the software both outputted an external file with a 3D model that could be used for stress analysis and a report, in PDF format, which contained the results from the simulation.

The engineers at the company, i.e. Vicura AB, had also performed an investigation where an analysis made in Transmissio3D was compared with simulations made on a similar case in the conventional FE software ABAQUS. The results obtained from both of the software showed similar trends, but the computational time for the simulations that were performed in Transmission3D were significantly faster.

### 3.3.2 Generation of a Generalized Model

Transmission3D differs from other FE programs in that sense that it does not require any 3D model as input to the preprocessing procedure. A model is instead generated by the FE program by defining a set of parameters which describe the layout of a gear pair.

The intention of using a generalized model in the analysis was due to an aspiration of being able to change the total appearance of the gears by only varying a few parameters, e.g. module and tooth characteristics. This was achieved by using the same layout as the test gear pair that was used in the FZG test procedure that was described in the *Theory Chapter*. The setup of the FZG gears was defined by two spur gears mounted at parallel shafts with a load that was transmitted from the driving wheel to the gear. Assumptions regarding the geometries of the gears were also made in addition to the definition of the general layout of the gear pair. These assumptions concerned the geometrical appearances of the gears.

A trial and error process began in order to find the specific parameters which defined the layout of the gears' teeth. During the literature study it was noticed that the parameters which are defined in the transversal plane for a helical gear are defined similarly as the parameters which define the spur gear. Based on this finding it was decided to define all parameters in the transversal plane. Transmission3D could then decide whether to generate a spur or a helical gear depending on the helix angle beta, e.g. if beta was equal to zero then a spur gear was generated. The parameters which define the tooth geometry are listed in Table 10.

**Table 10: List of the parameters which are required as input to Transmission3D**

| | **Parameter:** | **Nomenclature:** |
|---|---|---|
| *Gear Data* | Center distance | $a$ |
| | Number of teeth | $z$ |
| | Module | $m$ |
| | Pressure angle | $\alpha_0$ |
| | Circular tooth thickness | $s_t$ |
| | Face width | $b$ |
| | Helix angle | $\beta_b$ |
| | Outside diameter | $d_a$ |
| | Root diameter | $d_f$ |
| *Tool Data* | Tip radius of the hob | $\rho_0$ |
| | Protuberance | $pro$ |
| | Protuberance height | $hpro$ |

In the *Theory Chapter* it was mentioned that the shape of a gear tooth's root is defined by the tool geometry. A picture that illustrates the difference between using a standardized tool and a tool that includes a protuberance is shown in Figure 16. The purpose of using a protuberance is to create extra clearance in the root section (Karlebo Handbook, 1992).

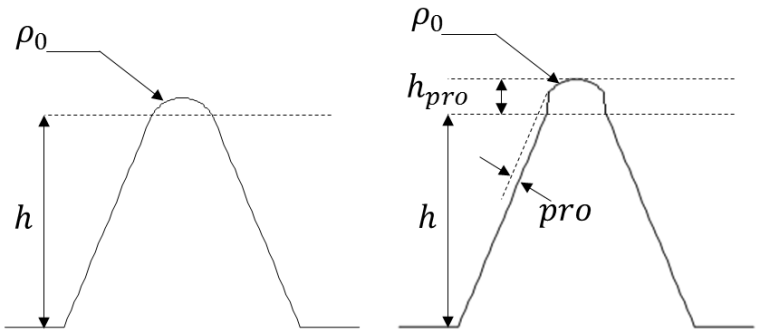


**Figure 16: Difference between a standard tool and a tool that includes a protuberance based on a description given by Vijayakar[1]. The parameter *h* indicates the height of the tool.**

During the trial and error process it was also decided to use infinitely stiff shafts such that only the gears would deform when the torque was applied. The design of the shafts could thus be given an arbitrary shape, due to the fact that the selection of shape would not affect the durability of the shafts.

The 3D model that represented the driving wheel consisted of two parts, one shaft and one ring that included all teeth. The two parts were assembled by using the same number of elements at the mating surfaces of the parts. The driving wheel was assumed to be created directly at the driving shaft and therefore was the shaft divided into different segments with varying diameters. The ring was then connected to the outer segments of the shaft in order to achieve an axial connection between the ring and the shaft. The two parts in meshed appearances are shown in Figure 17.

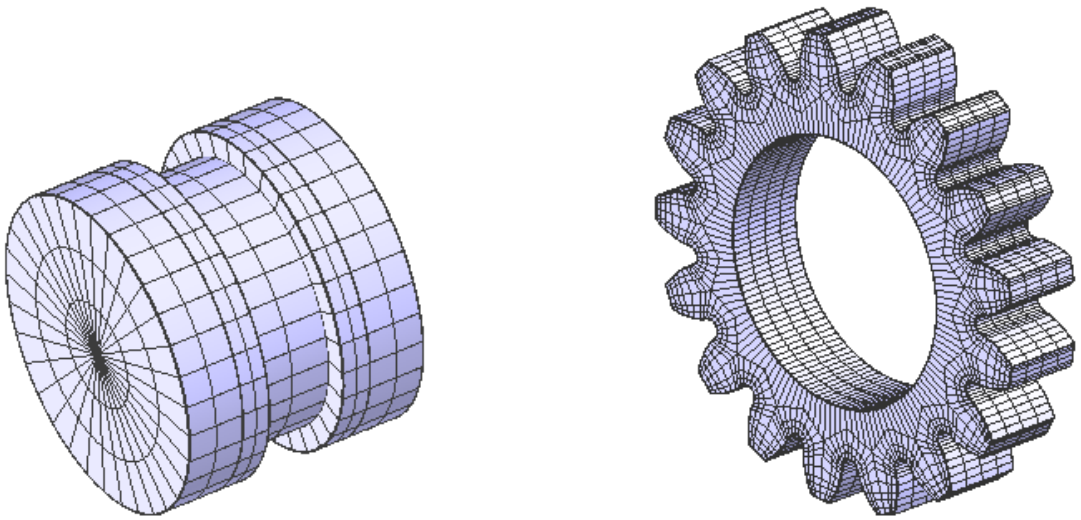

**Figure 17: Picture showing the meshed parts which define the driving wheel, i.e. the shaft and the ring structure.**

The outer diameter of the driving wheel's shaft was derived by calculating the mean value of the inner diameter of the ring that included the teeth and the root diameter of the driven wheel. Transmission3D defines the inner diameter of the ring according to

[1] Sandeep Vijayakar at ANSOL, email correspondence 19 February 2013

eq 38 (ANSOL, 2003). The outer diameter of the shaft is given by eq 39. The same diameter was then used for the driven wheel's shaft.

$$d_{ring,inner} = 2d_f - d_a \quad (38)$$

$$d_{shaft,outer} = \frac{d_{ring,inner} + d_f}{2} \quad (39)$$

Three different parts constituted the 3D model that represented the driven wheel. These parts were a driven shaft, a rim and a ring that included the teeth. The connections between the parts were made in a similar way as for the driving wheel by using the same number of elements for the mating surfaces of the different parts. The driven wheel was assumed to have been created as a separate piece and then been mounted at the driven shaft, and thereby could a uniform shape of the driven shaft be used. The meshed parts are shown in Figure 18.

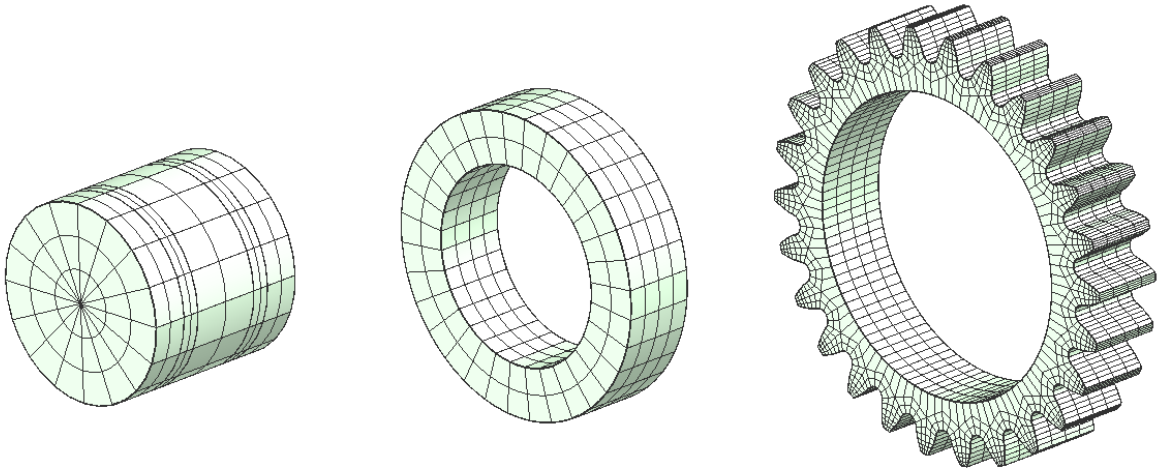

**Figure 18: Picture showing the meshed parts which define the driven wheel, i.e. the shaft, the rim and the ring structure.**

Transmission3D includes options for auto generating a mesh on the gear teeth by using so-called mesh templates. The templates adapt to the geometry of the teeth and the only thing that is required by the user is to define the accuracy of the template. The mesh template for the driving wheel tooth was selected to be finer than for the gear tooth. This choice was based on a fact presented by Dudley (1994) which states that the worst load position on spur gear teeth can be found at the lowest point of a driving wheel tooth where the entire load is carried by one pair of teeth. A zoomed in picture that shows the difference between the driving wheel's and driven wheel's mesh templates is shown in Figure 19.

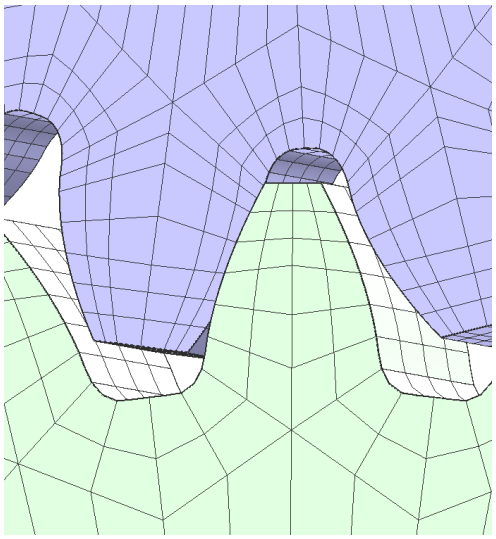

**Figure 19: Picture illustrating different meshes of the driving wheel and the driven wheel. The driving wheel is shown in purple color and the driven wheel in green color.**

For the shafts it was decided to use coarse meshes, which were defined manually, since these were not being investigated in the analysis. The only functions of the shafts were to transfer the loads and due to that fact could a rough mesh be used. General mesh data for the shafts are shown in Table 11 and 12 respectively.

**Table 11: Mesh data for the driving wheel**

| **Mesh attribute:** | | |
|---|---|---|
| *Element type* | | Cubic lagrangian |
| *Number of elements* | Radial direction | 3 |
| | Axial direction | 2 |
| | Circular Direction | 32 |

**Table 12: Mesh data for the driven wheel**

| **Mesh attribute:** | | |
|---|---|---|
| *Element type* | | Cubic lagrangian |
| *Number of elements* | Radial direction | 3 |
| | Axial direction | 2 |
| | Circular Direction | 16 |

The procedure that defines the gear pair could then be used for generating different types of spur and helical gear pairs. Examples of different gear pairs which have been generated by considering this procedure are shown in Figure 20.

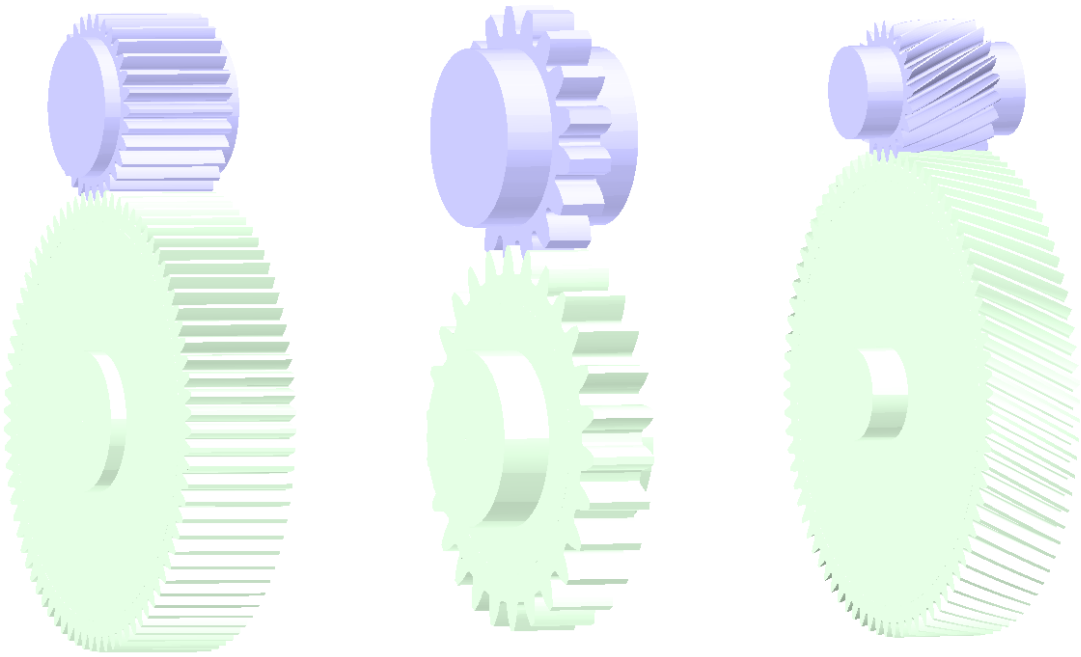

**Figure 20: Example of different models that have been generated by using the generalized procedure for generating a gear pair.**

## 3.4 Validation

The validation process was conducted in order to test how well an analysis made by the computational method performed compared to other analytical tools. The two tools which were used as references were the AGMA procedure, described in the beginning of the *Method Chapter*, and the computational program LDP. This section summarizes the Validation process briefly, while a more comprehensive description can be found in Appendix B: *Validation Report*.

### 3.4.1 The Studied Object

The model that was used in the validation process was based on test gears used by Leque (2011) in a study where spur gears were tested under high-speed and high-temperature conditions. The data which defines the gear geometry is presented in Table 13 and data for the micro geometry is given in Table 14.

**Table 13: Gear data obtained from Leque (2011) presented in mm and degrees**

| **Parameter:** | **Driving wheel** | **Driven wheel** |
|---|---|---|
| *Module, m* | 4.23 | |
| *Center Distance, a* | 91.5 | |
| *Number of Teeth, z* | 17 | 26 |
| *Pressure Angle,* $\alpha_n$ | 22.5 | |
| *Face Width, b* | 14 | 20.29 |
| *Tip Radius,* $d_a$ | 80.02 | 117.11 |
| *Root Radius,* $d_f$ | 62.87 | 99.95 |
| *Circular Tooth Thickness,* $s_t$ | 7.81 | 5.65 |

**Table 14: Micro geometry of the gears obtained from Leque (2011) presented in mm and degrees**

| **Modification:** | | **Driving wheel** | **Driven wheel** |
|---|---|---|---|
| *Tip relief:* | Magnitude | 36 | 36 |
| | Start roll angle | 34 | 30 |
| *Root relief:* | Magnitude | 5 | 5 |
| | Start roll angle | 12 | 15.6 |
| | End roll angle | 34 | 30 |
| *Lead crown:* | Magnitude | 5 | 8 |

The reason for why the gears used by Leque (2011) were used as references was due to the factors listed below:

- Sufficient data was presented in order to generate models in Transmission3D and LDP
- The layout of the test section in the test rig was designed in a similar way as the model used by the developed computational procedure
- Results on the contact stresses were shown which could be used as references during the evaluation process

A model was generated for the analysis based on the gear data that was obtained from Leque (2011). A picture showing the meshed model is shown in Figure 21.

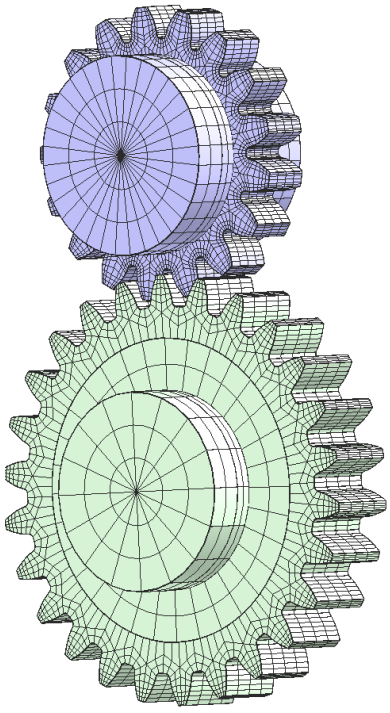

**Figure 21: Meshed gear pair that has been generated in Transmission3D.**

The micro geometry of the tooth flank was modified by using a standardized function in Transmission3D. This function only required the magnitude of the modification for a modification performed in the lead direction. For a profile modification it also required the roll angles where the modification was supposed to begin and end. The modification performed in the profile direction was assumed to be of linear type.

The material that Leque (2011) used for the automotive test gears was Society of Automotive Engineers, SAE, 4118 steel. Table 15 shows some mechanical properties

of the material based on data obtained from SteelSS (2011) and the mechanical properties used within the simulations. Furthermore, it was assumed that the bodies were made of uniform material.

**Table 15: Material data.**

| **Material parameters:** | **SAE4118 at 25°C (SteelSS, 2011)** | **Used in Transmission3D** | **Unit** |
|---|---|---|---|
| *Young's modulus of elasticity, E* | 190 – 210 | 210 | GPa |
| *Poisson's coefficient, ν* | 0.27 - 0.3 | 0.3 | |
| *Density, ρ* | 7700 – 7900 | 7900 | $kg/m^3$ |

### 3.4.2 Simulation Settings

The simulation settings were mainly based on default values given by Transmission3D, except from the delta time which is the gear mesh cycle time divided by the number of simulation steps minus one. Since this parameter varies for different gears, i.e. due to number of teeth and speed, it had to be calculated every simulation. An example on how the delta time is calculated is given in eq 40.

$$\Delta t = \frac{2\pi}{\omega_{pinion}\, z_{pinion}} \frac{1}{(n_{steps} - 1)} \quad (40)$$

The number of simulation steps was chosen as 11. This value was decided to be sufficient in order to obtain good results. If a lower value had been used then the calculation time would have been faster but to the cost of the accuracy of the results. A higher value would yield more accurate results but at the same time would have resulted in longer calculation times.

### 3.4.3 Setup of Cases

Leque (2011) performed simulations for two different cases with a constant speed of 13500 RPM and torque levels of 250 Nm and 340 Nm respectively. The gears which were tested by Leque (2011) included modifications, both in the lead and profile direction. Additional cases were, on the other hand, simulated in order to obtain sufficient data for making any conclusions.

In total were six different cases simulated, due to the fact that three different types of modifications were simulated at two different load stages. LDP was used as a reference for all simulations, while the results showed by Leque (2011) were only used for the cases with modifications performed in both lead and profile direction. The AGMA procedure was used as a reference for the cases without any modification.

## 3.5 The Contact Program

A computer based gear application, written in Python 2.7.3 (Python, 2013), was created in order to simplify the modeling work and to reduce the preprocessing time, i.e. the time it takes to generate a model in Transmission3D and define the simulation settings. The reason for making such a program was to eliminate repetitive steps in the preprocessing and the post processing steps. This was achieved by increasing the level of automation.

### 3.5.1 Program Structure

The gear application constitutes of a main program that includes the graphical user interface, GUI, which interacts with the user. The main program also runs other subroutines, i.e. modules, in order to perform different operations. The decision of using a modular design (Ulrich and Eppinger, 2012) of the gear application was made in order to allow for addition of more functions in the future. Another benefit of using the modular approach was that the entire gear application did not required to be recompiled every time when a subroutine was modified. A schematic picture that illustrates the layout of the gear application is shown in Figure 22.

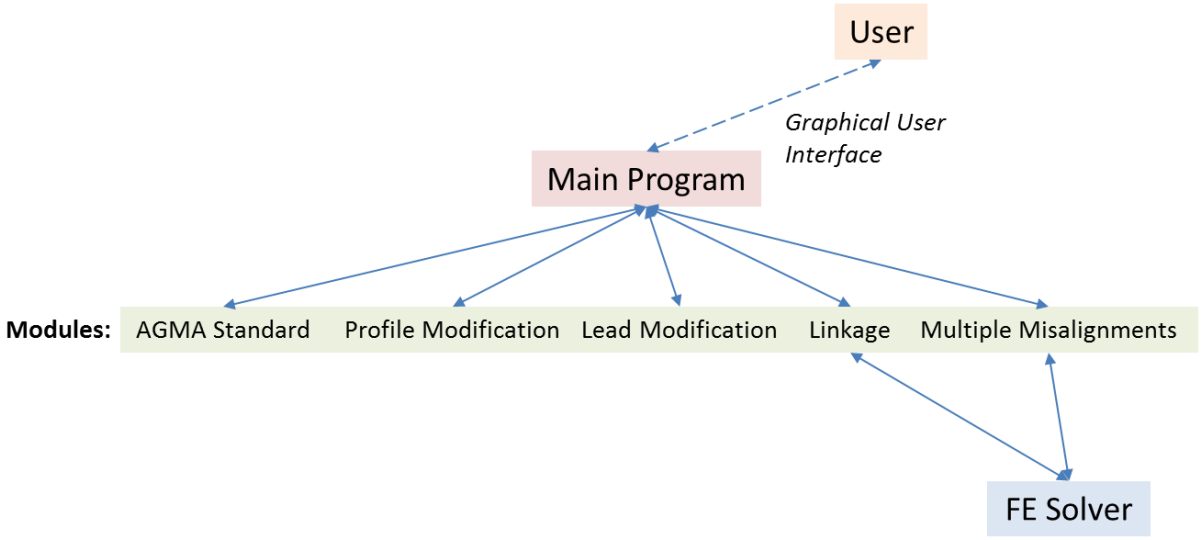


**Figure 22: The layout of the gear application.**

### 3.5.2 The GUI

The intention of making a GUI was to simplify the interaction between the user and the FE program. The user, in this case, was assumed to be a mechanical designer with basic knowledge in gear design and of that reason it became necessary to eliminate the FE related parameters and instead focus on the parameters which describe the gear geometry. This implies that the user does not need any knowledge about the FE method in order to perform a contact analysis.

The GUI was created in Python 2.7.3 which is an open source programming language. The advantage of using an open source programming language was that it is free of charge, both for private as well as commercial use (Python, 2013). Another benefit of using Python was due to the fact that it includes several subroutines, i.e. modules, which involve functions that can be used for different purposes, e.g. mathematics and graphical work.

The visual part of the GUI was generated with help of a python module called Tkinter (Lundh, 1999). The module was used for creating the environment that the user interacts with during the usage of the gear application. This involves buttons, entries, pictures and different menus which all have been generated by using the Tkinter module.

### 3.5.3 Communication with the FE Program

Transmission3D offers the possibility to read instructions from a text file, which includes the user commands, instead of having the user to interactively define the

input to the software in the software's own GUI. This option was used when the link between Transmission3D and the developed gear application was established.

The general idea behind the linkage was to use the own developed gear program in order to create the parameters which defined the model and the loading conditions, and thereafter launch Transmission3D directly from the gear program. This was achieved by using a batch file, e.g. a file including commands for opening Transmission3D from the command prompt and to make Transmission3D performing the tasks which were defined in the script file.

A Python module, called linkage, was created for making the script file and the batch file. After the script and batch files had been created the module launched the batch file which in its turn started the FE simulation. A schematic picture illustrating the communication flow is shown in Figure 23.


**Figure 23: The communication flow used by the computer program.**

The automation process of the computational procedure required that more simplifications had to be done in order to cover all the aspects which characterized the analysis. For example it was decided to use a default gear material, i.e. SAE4118, in the program. This decision was based on a wish of reducing the number of parameters that the user had to define during the setup of the analysis.

A function for calculating the delta time, which was described in the Validation process, was implemented into the linkage module. The delta time was dependent of the parameters that were required as input to the computational method and the number of time steps which was chosen as 11 based on experiences from the Validation process, and thereby could the function be automated.

### 3.5.4 Options for Defining the Micro Geometry

In the *Theory Chapter* it was shown that a modification of the gear tooth at sometimes may be required, due to unfavorable loading conditions. Of that reason, it was decided to incorporate an option for modifying the micro geometry into the gear program.

In the Validation process it was shown that Transmission3D included standardized functions for performing modifications in the lead and profile directions. Beside these functions Transmission3D also included options for reading mathematical curves which describe the geometry in the lead and profile direction. These curves were defined by a position vector and a magnitude of modification vector which were sent to Transmission3D. Based on these vectors, Transmission3D could then generate the shapes of the lead and profile geometries.

The position of a modification that is performed in the lead direction was calculated according eq 41. A picture that shows how the positions in the lead direction are defined in Transmission3D is shown in Figure 24.

$$\zeta_i = 2\frac{x_{pos}}{b} - 1 \quad (41)$$

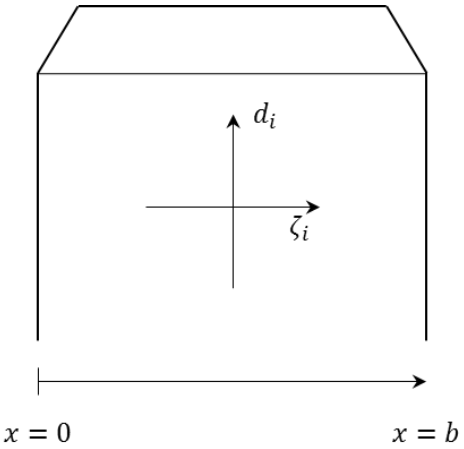


**Figure 24: Picture showing how the positions in the lead direction are defined.**

The positions of the modifications which are done in the profile direction are described by a vector that contains the corresponding roll angles for the modifications. The roll angle, $\theta_i$, was obtained by using an expression defined by Dudley (1994), which can be seen in eq 42.

$$\theta_i = \tan \alpha_i \quad (42)$$

The angle, $\alpha_i$, which occurs in the expression above is the profile angle at the contact point (Kahraman, Houser & Xu, 2005). The profile angle can be obtained by calculating the arccosine of the operating base diameter divided by a given diameter, $d_i$, which can be seen in eq 43.

$$\alpha_i = \cos^{-1}\left(\frac{d_b}{d_i}\right), \qquad where\ d_l \leq d_i \leq d_a \quad (43)$$

The lower limit of the diameter, $d_i$, is known as the limit diameter, $d_l$, and is the diameter where the SAP is positioned. The limit diameter can be obtained by using the AGMA 913-A98 standard which contains a methodology for specifying the geometry of spur and helical gears (AGMA, 1998). A picture showing the lower and upper limits, i.e. the limit and the tip diameters, is shown in Figure 25.

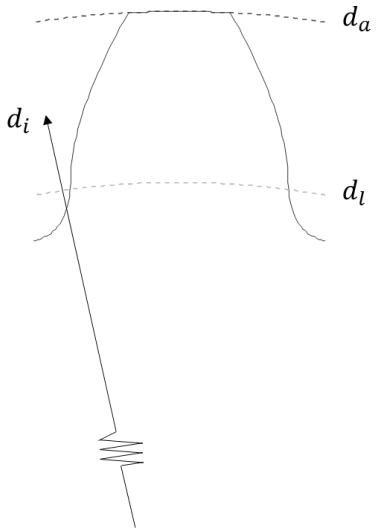


**Figure 25: Illustration of the diameter used in eq 43 with diametric boundaries.**

### 3.5.5 Estimation of Contact Stresses

A function for calculating an initial estimation of the contact stresses was added to the gear program. The purpose of making this function was to enable an initial estimation of the maximum contact stress before a simulation is started. The function was based on the AGMA procedure that was described in beginning of the *Method Chapter*.

### 3.5.6 Option for Axial Misalignments

A factor that has been proved to have an impact on the contact pattern, beside gear design and loading conditions, is axial misalignments of the gears (Houser, Harainto and Talbot, 2006). According to Houser, Harianto and Talbot (2006) the misalignments may be due to manufacturing errors of housings and gears which in its turn affects the gears in that sense that they avoid from their ideal positions in the gear mesh. Based on this knowledge it was decided to add an option for analyzing the misalignments of the gears to the gear program.

The misalignments of the gears were achieved by letting one of the gears, in this case the driving wheel, rotate about its tangential and radial axes in order to change the contact pattern. Pictures that illustrate how a misalignment was achieved by rotating the driving wheel around its *X* and *Y* axes are shown in Figure 26. The positions of the driving wheel and the gear were defined in the same way as Houser, Harianto and Talbot (2006) defined the gear pair that they had used in their study, i.e. by letting the driving wheel be positioned beneath the driven wheel.

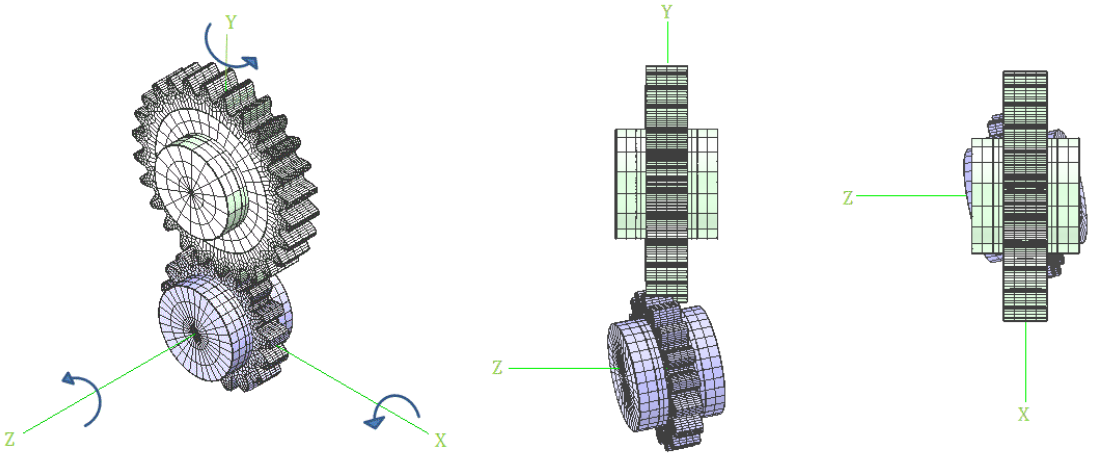


**Figure 26: Example of how a misalignment is defined in Transmission3D.**

The option for simulating multiple misalignments in the gear program was defined in a manner such that it allowed variation in both torque levels as well as misalignments. By considering this option it became possible to simulate duty cycles where a drive cycle is represented by different load stages.

## 3.6 Simulations Performed with the Contact Program

More simulations were performed after a first draft of the computer program had been created. These simulations were performed in order to evaluate the outcome from the gear program. The intention was then, with help of the outcome, to optimize the gear program and to obtain knowledge for future recommendations regarding gear design.

The model that was used for the simulation was the same model that was used in the validation process, i.e. the model obtained from Leque (2011). The reason for using the same model was due to the fact that some interesting findings, regarding the tip relief, had been discovered during the validation process. Another motivation for using the same model was the availability of public data, i.e. the report written by Leque (2011) contained sufficient information to generate a model for the analysis.

### 3.6.1 Analysis of Different Profile Modifications' Impact on the Contact Stresses

A demand of evaluating the influence from linear versus quadratic reliefs arose from the findings made in the validation process, see Appendix B: *Validation Report*. In the report it was noticed that linear root and tip reliefs seemed to have an influence on the high stresses, seen in Transmission3D, which appeared in the root and tip regions.

Three different models were made in order to investigate the influence of the type of profile modification. The first model did not include any profile modification, the second included linear tip and root reliefs and the last included parabolic tip and root reliefs. The two types of profile modification are shown in Figure 27 and 28, where the magnitude of the profile modification is plotted against the roll angles. The values on the tip and root reliefs were based on the profile modification values used by Leque (2011), which were shown in Table 14.

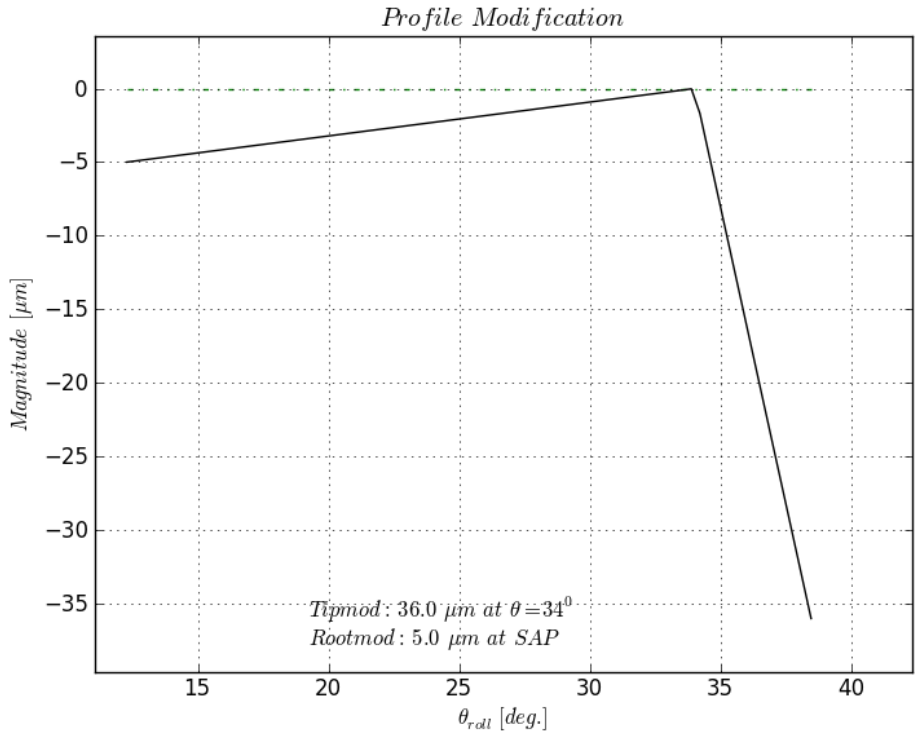


**Figure 27: Picture showing the shape of a linear profile modification.**

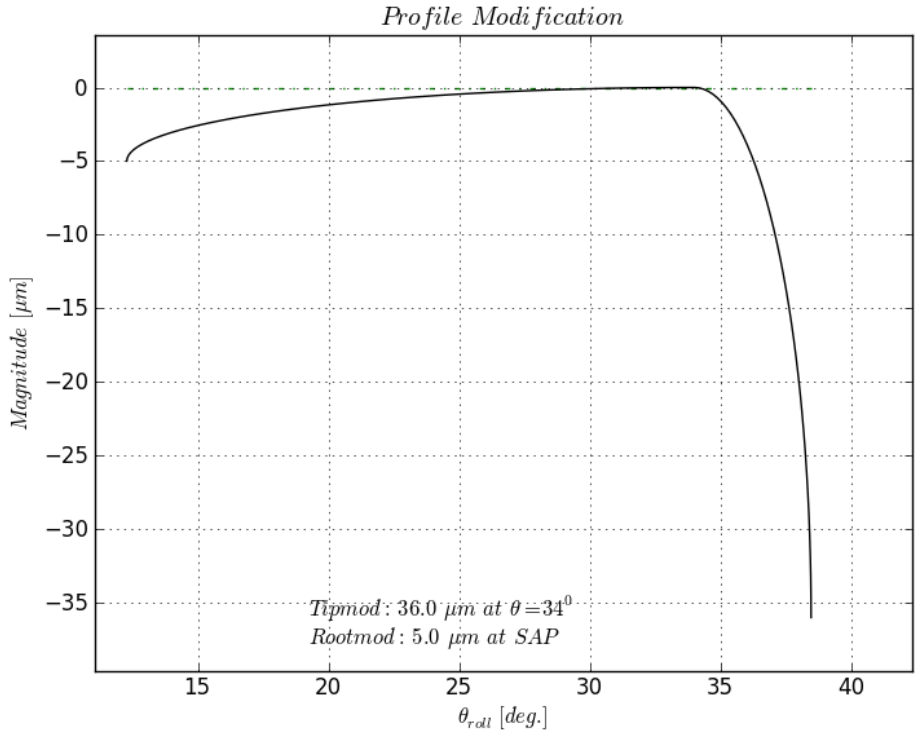


**Figure 28: Picture showing the shape of a parabolic profile modification.**

In total were six different simulations made in Transmission3D, i.e. three including edge contact and three without any edge contact. The option to simulate without any edge contact in Transmission3D was made in order to avoid influences from other sharp parts in the geometry, except from the tip and root transitions, such as sharp

corners positioned at the edges of the gear face and at the highest point of the tooth. Examples of critical areas, where there is a risk of fictitious stresses, are indicated in Figure 29.

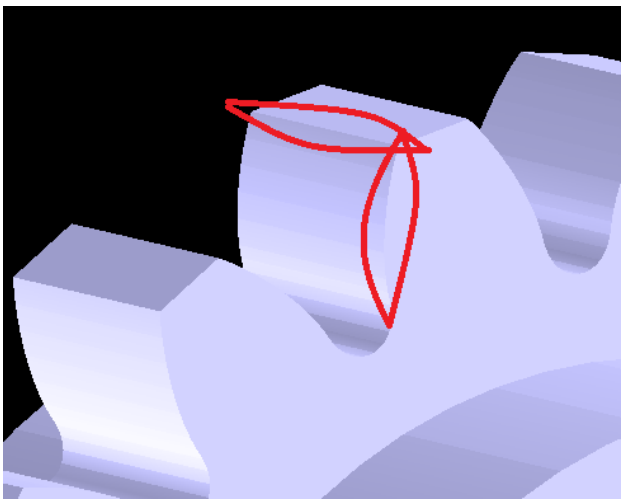

**Figure 29: Picture that indicates the areas, on a gear tooth, where there is a risk of fictitious stresses.**

Three simulations, with identical profile modifications as the ones used in Transmission3D, were simulated in LDP in order to obtain data for making a comparison of the results. The reason for making this comparison was based on the fact that the function that was used for modifying the gear profile had to be evaluated before it was included in the developed gear program.

### 3.6.2 Investigation of the Impact from Lead Modification

The simulations which were performed to investigate the influence from lead modification were made in order to show how a lead crown could be used in order to prevent, or at least reduce, the impact from axial misalignments. Simulations of an unmodified gear and a lead modified gear were therefore performed for both ideal conditions, i.e. operating conditions with no axial misalignments, and for operating conditions with axial misalignments. The model used in the Validation process was, once again, used but with the exception that the lead modification was removed from one of the gear pairs that was analyzed.

The interest of only evaluating the impact from lead modification led to the fact that only the lower torque stage, i.e. 250 Nm, was used within the simulations. It was considered as sufficient since a higher torque stage would only increase the magnitude of the contact stresses but not affect the load distribution, i.e. how the appearance of the load pattern changes. The rotational speed of the driving wheel was kept at 13500 RPM.

No edge contact was used in the simulations. This choice was based on the findings from the validation process, which can be seen in Appendix B: *Validation Report*, where high edge stresses were noticed at the edges of the gear tooth despite the fact that the gears used in the simulations were operating under ideal conditions.

An aspiration of investigating which of the rotations that gave rise to the worst misalignments resulted in nine different simulations. The setup of the simulations is shown in Table 16.

**Table 16: Setup of the simulations which were used for investigating the impact of lead modification**

| Simulation no. | Tangential rotation [mrad]: | Radial rotation [mrad]: |
|---|---|---|
| *1* | 0 | 0 |
| *2* | 1.0 | 0 |
| *3* | -1.0 | 0 |
| *4* | 0 | 1.0 |
| *5* | 0 | -1.0 |
| *6* | 1.0 | 1.0 |
| *7* | -1.0 | -1.0 |
| *8* | -1.0 | 1.0 |
| *9* | 1.0 | -1.0 |

# 4. Results and Discussion

This chapter starts with a demonstration of the results that have been obtained from the analytical part of the study. It also gives a presentation of the computer program that has been developed during the work with the thesis.

## 4.1 Validation

This section gives a summary of the results which were obtained from the validation process. A thorough description of the results is given in Validation Report which is appended in Appendix B: *Validation Report*.

The validation process showed maximum contact stresses at positions where high stresses were not expected and of that reason were only contact stresses which were located at a distance from the sharp edges studied. Figure 30 shows the stress pattern over an unmodified tooth flank which, according to the literature (Dudley, 1994), should show maximum stresses at the first position on a gear tooth where the entire load is carried by one pair of teeth but instead shows maximum stresses at the edges.

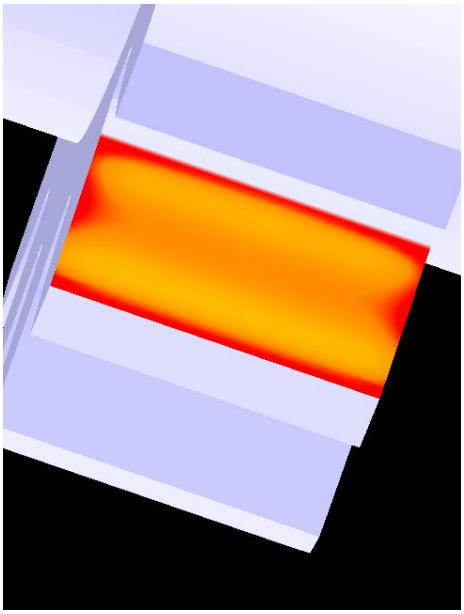

**Figure 30: Stress distribution over an unmodified tooth flank.**

A summary of the results that were obtained from the validation process is given in Table 17. The contact stress measured at the worst position according to Dudley (1994) was reported in the table instead of listing the maximum stresses which occur in the tip, root and edge sections of the tooth flank. This was done in order to enable the comparison between the gear programs.

**Table 17: Summary of the results which were obtained from the validation process**

| Type of Modification: | Method: | 250 Nm | 340 Nm | Unit: |
|---|---|---|---|---|
| *Lead and profile modification* | T3D | 1682 | 1912 | MPa |
| | LDP | 1692 | 1924 | MPa |
| | Leque (2011) | 1695 | 1921 | MPa |
| *Lead modification* | T3D | 1652 | 1878 | MPa |
| | LDP | 1687 | 1894 | MPa |
| *No modification* | T3D | 1944 | 2314 | MPa |
| | LDP | 1805 | 2115 | MPa |
| | AGMA standard | 1897 | 2212 | MPa |

### 4.1.1 Discussion

The gear programs showed similar values of the contact stresses if the severe edge stresses, seen in Transmission3D, were neglected. The largest difference was obtained for the case with an unmodified gear where the results from the ANSI/AGMA standard were located between the values obtained from the computational programs. A warning should, thus, be raised regarding the results which were obtained from the ANSI/AGMA standard since the equations which are used within the standard involve parameters which are decided by the designer and are typically estimated based on experience within the field of application (Budnas and Nisbett, 2008).

From the Validation process it could be seen that the option to include edge contact in Transmission3D had an impact on the compact stresses, especially at those located near sharp transitions in the geometry. It can be discussed whether these stresses are true or not. The most likely is that the results show fictitious values, due to bad FE mesh at the sharp geometrical transitions, but gives a realistic picture of the stress distribution. Sharp edges in the geometry will result in stress concentrations, since the large forces that are applied on infinitesimal areas will result in infinitely large stresses (Sundström, 2008).

A warning should be raised regarding the values on the contact stresses which were obtained from Transmission3D, since they had to be estimated manually by studying the post processing model. The real values might instead be located within a plus, or minus, five percent interval of the measured values. The decision to not repeat the simulations was based on the fact that similar cases were going to be simulated again in the following analysis.

## 4.2 Linear vs. Parabolic Profile Modification

The results which were used for testing which kind of profile modification that yielded the lowest contact stresses are presented within the following section. The results are presented in diagrams which show how the contact stress varies during the mesh cycle, i.e. the active period of a gear tooth.

The red curve, in the diagrams, shows the contact stress for a tooth entering the mesh cycle while the green curve shows the contact stress for a tooth that exits the mesh. A gear tooth experiences both conditions in reality and therefore can both curves be combined into one total curve that describes the gear's behavior during the entire mesh cycle.

The positions where both curves are not equal to zero indicate that more than one gear pair is active, i.e. carries the load. An example of two co-operating pairs can be seen in Figure 31.

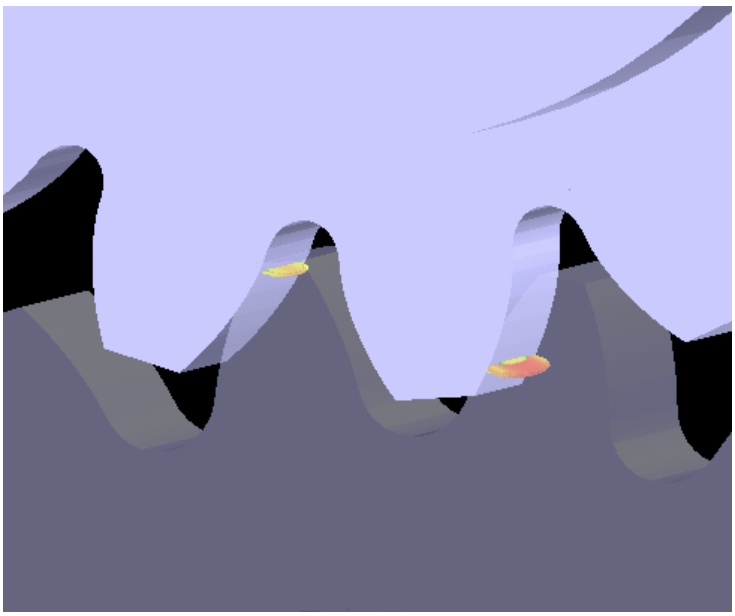

**Figure 31: Picture showing two active gear pairs.**

### 4.2.1 Simulations Including Edge Contact

The reason for performing simulations including edge contact was to include the stress pattern over the entire tooth flank, despite the risk of fictitious stresses at complex geometries. It was also important to investigate what influence the profile modification had on the fictitious stresses.

The simulation that did not included any profile modification resulted in a contact stress of 4007.7 MPa, which was the highest contact stress that was obtained from the simulations. A plot on how the contact stress varies with the mesh cycle time is shown in Figure 32.

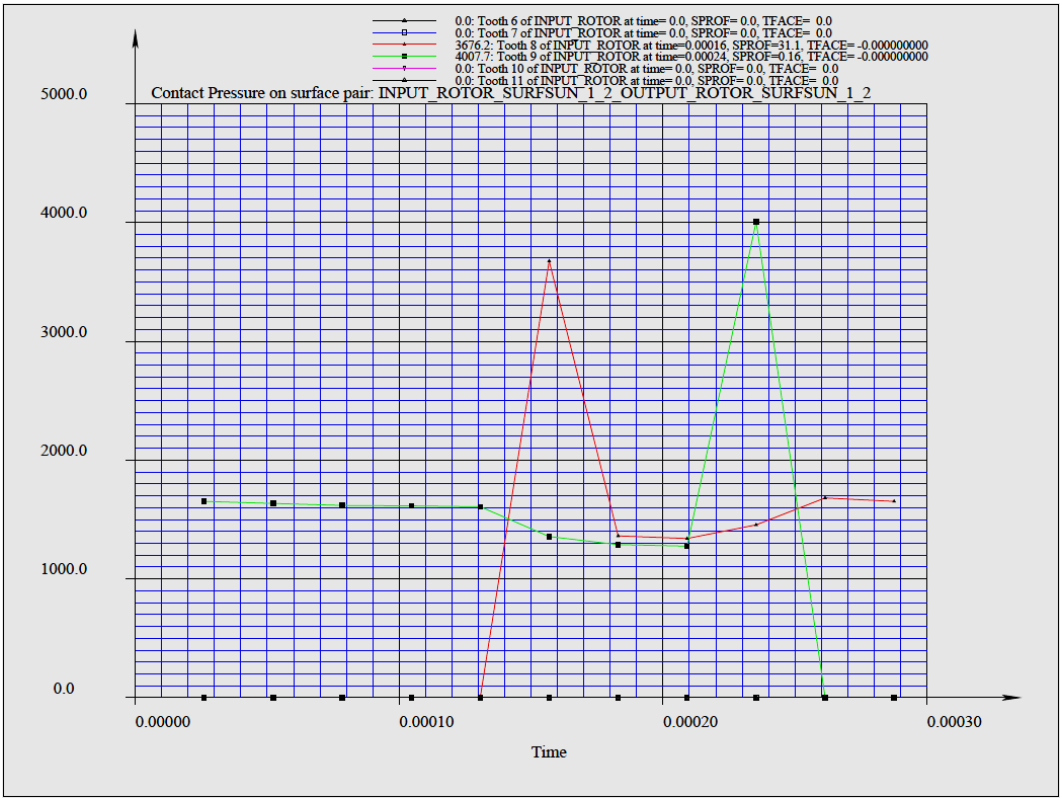


**Figure 32: Picture showing the contact stresses plotted versus time for gears without any profile modification.**

The contact stress was obtained as 1937.8 MPa for the case with linear profile modification. The plot over contact stress versus time is shown in Figure 33.

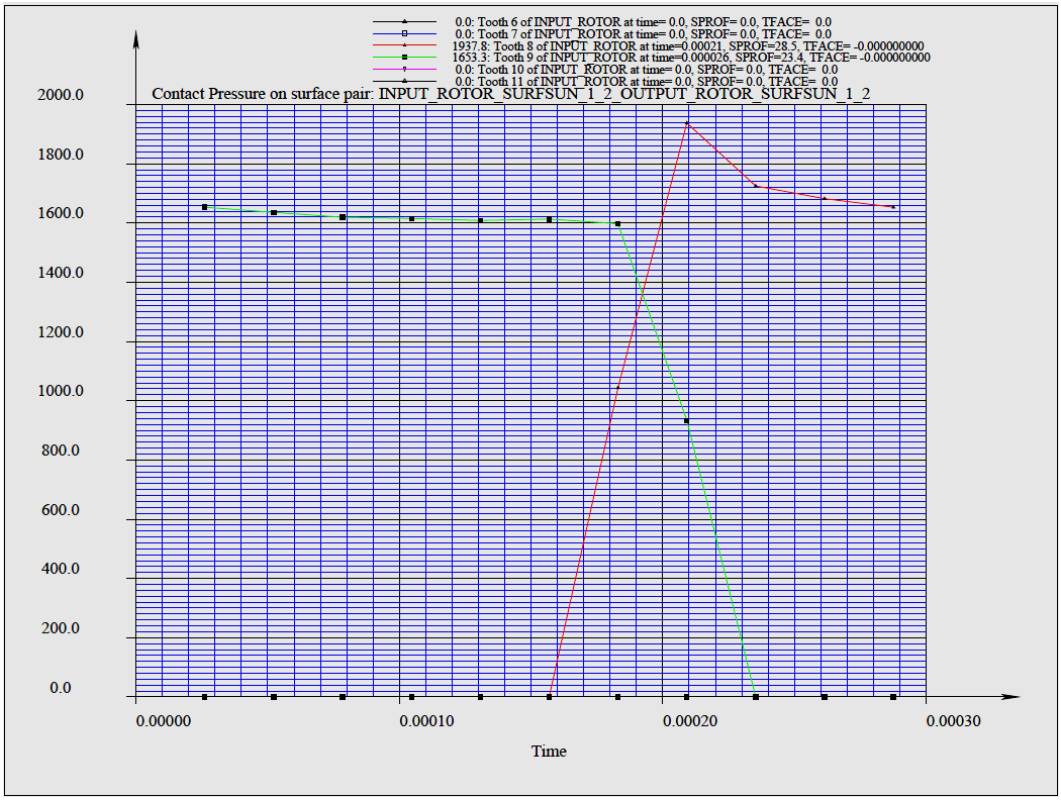


**Figure 33: Picture showing the contact stresses plotted versus time for gears with linear profile modification.**

The simulation with parabolic profile modification showed the lowest contact stress of 1731.5 MPa. The contact stress plotted against time is shown in Figure 34.

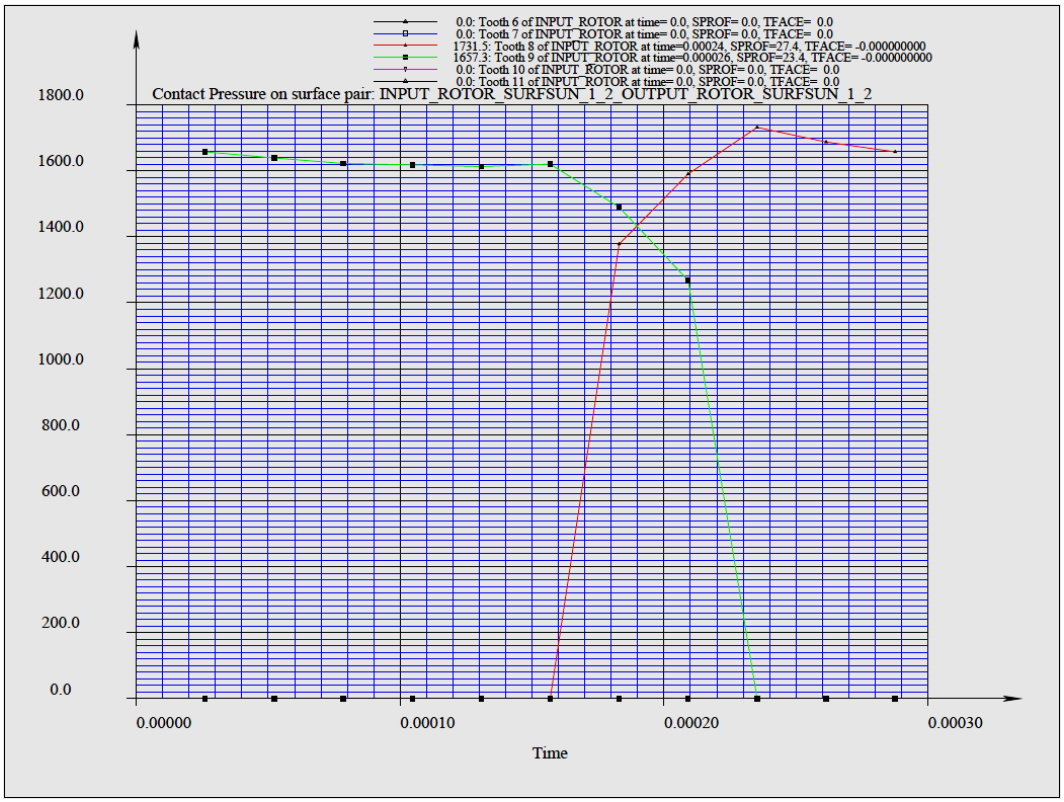


**Figure 34: Picture showing the contact stresses plotted versus time for gears with parabolic profile modification.**

### 4.2.2 Simulations Excluding Edge Contact

In the following section are the simulations which did not include any edge contact presented. The purpose of testing without any edge contact was to eliminate fictitious stresses that would had appeared at complex parts in the model's geometry, e.g. sharp corners and edges.

The case with no profile modification resulted in the lowest contact stress of 1723.7 MPa. A diagram that shows how the contact stress varies with the mesh time is shown in Figure 35.

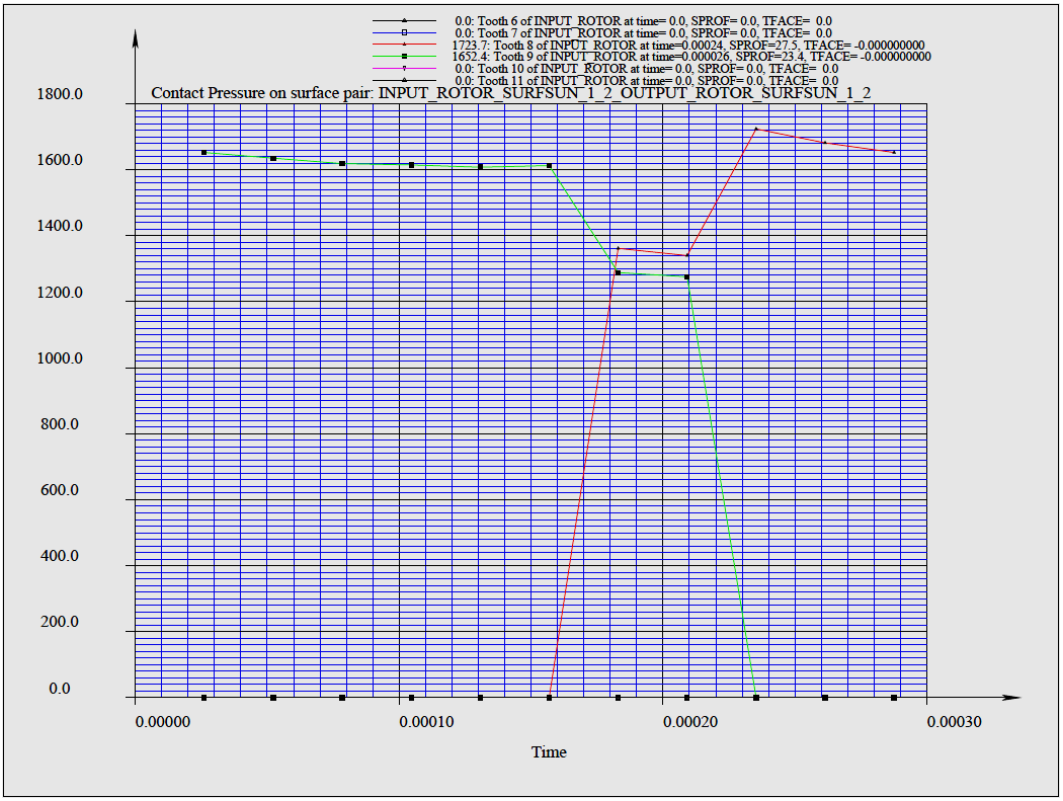


**Figure 35: Picture showing the contact stresses plotted versus time for gears which do not have any profile modification.**

The highest contact stress, in the simulations, was obtained for the gears which had linear profile modification. The value of the maximum contact stress was obtained as 1937.8 MPa, which can be seen in Figure 36.

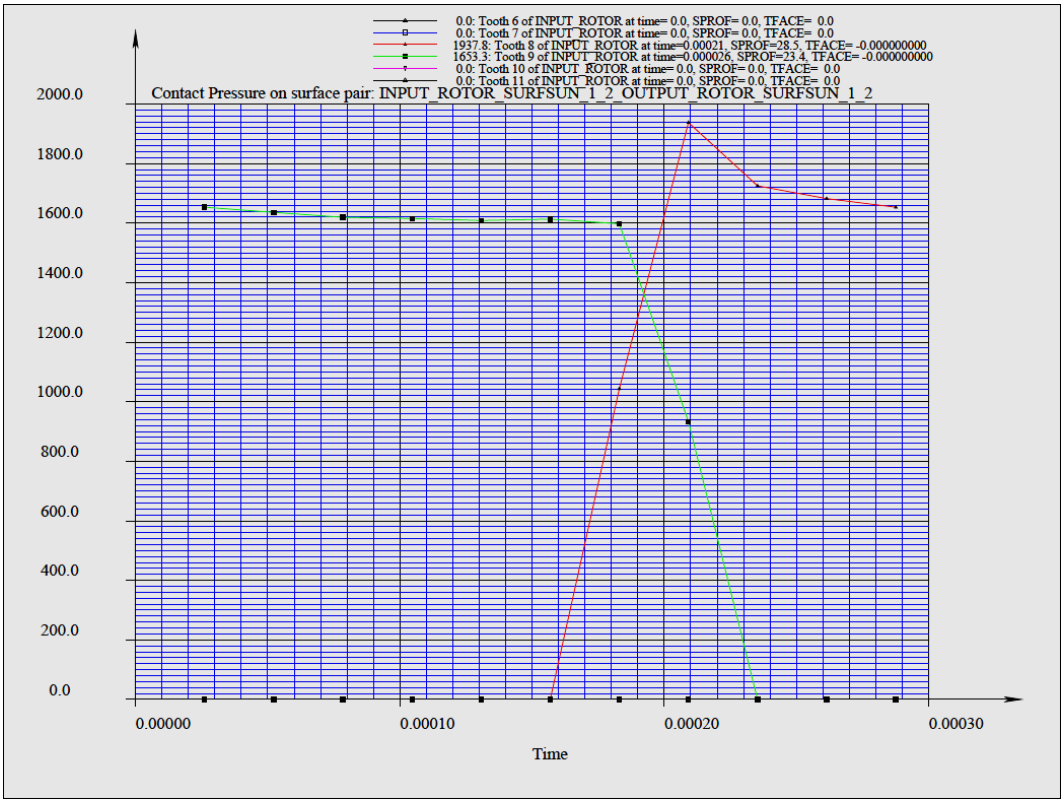


**Figure 36: Picture showing the contact stresses plotted versus time for gears with linear profile modification.**

The gears which had parabolic profile modifications showed a maximum contact stress of 1731.5 MPa. Figure 37 shows how the contact stress varies with time for gears with parabolic profile modification.

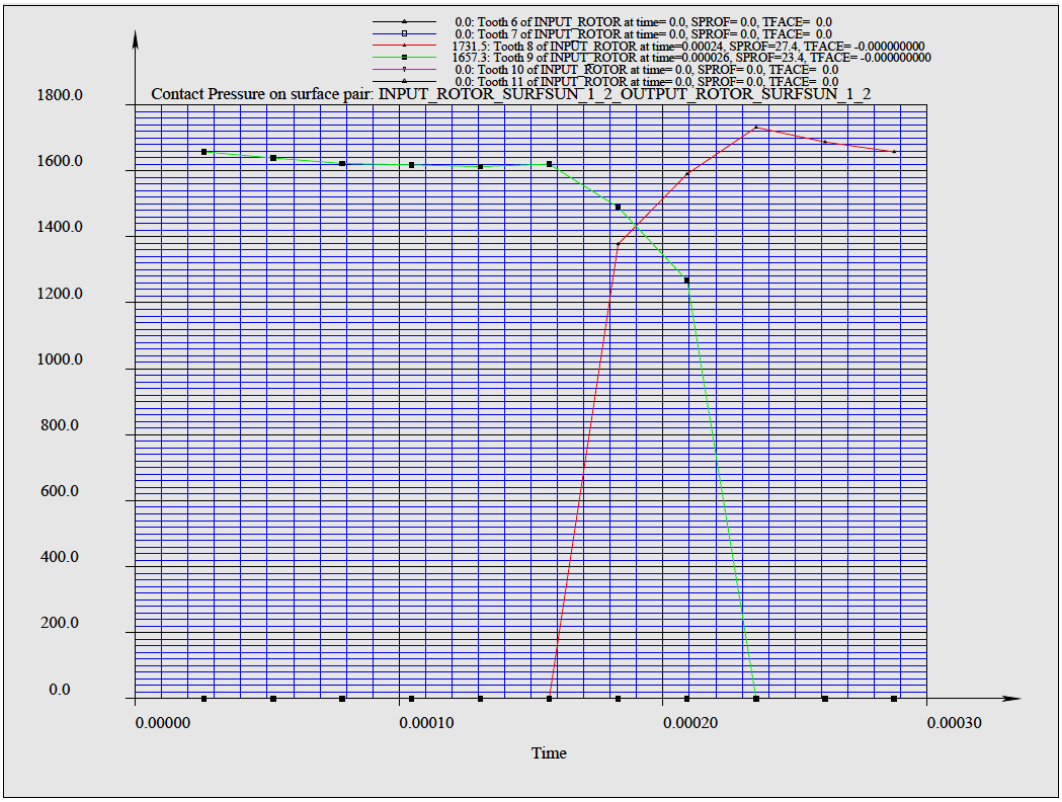


**Figure 37: Picture showing the contact stresses plotted versus time for gears with parabolic profile modification.**

Figure 38 is used to clearly illustrate the difference between the contact patterns which were obtained from the simulations. In the picture it can be seen that the simulation which included edge contact for an unmodified gear deviated from the general pattern. It can also be seen that the gear with linear profile modification show larger stresses.

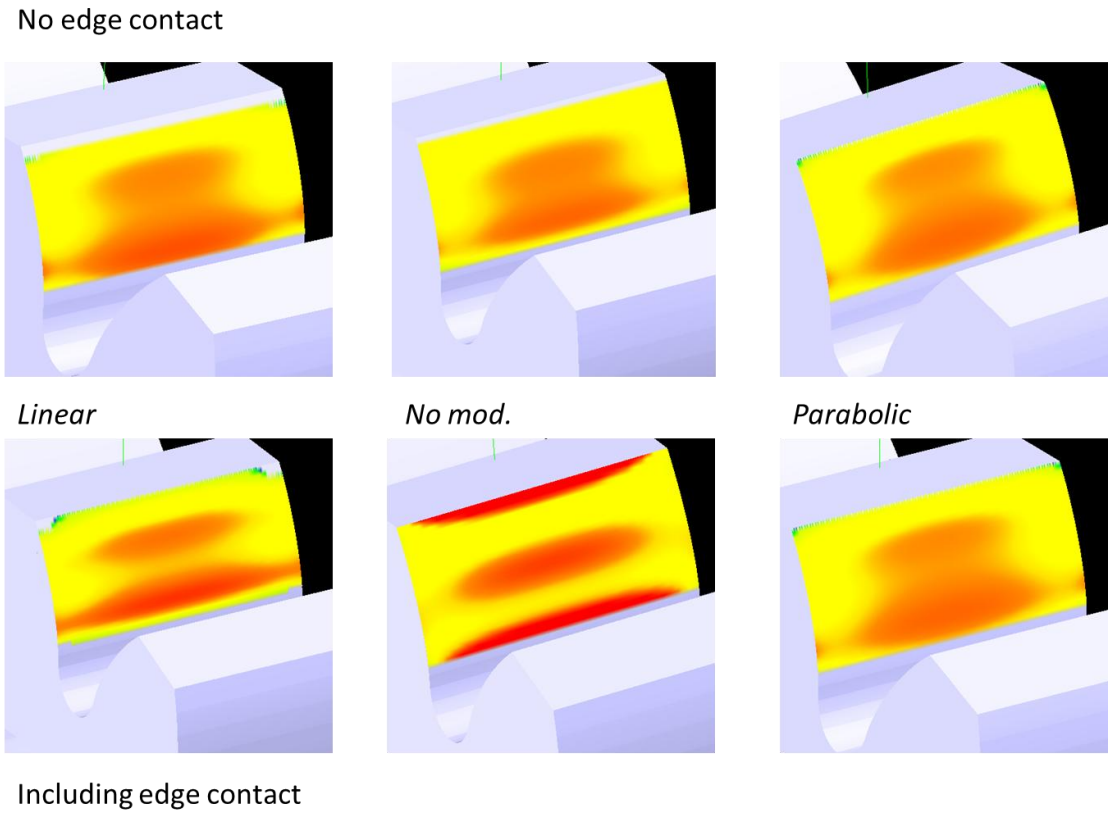


**Figure 38: Comparison of different contact patterns. Sharper red color indicates that the contact stresses are higher.**

### 4.2.3 Comparison with LDP

The results from the corresponding simulations performed in LDP are shown in Table 18 together with the maximum contact stresses from the simulations performed in Transmission3D. In the table it can be seen that the maximum contact stress obtained from LDP does not vary for the different types of profile modification, i.e. no, linear or parabolic modification.

**Table 18: Table that shows the results obtained from LDP and Transmission3D**

| Type of Profile Modification: | LDP (No edge contact) | Transmission3D (No edge contact) | Transmission3D (Including Edge Contact) |
|---|---|---|---|
| *None* | 1692 MPa | 1723.7 MPa | 4007.7 MPa |
| *Linear* | 1692 MPa | 1937.8 MPa | 1937.8 MPa |
| *Parabolic* | 1692 MPa | 1731.5 MPa | 1731.5 MPa |

If the contact patterns obtained from the different simulations made in LDP instead are compared it can be shown that profile modification has an impact on the contact stresses, but the difference between linear and parabolic profile modification is not as significant as it is in Transmission3D. The Figures 39 to 41 show the contact patterns, which were obtained from the simulations with no edge contact, for the different profile modifications.

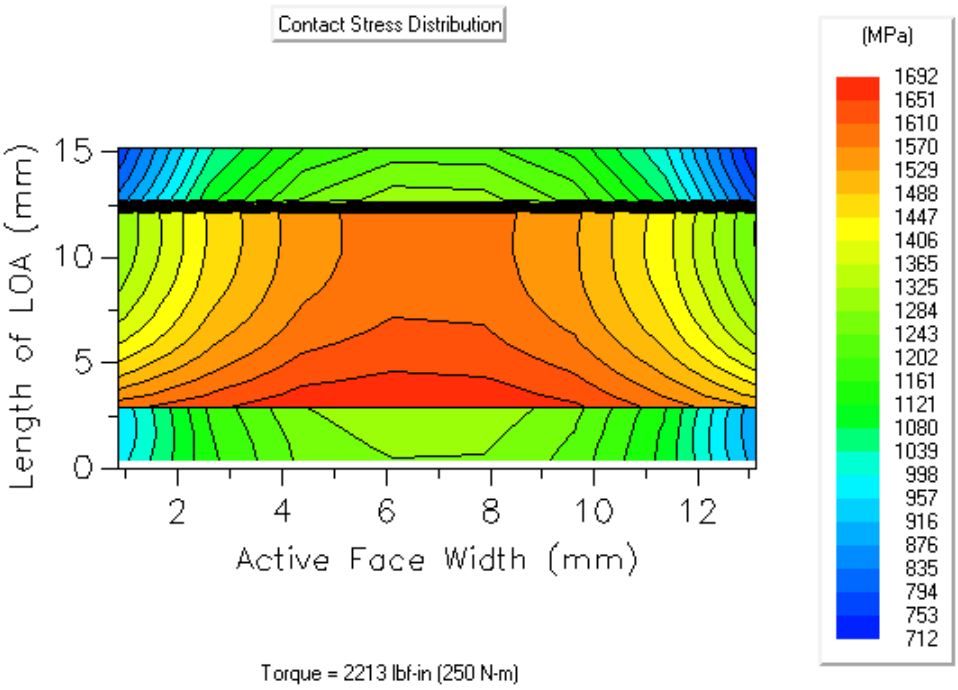


**Figure 39: Contact pattern obtained from LDP for a gear without profile modification.**

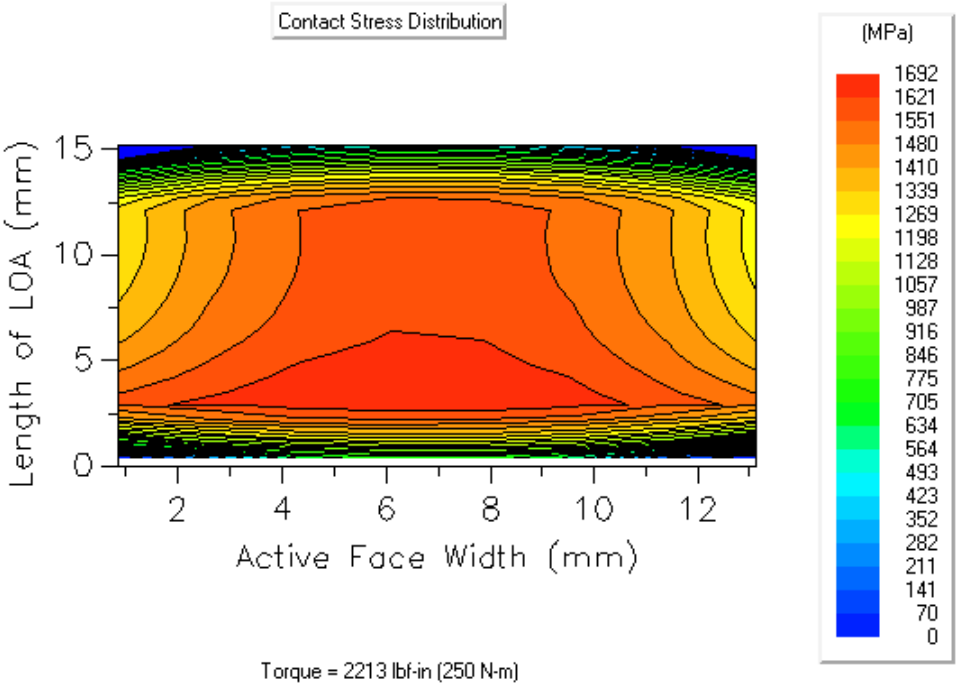


**Figure 40: Contact pattern obtained from LDP for a gear with linear profile modification.**

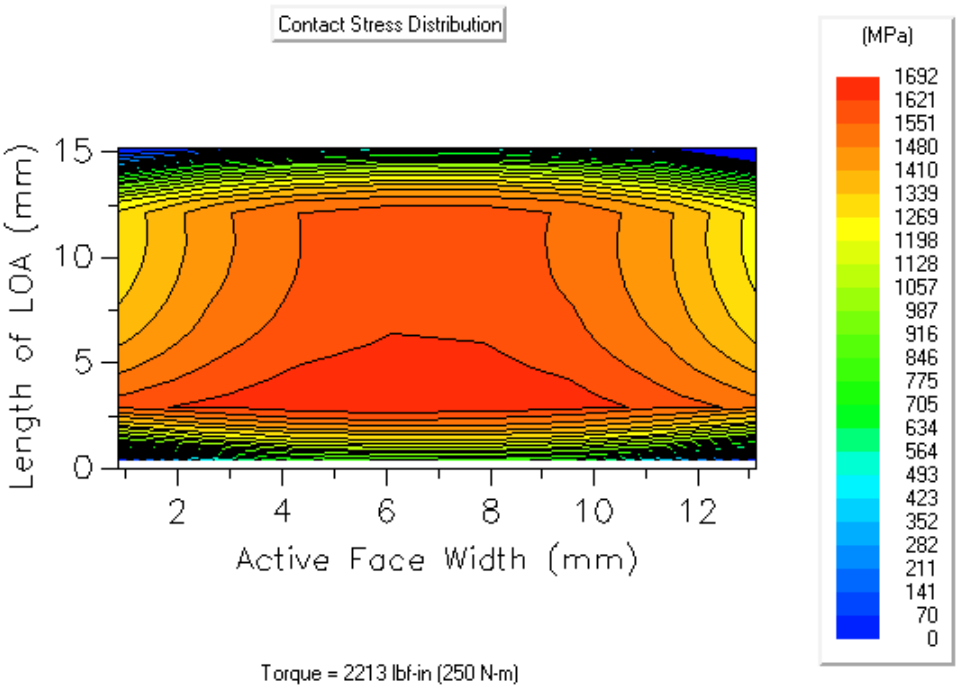


**Figure 41: Contact pattern obtained from LDP for a gear with parabolic profile modification.**

### 4.2.4 Discussion

From the simulations it can be seen that edge contact only has an influence on the gears which did not have any profile modification. The gears which included a profile modification, i.e. linear or parabolic, were not affected by the selection of including edge contact or not.

The maximum contact stress was obtained at the same location for all the simulations except from the simulation with edge contact that was performed for an unmodified profile. The maximum contact stress, in this case, was obtained at the position where the tooth exits the gear mesh, i.e. at the tip of the gear tooth. This is not in compliance with the literature which says that the maximum contact stress in a gear pair should be located at the lowest position of a driving wheel tooth where the one pair of teeth carries the entire load (Dudley, 1994). Neither do the results from LDP indicate that the maximum contact stress would occur at any other place than the location indicated by the other simulations.

An interesting discovery was that LDP did not shift value of the maximum contact stress for none of the different types of reliefs. The only change that was noticed in the simulations was the increase in the contact stresses which were located in the tip and root sections when it shifted from an unmodified to a modified tooth profile. One reason for why any change of the different profiles was not noticed is probably due to the choice of neglecting edge contact in the analysis. If edge contact had been included in the simulations would a difference between the linear and parabolic shape probably been seen, but since LDP only was used as a reference for the Transmission3D simulations it was considered to be excessive to perform more simulations in LDP.

## 4.3 Investigation of the Impact from Lead Modification

This section shows the results from the simulations which were used in order to investigate the impact from lead modification. The results are reported in tables which

show the maximum contact stresses for the simulations. Pictures that illustrate the contact pattern for each simulation are also shown in addition to the tables that include the maximum contact stresses.

### 4.3.1 Gears without Lead Modification

The maximum contact stresses which were obtained from the simulations for the gears that did not had any modification are reported in Table 19. From the table it can be seen that when only tangential rotation is applied to a gear pair is the contact stress increased compared to the case when only radial rotation is used. Another discovery was that when the tangential and the radial rotations are applied with the same direction increases the maximum contact stress compared to the case when only one of the rotations has been applied. It was also noticed during the simulations that the maximum contact stress decreased when the rotations had different signs.

**Table 19: Maximum contact stresses for the simulations without lead modification**

| **Simulation:** | **Tangential rotation [mrad]:**<br>**Radial rotation [mrad]:** | **Maximum contact stress [MPa]:** |
|---|---|---|
| *1* | 0 | 1733.3 |
| | 0 | |
| *2* | 1.0 | 1967.3 |
| | 0 | |
| *3* | -1.0 | 1968.2 |
| | 0 | |
| *4* | 0 | 1837.4 |
| | 1.0 | |
| *5* | 0 | 1837.2 |
| | -1.0 | |
| *6* | 1.0 | 2061.3 |
| | 1.0 | |
| *7* | -1.0 | 2062.6 |
| | -1.0 | |
| *8* | -1.0 | 1869.8 |
| | 1.0 | |
| *9* | 1.0 | 1869.5 |
| | -1.0 | |

Contact patterns were used to visually display how the stress distribution was affected by the misalignments. The contact patterns for the different simulations are shown in Figure 42 to 46. The stresses which are shown in the figures are reported in MPa.

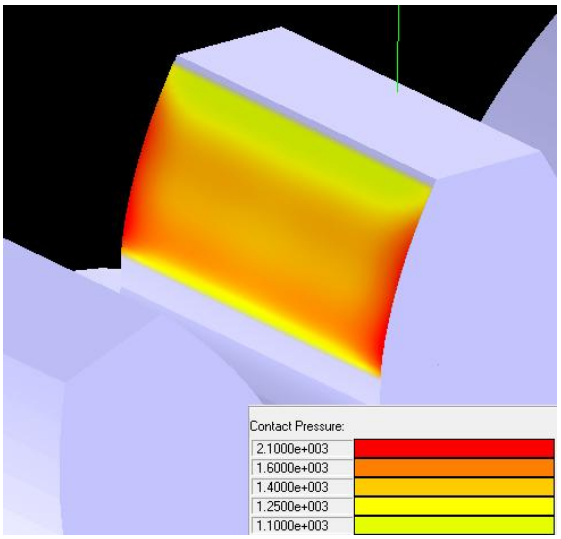


**Figure 42: Contact pattern for an unmodified gear with (tan., rad.) = (0, 0) mrad misalignment.**

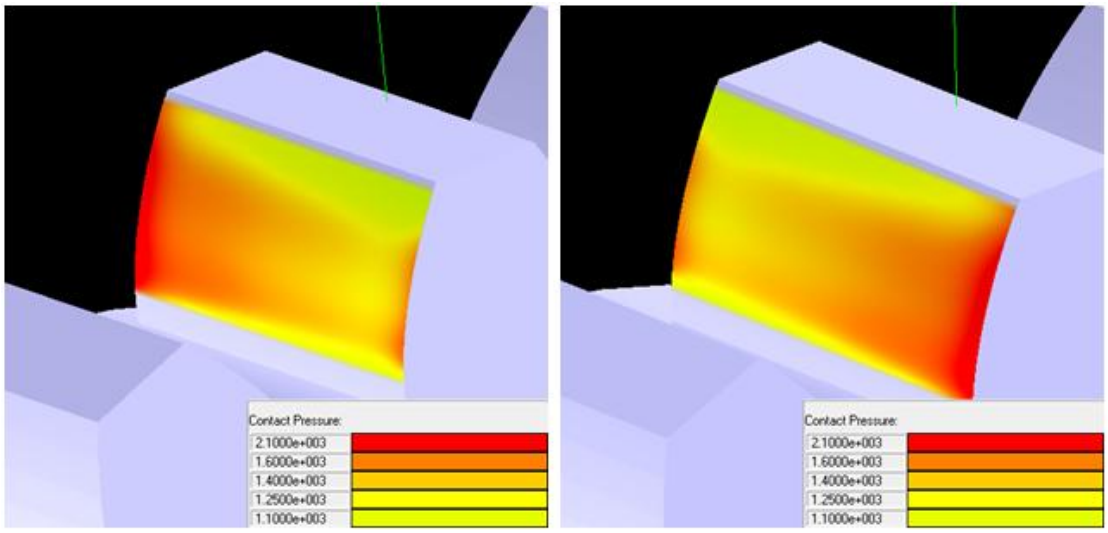


**Figure 43: Contact patterns for unmodified gears with (tan., rad.) = (1.0, 0) and (tan., rad.) = (-1.0, 0) mrad misalignments.**

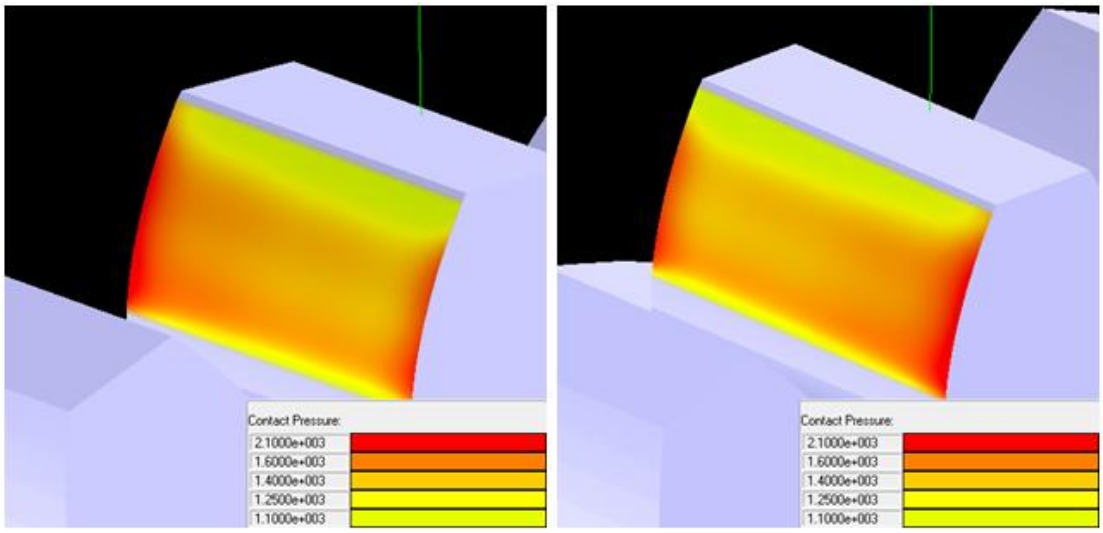


**Figure 44: Contact patterns for unmodified gears with (tan., rad.) = (0, 1.0) and (tan., rad.) = (0, -1.0) mrad misalignments.**

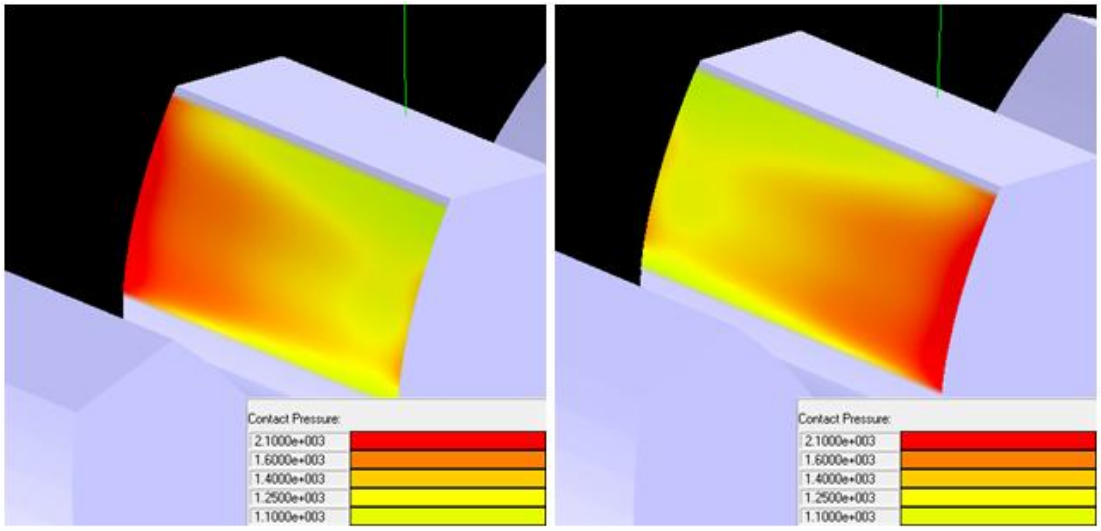


**Figure 45: Contact patterns for unmodified gears with (tan., rad.) = (1.0, 1.0) and (tan., rad.) = (-1.0, -1.0) mrad misalignments.**

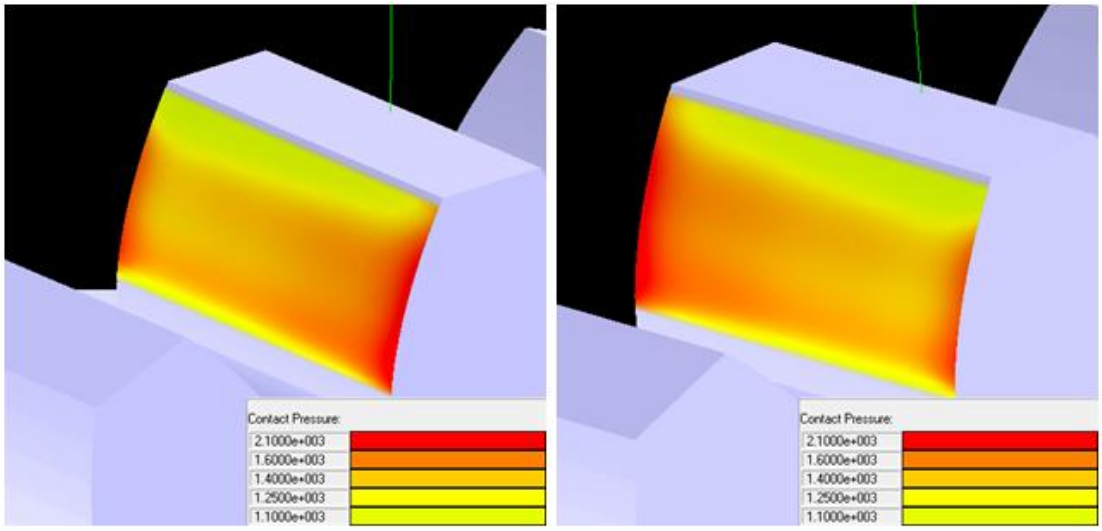


**Figure 46: Contact patterns for unmodified gears with (tan., rad.) = (-1.0, 1.0) and (tan., rad.) = (1.0, -1.0) mrad misalignments.**

### 4.3.2 Gears with Lead Modification

Simulations which were similar to the ones carried out for the gears with no modification were performed on lead modified gears in order to investigate how the lead modification affects the contact stresses. The maximum contact stresses which were obtained from the simulations are shown in Table 20.

**Table 20: Maximum contact stresses for the gears with lead modification**

| Simulation: | Tangential rotation [mrad]: / Radial rotation [mrad]: | Maximum contact stress [MPa]: |
|---|---|---|
| *1* | 0 / 0 | 1741.8 |
| *2* | 1.0 / 0 | 1782.5 |
| *3* | -1.0 / 0 | 1782.6 |
| *4* | 0 / 1.0 | 1747.3 |
| *5* | 0 / -1.0 | 1747.3 |
| *6* | 1.0 / 1.0 | 1851.7 |
| *7* | -1.0 / -1.0 | 1851.7 |
| *8* | -1.0 / 1.0 | 1753.9 |
| *9* | 1.0 / -1.0 | 1753.9 |

Contact patterns were also shown for the lead modified gears in order to visually display the results. The contact patterns for the different misalignments are shown in Figure 47 to 51. The contact stresses which are shown in the pictures are reported in MPa.

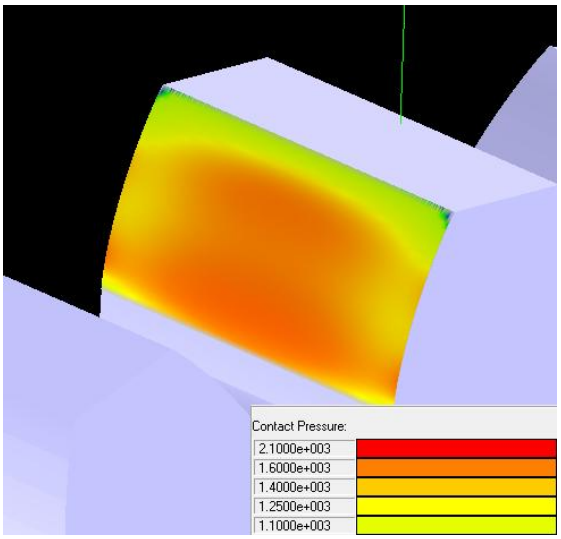


**Figure 47: Contact pattern for a lead modified gear with (tan., rad.) = (0, 0) mrad misalignment.**

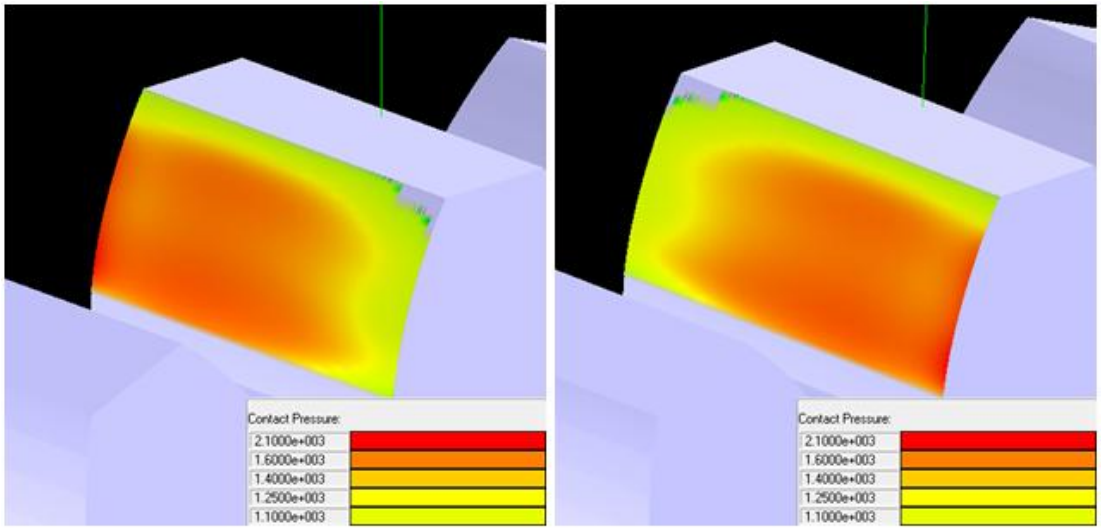


**Figure 48:Contact patterns for lead modified gears with (tan., rad.) = (1.0 , 0) and (tan., rad.) = (-1.0 , 0) mrad misalignments.**

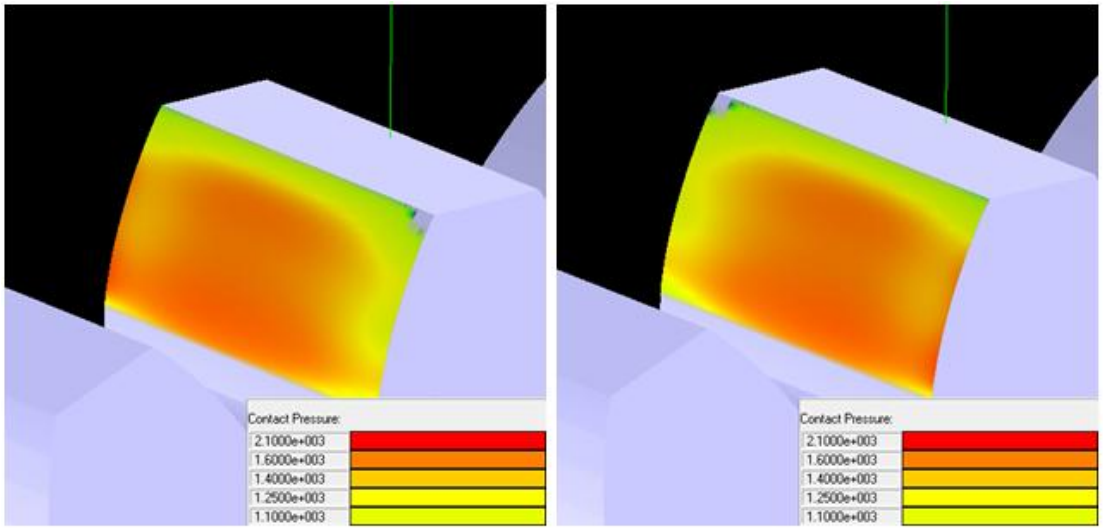


**Figure 49: Contact patterns for lead modified gears with (tan., rad.) = (0 , 1.0) and (tan., rad.) = (0, -1.0) mrad misalignments.**

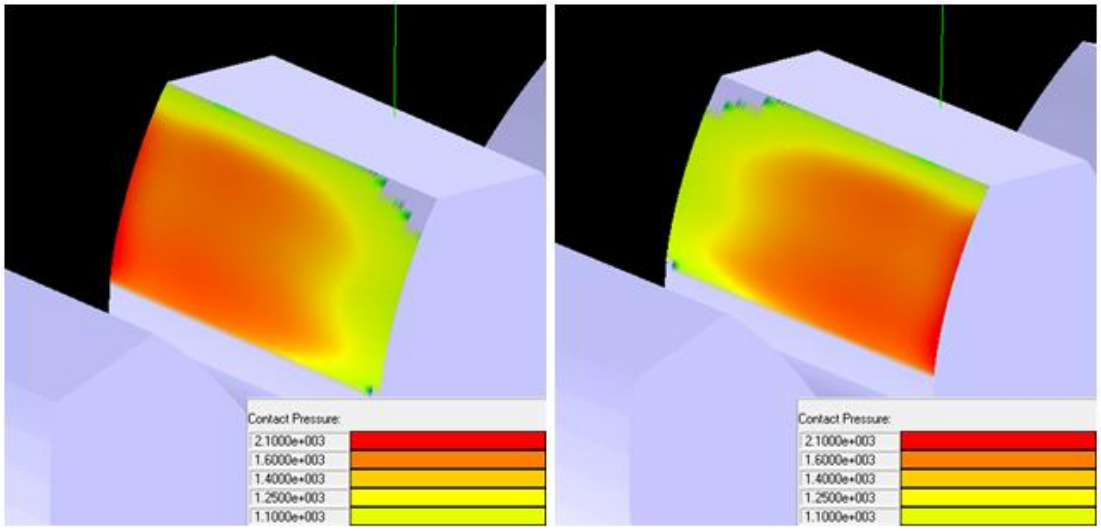


**Figure 50: Contact patterns for lead modified gears with (tan., rad.) = (1.0, 1.0) and (tan., rad.) = (-1.0, -1.0) mrad misalignments.**

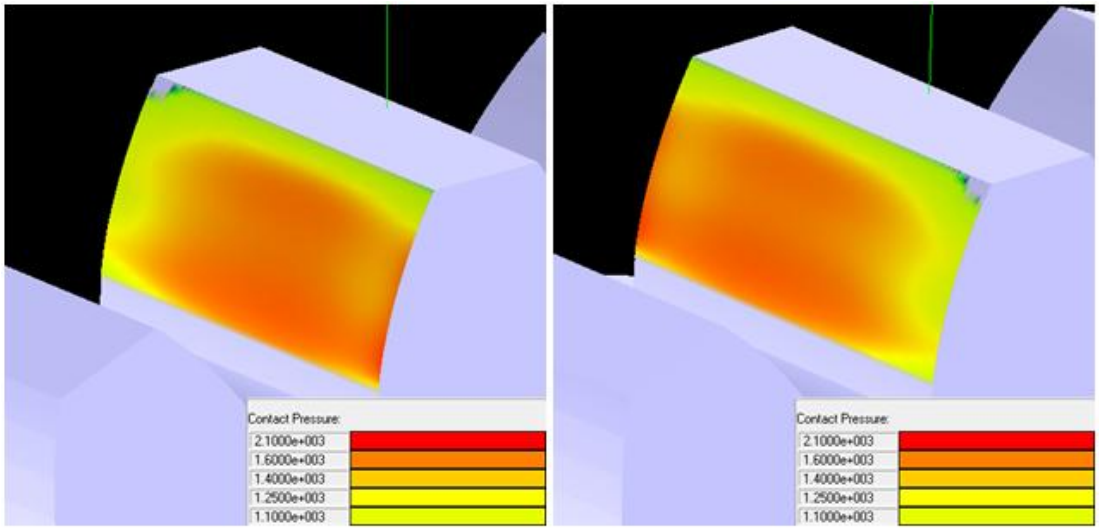


**Figure 51: Contact patterns for lead modified gears with (tan., rad.) = (-1.0, 1.0) and (tan., rad.) = (1.0, -1.0) mrad misalignments.**

### 4.3.3 Comparison of the Results

By comparing the results which were obtained from the simulations performed for an unmodified gear with the results for the lead modified gear, it was noticed that the lead modification reduced the maximum contact stress by approximately 210 MPa. Figure 52 is used in order to illustrate the differences between the unmodified and lead modified teeth. In the picture, it can be seen that the load is distributed over a larger area for the lead modified gears.

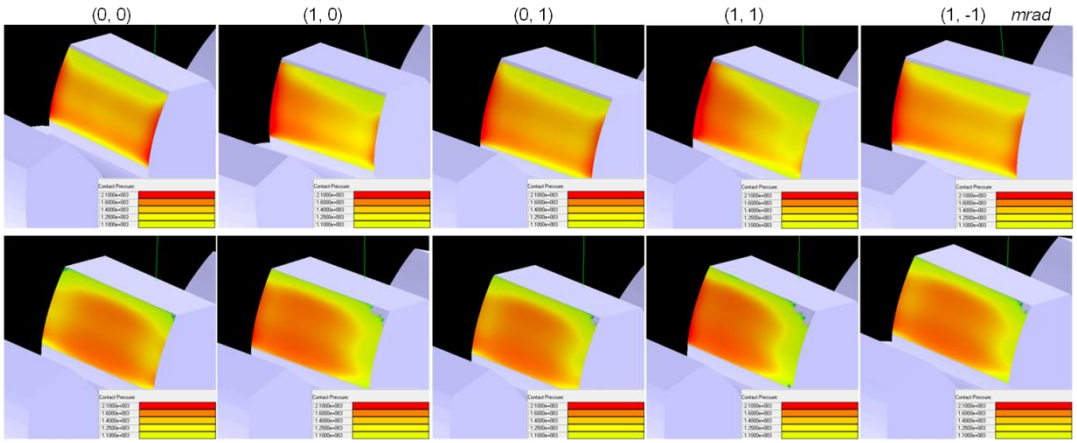


**Figure 52: Comparison of the unmodified gear with the lead modified gear.**

### 4.3.4 Discussion

From the simulations it can be seen that the gear's ability to withstand the impact from axial misalignments is improved by performing a lead modification. This is in compliance with the theoretical findings from the literature study that were obtained from Houser, Harianto and Talbot (2006) and Dudley (1994).

The only case which shows that an unmodified gear would give lower contact stresses is when there exist no misalignments of the gears. The probability of having such conditions in reality is very low due to the likelihood of errors in manufacturing and assembly.

The contact stresses would probably have been reduced even further if the lead modification also had been sloped such that the load was applied orthogonally to the

active tooth flank. The load would then have been distributed over a larger area which implies that the contact stresses would decrease. The reason for why a sloped lead modification was not made in the study was due to the fact that every misalignment would had required a specific slope, and the investigation of which misalignment that gave rise to the worst contact stresses would not had been possible to perform.

It was also seen in the simulations, for both the unmodified and modified gears, that the contact stresses increased for misalignments with similar signs of the rotations and decreased for different signs of the rotations. This implies that the rotations collaborate and creates more severe misalignments in some cases while in other cases they take out each other and give rise to less harmful misalignments.

## 4.4 Presentation of the Contact Program

A final version of the computer program was made after the simulations that investigated the impact from lead and profile modification had been completed. A brief description of the gear program and its output is given within the following section.

### 4.4.1 The GUI

The computer program starts in a menu where general information about the gear pair is defined. This information considers loading conditions, i.e. speed and torque, if an idler stage should be included in the gear set, if the gears are subjected to any axial misalignments and if edge contact is included in the simulation. The work directory is also specified from the start menu. From the start menu it is possible to either read gear data from a dat-file or to manually define gear data. A picture of the start menu is shown in Figure 53.

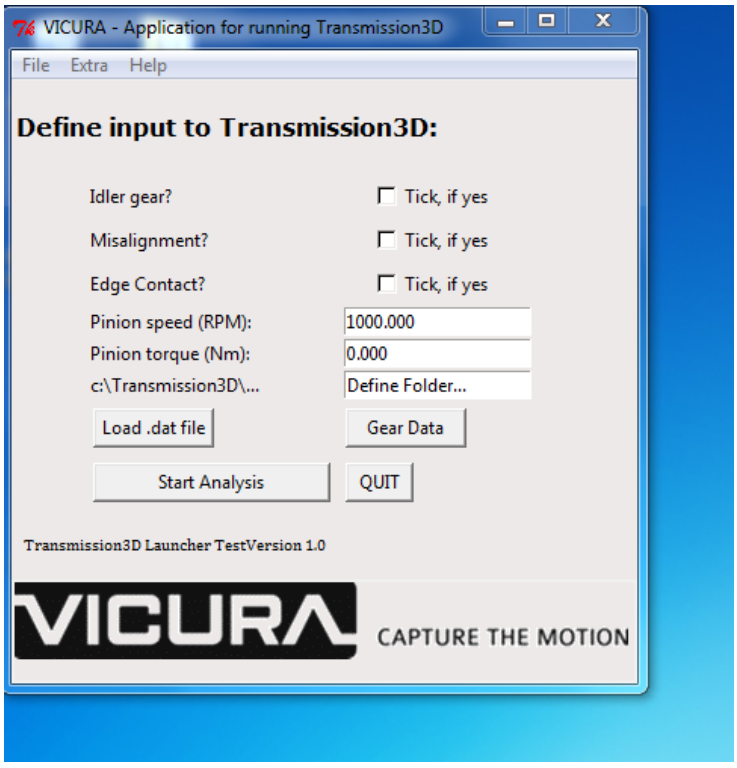


**Figure 53: Picture of the computer program's start menu.**

The computer program offers the possibility to manually define the geometries of the driving wheel and the gear. This is achieved by entering the menu for specifying the

gear data. It is also possible to obtain an initial estimation, according to the ANSI/AGMA 2101-D04 standard, of the contact stresses from this menu. The gear parameters which Transmission3D requires in order to create a FE model were shown in the method chapter and were described in the theory section. An example picture of the menu which is used for defining the gear geometry is shown in Figure 54.

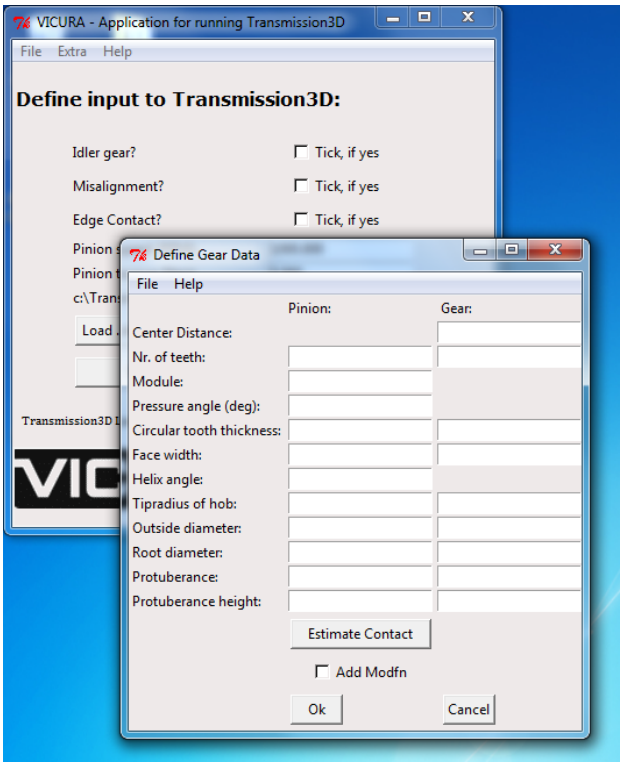


**Figure 54: Picture of the menu that is used for defining the gear geometry.**

After the general gear data has been defined, either by reading input from an external file or by defining the input manually, it is possible to define the micro geometry of the gear tooth. The modification of the micro geometry is defined within its own menu where the geometrical shape of the tooth flank is defined. The modification can then be previewed before it is sent to Transmission3D. An example of a lead modification, i.e. a symmetric crown, is shown in Figure 55.

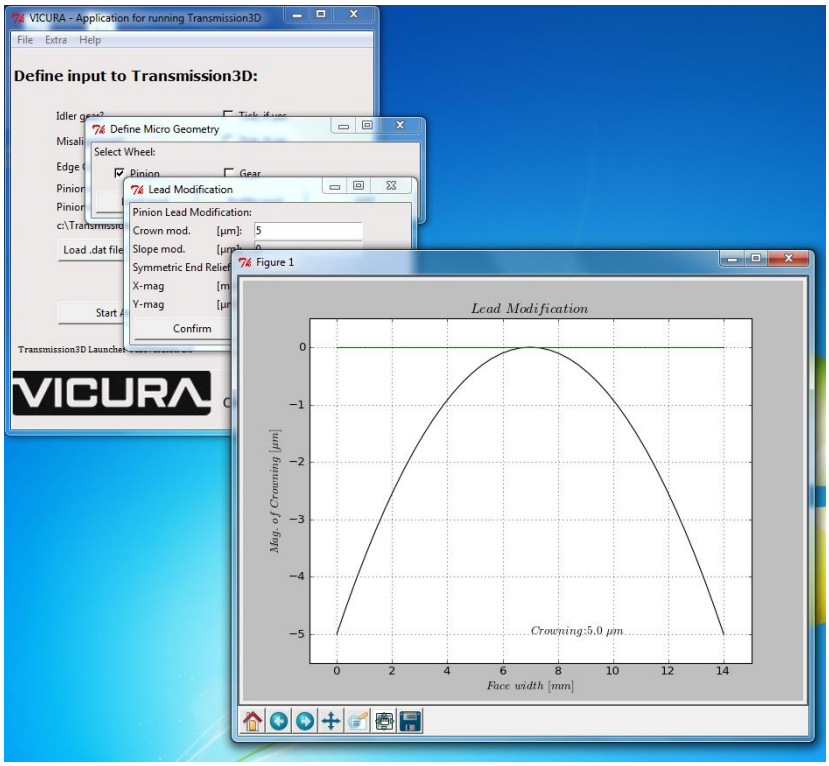


**Figure 55: Picture showing a plot that has been obtained from the lead modification menu**

The possibility to run several simulations for different misalignments is given in the multiple misalignments menu where several misalignments may be defined for different torque levels. A picture showing the menu that is used for defining the misalignments is shown in Figure 56.

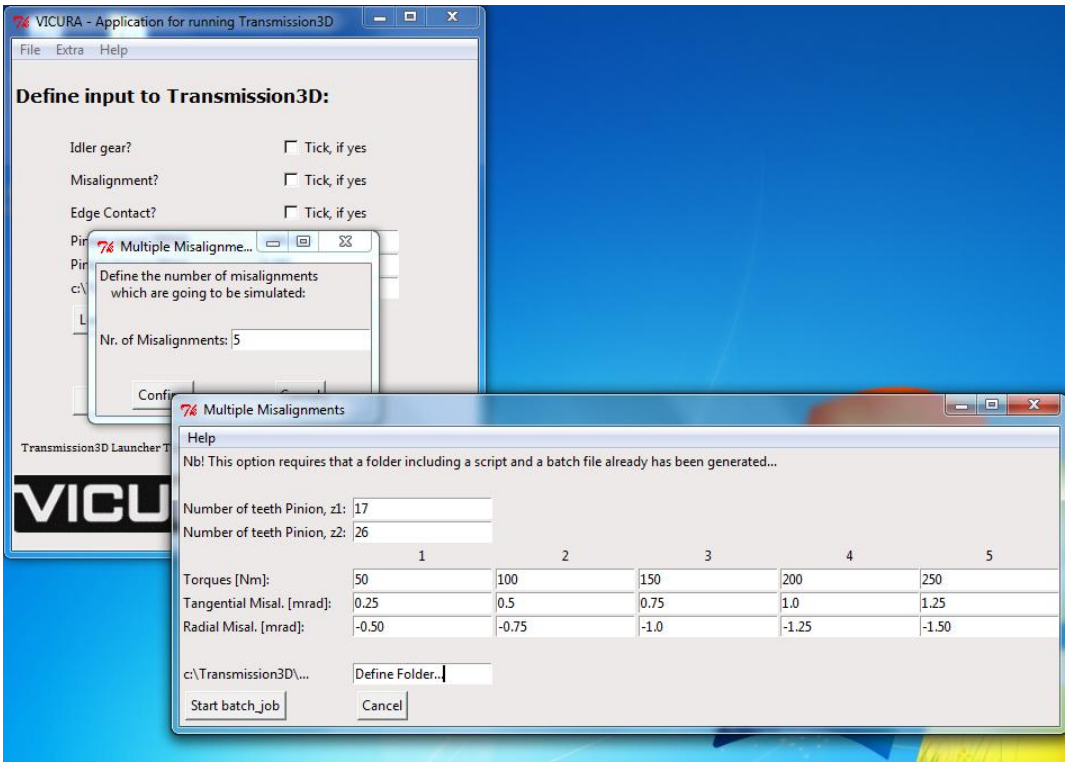


**Figure 56: Picture showing the multiple misalignments menu.**

### 4.4.2 Output from the Contact Program

Transmission3D includes options to output post processing results in various formats, e.g. diagrams and 3d models with stress distributions, in order to visually display the results from the simulations. These options were added to the developed tool which specifies what kind of results that should be saved and where the results are to be stored.

A test simulation was performed in order to display the output from the tool after the final version had been created. The model that was simulated was the model obtained from League (2011), which had been used within the previous simulations.

Transmission3D offers the possibility to generate plots of the maximum contact stresses versus time and the contact stresses across the active face width. These two options were used by the computer program and examples of the diagrams are given in Figure 57, where the contact stresses versus the face width is shown to the left and the contact stresses versus the mesh time is shown to the right.

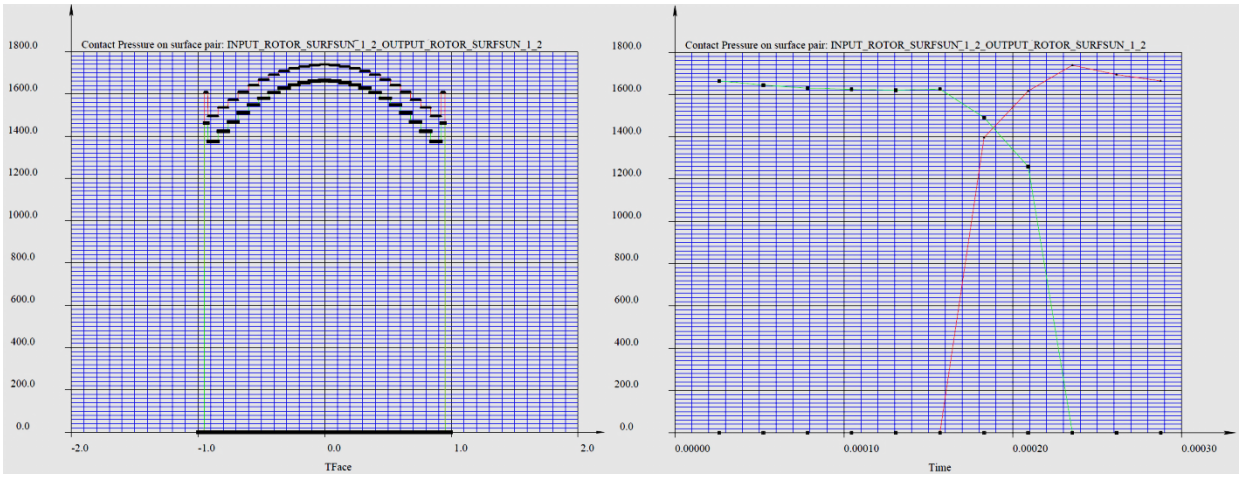


**Figure 57: Examples of diagrams which show the maximum contact stresses. The first picture shows a plot on contact stresses over the face width, whilst the other shows how the contact stress varies with time.**

Another attribute that was given as output from the tool was the contact stress pattern over the tooth face. An example of the contact pattern, which was obtained from the gear program, is shown in Figure 58.

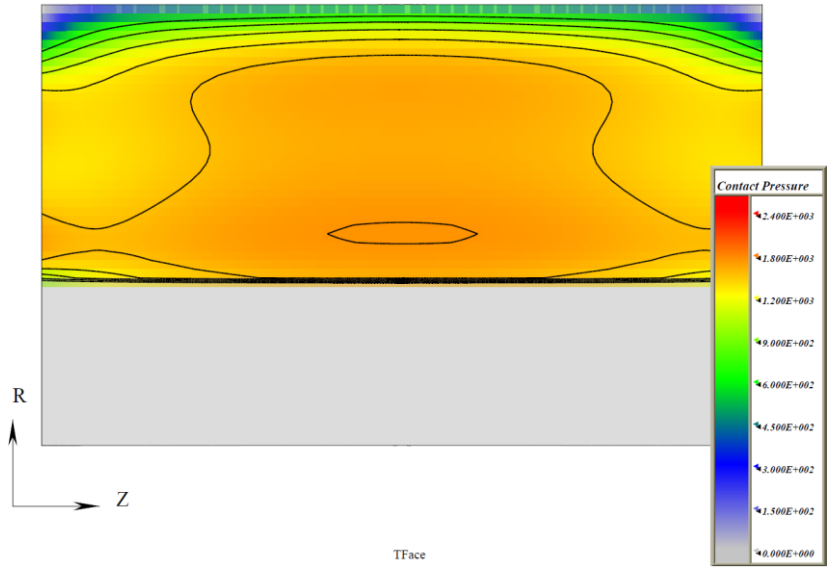


**Figure 58: Example of contact pattern, over a gear tooth, obtained from the gear program.**

The last result that was given by the tool was a diagram showing the subsurface shear stress. The reason for adding this diagram into the output results was due to a fact that was presented in the literature study which stated that pitting fatigue may result from plastic deformation under the tooth face. (Glaeser and Shaffer, 1996). Figure 59 shows an example of a diagram that displays the subsurface shear stresses.

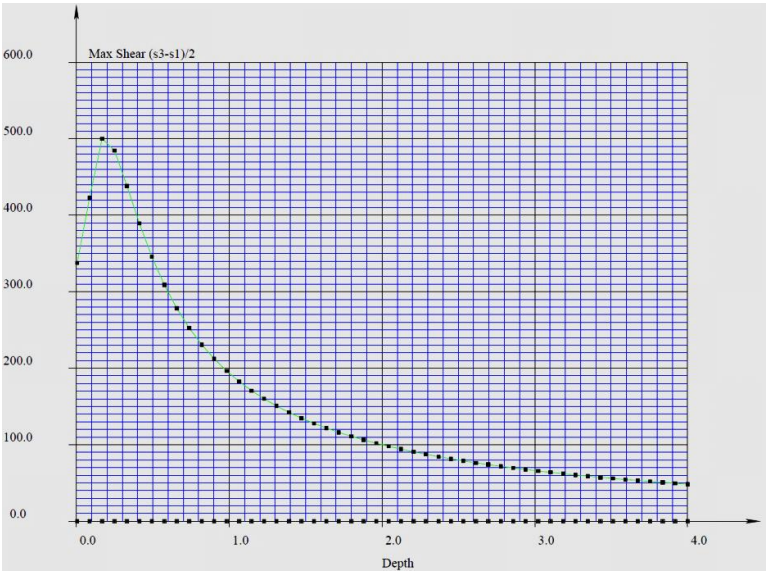


**Figure 59: Diagram showing the subsurface shear stresses. Pitting fatigue may start if this stress is larger than the yield strength of the material.**

A file including a 3d model and post processing results was generated in addition to the results which were reported as diagrams and contact patterns in the PDF file. The 3d model could then be opened within its own GUI, i.e. Iglass, where the model could be analyzed. Examples of the post processing file's interface and contact stresses are shown in Figure 60.

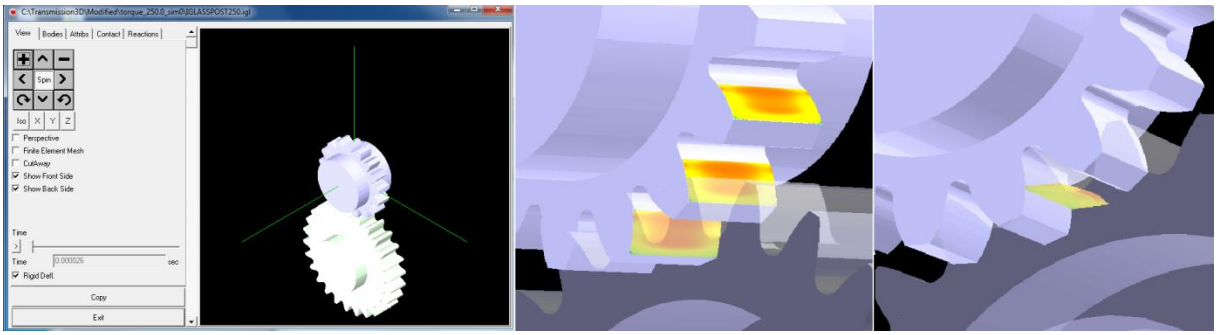

**Figure 60: Post processing made in the Iglass interface. The first picture shows the post processor's interface, the second shows the contact stress distribution on a tooth flank and the third picture shows the stress distribution along LOA.**

### 4.4.3 Discussion

What can be noticed from the presentation of the tool that has been developed is that the tool's focus has been directed at analyzing the characteristics of pitting fatigue, while other gear failures such as scuffing and abrasion are given less attention. This choice of focus was consciously made due to the delimitations which were done in the beginning of the project and the FE software's limitations.

An aspect which speaks for not putting the focus on abrasion was due to the fact that abrasion is initiated by impurities in the gear lubricant which might have been added from internal or external processes (Davies, 2005). If the impurities have been added

from an internal process it might be likely that the impurities are caused by material loss caused by another contact failure, e.g. pitting fatigue or scuffing. Of that reason it may be wise to investigate the primary source of the failure, which in this case might be pitting or scuffing, instead of investigating the secondary source.

The decision to not include scuffing in the computer program was mostly due to the limitations in the FE software, i.e. the used FE software did not include any options to analyze the lubricant properties or temperature. Scuffing may, on the other hand, be prevented by lowering the contact stresses and reducing high sliding velocities (Davis, 2005) and these properties can be analyzed with help of the FE software.

Another reason for why a scuffing function was not added to the tool was due to the fact that LDP, the program that was used in the validation process, includes options for analyzing the lubricant properties, e.g. film thickness and temperature distribution. Based on that aspect, it might be more suitable to link LDP to the tool in the future instead developing own functions for estimating the lubricant properties.

# 5. Conclusion

The outline for the thesis was to acquire knowledge in contact mechanics and then generate a computer based application that could be used for analyzing contact mechanics in gears. This concluding section will summarize the findings which have been made during the study and give recommendations for future work.

## 5.1 Summary

This section summarizes the different topics that have been covered by the study. Each topic is treated separately in order to summarize the most vital findings from every part of the work.

### 5.1.1 Literature Study

From the literature study it was shown that contact failures may originate from different sources. Scuffing, pitting, abrasion and case crushing are all examples of failures that are linked to contact mechanics. During the literature study it was noticed that there is a lack of a shared terminology in mechanical standards, i.e. European standards tend to use one definition for different failures while American standards uses another.

The literature study also showed that there exist well developed theoretical methods for analyzing pitting fatigue. The one that was used in this study was the ANSI/AGMA 2101-D04 standard but similar methodologies that can be used for contact stress analysis are given by ISO and DIN. The main parameter that is studied in the standard is the surface stress which is then compared with an S-N diagram to decide whether the gear will suffer any damage or not. Another parameter that is not given as much attention, but still is equally important, is the subsurface shear stress since this parameter decides whether a plastic deformation will take place beneath the tooth surface and thus initiate pitting.

The contact phenomena known as scuffing is harder to estimate since it can take place at any occasion, compared to pitting which appears after a certain number of life cycles. Scuffing is highly dependent of the lubricant properties, e.g. minimum film thickness and flash temperature, which make it more of a tribological question than a mechanical question. On the other hand, findings from the literature study also show that mechanical factors such as surface stresses, friction and sliding velocities affect scuffing which indicate that mechanical parameters can be optimized in order to prevent scuffing.

Two different test procedures which are used for analyzing contact failures were described in the theory section, i.e. RCF testing and FZG testing. The former one is used as a screening process in order to find a possible gear material with good pitting properties, while the latter one is used for evaluating the properties of the lubricant.

### 5.1.2 Analysis

The initial validation was made in order to compare the outcome from the FE software, i.e. Transmission3D, which were to be used in the computer program with another computational program, i.e. LDP, in order to check the validity of the results. The validation gave an indication of consistency between the programs, but also showed that the model that was used in Transmission3D had to be improved since the results from Transmission3D showed severe stresses at positions which were not

expected according to the theory, e.g. in corners and at sharp edges, or noticed in LDP. The occurrence of severe stresses in Transmission3D was thought to be associated with the fact that Transmission3D is an FE based program, which implies that there is a risk of severe stresses at positions that are hard to mesh.

Based on the findings from the initial validation arose a need of further testing. The first test was performed in order to investigate how much the type of profile modification, i.e. linear or parabolic, affects the contact stresses. From the simulations it was shown that LDP did not show any difference between the two types, while Transmission3D showed a large difference between linear and parabolic modifications. Based on the findings it was concluded that a parabolic shape of the root and tip reliefs is the optimal design since it gave lower contact stresses and of that reason it was decided to only use parabolic reliefs in the following simulations.

The second test was performed in order to investigate how the impact from axial misalignments could be reduced by adding a lead crown to the tooth flank. Axial misalignments are known to create even worse contact conditions, e.g. shifting the load towards the edges of the tooth face, and of that reason it is important to prevent the impact from misalignments. From the simulations, it was noticed that the lead crown reduced the contact stresses significantly. The only case which showed larger contact stresses for a gear tooth with lead crown than for an unmodified tooth was the case without misalignments, which in reality is unlikely due to errors from manufacturing and assembly. It was also noticed from the simulations that some misalignments, i.e. the ones with equal signs of the radial and tangential rotations, gave more severe contact stresses than the misalignments which were defined by rotations with opposite signs.

### 5.1.3 The Contact Program

The purpose of making a computer program was to simplify the interaction between the mechanical designer and the computational software. This task has been achieved by making a GUI that requires that the user defines the parameters which define the gear pair and the loading conditions, in turn reducing the complexity of running a contact analysis compared to running the analysis directly from the FE program's interface. The FE program’s interface requires the user to manually define all the connections between the different parts which define the gear, e.g. shafts and rims, and FE related parameters such as mesh attributes and material data. These tasks have been automated in the gear program which implies that the user only needs to have knowledge in gear design.

The computer program enables complex geometries of the gear’s teeth, e.g. lead and profile modifications, but the rest of the model, e.g. shafts and rim, have standardized shapes. The gear model has to be generated from the FE program’s own interface if complex structures of the shafts and rims are demanded. The computer program should thus only be used for analysis where complex shapes of the gear’s shaft and rim are not required, and for cases which involve more complex geometries follows a recommendation of using the FE program’s interface when a model shall be generated.

## 5.2 Overall Conclusion

The study has shown what failures that may be expected due to bad contact performance of a gear pair. The procedures which are available for analyzing contact

mechanics in gears, including both theoretical and practical methods, have also been described.

During the analytical work it has been proved that the computational procedure used in the FE program, Transmission 3D, is valid for making an analysis of contact mechanics in gears. Another finding that has been discovered is that the analytical methods which have been used in the study, in general, show similar results, but due to the natures of the used analytical methods there will be a variation in the absolute values.

The micro geometry of the gear tooth has been proven to have an impact on the contact stresses. For tip and root reliefs it was shown that parabolic reliefs gave lower contact stresses on the tooth surfaces compared to linear reliefs. It was also shown that lead crowning reduced the severe contact stresses caused by axial misalignments.

Finally, a computer based application for analyzing contact mechanics in gears has been developed and also been proven to work for gear models that do not require any complex shaft or rim geometry. The advantage of using this application is the reduction of pre- and post-processing time, while the drawback is the absence of functions for varying the geometries of the gear's shaft and rim.

## 5.3 Future Recommendations

A future recommendation would be to add other analytical procedures, e.g. tooth bending calculations and lubricant analysis, to the computer program in order to create an application that can be used for general gear analysis instead of only focusing the application on contact mechanics. The different analytical procedures could then use the same model as input which in its turn would decrease the total pre-processing time. The risk of ambiguous input to the different methods would also decrease since the same model would be used as input to all methods.

Another recommendation would be to add functions such that more complex geometries could be represented by the model. This could be done in combination with a study that investigates the influence that varying shaft and rim geometries have on the contact durability.

Finally, there is a need for physical testing in order to validate the outcome from the computational procedure with realistic data. A suitable candidate for such testing would be to perform an FZG test where the load pattern is studied and the contact stresses can be calculated from the measured load stages. The same analysis could then be performed with the computer program in order to investigate how well the computational analysis reflects the actual conditions.

Physical testing could also be made in order to obtain material data on different gear materials such that S-N curves for different gear materials could be stored in a future material library that is included in the computer program. A motivation for testing different gear materials was described in the literature study, where it was shown that the selection of material had an impact on the contact durability. RCF may be used for this kind of testing, since it can be used for evaluating the pitting performance of different gear materials and at the same time is cheaper than more detailed gear tests since it uses cylindrical disks instead of real gears.

# List of References


American Gear Manufacturers Association (1995). *ANSI/AGMA 1010-E95 Appearance of Gear Teeth – Terminology of Wear and Failure*. Alexandria VA: AGMA

American Gear Manufacturers Association (1999). *AGMA 908-B89 Geometry Factors for Determining the Pitting Resistance and Bending Strength of Spur, Helical and Herringbone Gear Teeth*. Alexandria VA: AGMA

American Gear Manufacturers Association (2003). *AGMA 925-A03 Effect of Lubrication on Gear Surface Distress.* Alexandria VA: AGMA

American Gear Manufacturers Association (2004). *ANSI/AGMA 2101-D04 Fundamental Rating Factors and Calculation Methods for Involute Spur and Helical Gear Teeth*. Alexandria VA: AGMA

Ansol (2003). *Transmission3D User's Manual*. Hillard OH: Advanced Numerical Solutions

Budynas, R. & Nisbett, K. (2008). *Shigley's Mechanical Engineering Design*. New York: McGraw-Hill

Bergseth, E. (2012). *On tribological design in gear contacts*. Stockholm: Royal Institute of Technology

Childs, P. (2004). *Mechanical Design*. Oxford: Elsevier Butterworth-Heinemann

Coy, J., Townsend, D. & Zaretsky, E. (1985). *Gearing*. Cleveland OH: NASA Lewis Research Center (NASA Reference Publication, 1152)

Davis, J. (2005). *Gear Materials, Properties and Manufacture.* Materials Park OH: ASM International

Dudley, D. W. (1994). *Handbook of Practical Gear Design*. Lancaster: Technomic Publishing Company

Frazer, R.C., Shaw, B.A., Palmer, D. & Fish, M. (2010). Optimizing Gear Geometry for Minimum Transmission Error, Mesh Friction Losses and Scuffing Risk Through Computer-Aided Engineering. *Gear Technology*, August 2010. Available: www.geartechnology.com [2013-05-20]

Glaeser, W.A. & Shaffer, S.J. (1996). Contact Fatigue. *ASM Handbook, Volume 19: Fatigue and Fracture*. Available: http://www.asminternational.org/content/ASM/StoreFiles/06197G_Sample.pdf [2013-03-07]

Gopinath, K. & Mayuram, M.M. (2013) *Machine Design II. Module 2- Gears. Lecture 8 – Spur Gear Design*. Madras: Department of Mechanical Engineering, IIT Madras. Available: http://nptel.iitm.ac.in/courses/IIT-MADRAS/Machine_Design_II/ [2013-02-20]

Gurumani, R. & Shanmugam, S. (2011). *Modeling and Contact Analysis of Crowned Spur Gear Teeth*. Tiruchirappalli: Department of Mechanical Engineering, National Institute of Technology

Harianto, J. & Houser, D. (2002). *Load Distribution Program*. Columbus OH: The Ohio State University

Houser, D., Harianto, J. & Talbot, D. (2006). Gear Mesh Misalignment. *Gear Solutions*, June 2006. Available: gearsolutionsonline.com [2013-04-25]

International Organization for Standardization (2000). *ISO 14635-1 Gears – FZG test procedures – Part 1: FZG test method A/8,3/90 for relative scuffing load-carrying capacity of oils*. 1st. Ed. Genève: ISO

International Organization for Standardization (2009). *ISO 10825 Gears – Wear and damage to gear teeth – Terminology*. 1st. Ed. Genève: ISO

Intertek (2013). *FZG Gear Testing*. Available: http://www.intertek.com/automotive/atf/fzg/ [2013-05-07]

Kahraman, A., Houser, D. & Xu, H. (2005). *Development of a Generalized Mechanical Efficiency Prediction Methodology for Gear Pairs*. Columbus OH: The Ohio State University

Karlebo Handbok. Utgåva 14. (1992). *Maskinelement. Kuggväxlar*. Stockholm: Liber AB

Lawcock, R. (2006). *Rolling Contact Fatigue of Surface Densified Gears*. Ontario: Stackpole Ltd

Leque, N. (2011). *Development of an Experimental Methodology for Evaluation of Gear Contact Fatigue under High-Power and High-Temperature Conditions*. Columbus OH: The Ohio State University. Available: OhioLink ETD Center [2013-04-05]

Liu, G.R. & Quek, S.S. (2003). *The Finite Element Method A Practical Course*. Oxford: Butterworth-Heinemann

Lundh, F. (1999). An introduction to Tkinter. Available: http://www.pythonware.com/library/tkinter/introduction/ [2013-04-16]

Mägi, M. & Melkersson, K. (2009). *Lärobok i Maskinelement*. Göteborg: EcoDev International

Ognjanovic, M. (2004). *Progressive Gear Teeth Wear and Failure Probability Modeling*. Tribology in industry, Volume 26, No 3&4, 2004. Available: http://www.tribology.fink.rs/journals/2004/3-4/7.pdf [2013-05-02]

Python (2013). *About*. Available: http://www.python.org/about/ [2013-01-23]

Råde, L. & Westergren, B. (2004). *Mathematics Handbook for Science and Engineering*. Lund: Studenlitteratur

Shigley, J., Mischke, C. & Browne, T. (2004). *Standard Handbook of Machine Design*. New York: McGraw-Hill

Shipley, E. (1967). *Gear Failures*. Cleveland OH: XTEC Inc.

Siemens (2013). *CAE / Computer-Aided Engineering*. Available: http://www.plm.automation.siemens.com/en_us/plm/cae.shtml [2013-05-08]

Special Steel Co. (2011). *Data Table for: Carbon Steel: SAE 4118RH*. Available: http://www.steelss.com/Carbon-steel/sae-4118rh.html [2013-04-05]

Sundström, B. (ed.). (2008). *Handbok och Formelsamling i Hållfasthetslära*. Stockholm: E-Print AB

Townsend, D. & Zaretsky, E. (1982). *Effect of Shot Peening on Surface Fatigue Life of Carburized and Hardened AISI 9310 Spur Gears*. Cleveland OH: NASA Lewis Research Center (NASA Technical Paper, 2047)

Townsend, D., Chevalier, J. & Zaretsky, E. (1973). *Pitting Fatigue Characteristics of AISI M-50 and Super Nitralloy Spur Gears*. Cleveland OH: NASA Lewis Research Center and U.S. Army Air Mobility R&D Laboratory (NASA Technical Note, D-7261)

The University of Utah. (2006). *Contact Stresses and Deformations*. ME EN 7960 – Precision Machine Design Topic 7. Salt Lake City UT: Department of Mechanical Engineering, The University of Utah. Available: http://www.mech.utah.edu/~me7960/lectures/Topic7-ContactStressesAndDeformations.pdf [2013-05-03]

Ulrich, K. & Eppinger, S. (2012). *Product Design and Development.* New York: McGraw Hill

Vicura AB (2013). *Overview*. Available: http://www.vicura.se/en/about-vicura/vicura-overview [2013-01-23]

# Appendix A: Contact Stress Calculations according to AGMA

This appendix describes the procedure of calculating the contact stresses in external spur and helical gears according to the ANSI/AGMA 2101-D04 standard (AGMA, 2004). The described procedure differs from the standard in that sense that the equations for the helical gear only considers helical gears of conventional type. The expression for calculating the contact stresses is given by eq 1 and nomenclature for the included parameters are shown in Table 1.

$$\sigma_H = Z_E \sqrt{F_t K_0 K_V K_S \frac{K_H}{d_{W1} b} \frac{Z_R}{Z_I}} \quad (1)$$

**Table 21: Presentation of the parameters which are included contact stress equation**

| **Parameter:** | **Description:** |
|---|---|
| $Z_E$ | Elastic coefficient, see eq 2 |
| $F_t$ | Tangential transmitted load [N] uniformly distributed along the face width, see eq 5 |
| $K_0$ | Overload factor |
| $K_v$ | Dynamic factor, see 6 |
| $K_s$ | Size factor |
| $K_H$ | Load distribution factor, see eq 10 |
| $d_{W1}$ | Operating pitch diameter of the driving wheel, see eq 4 |
| $b$ | Face width of the narrower member in the gear pair |
| $Z_R$ | Surface condition factor |
| $Z_I$ | Geometry factor for pitting resistance, see eq 20 |

The elastic coefficient is given by eq 2 and includes the material properties of the gear, i.e. Young's modulus of elasticity and Poisson's coefficient. If the same material is used for both gears then the expression can be simplified to eq 3.

$$Z_E = \sqrt{\frac{1}{\pi \left[\left(\frac{1-\nu_1^2}{E_1}\right) + \left(\frac{1-\nu_2^2}{E_2}\right)\right]}} \quad (2)$$

$$Z_E = \sqrt{\frac{1}{2\pi \left(\frac{1-\nu^2}{E}\right)}} \quad (3)$$

The operating pitch diameter is obtained by eq 4. The expression includes the shaft distance, a, and the speed ratio, u.

$$d_{W1} = \frac{2a}{u+1} \quad (4)$$

The tangential transmitted load is given by the expression shown in eq 5. The torque *T* that is used in the equation is the torque of the driving wheel (AGMA, 2004).

$$F_t = \frac{2000T}{d_{W1}} \quad (5)$$

According to the AGMA standard it is stated that a value on the $K_0$ factor can only be determined if sufficient experience has been acquired within the field of application (AGMA, 2004). Budynas and Nisbett (2008) show example values that ranges from 1 to 2.25 depending on the load stage of the application, e.g. from uniform load to heavy shock. Childs (2004) gives examples of similar values and presents numbers which are ranging from 1 to 2.75 depending on load stage.

The dynamic factor is given by eq 6 and is determined by the parameters C and B, which are given by eq 7 and 8 respectively, and the pitch line velocity at the operating pitch diameter, $v_t$, which can be seen in eq 9.

$$K_V = \left(\frac{C}{C + \sqrt{196.875 v_t}}\right)^{-B} \quad (6)$$

$$C = 50 + 56(1 - B) \; for \;\; 6 \leq A_V \leq 12 \quad (7)$$

The factor $A_V$ which occurs in eq 8 is known as the transmission accuracy number. This number is used in order to define the quality of the gears. Higher transmission accuracy numbers indicate higher quality, while a lower number means less good quality. According to the AGMA standard the expression shown above for the dynamic factor is only valid for transmission accuracy numbers that ranges from six to twelve (AGMA, 2004).

$$B = 0.25(A_V - 5.0)^{0.667} \quad (8)$$

$$v_t = \frac{\pi \omega_1 d_{W1}}{60000} \quad (9)$$

The rotational speed, $\omega_1$, included in the expression for the pitch line velocity is the rotational speed of the driving wheel. The rotational speed should be defined in RPM (AGMA, 2004).

Budynas and Nisbett (2008) describe the size factor, $K_s$, as a factor that compensates for non-uniformity of material properties with respect to the tooth dimensions, e.g. tooth size and face width. According to the AGMA standard the size factor should be defined as unity, i.e. $K_s=1$, if no detrimental size effects are known to exist otherwise the size factor should be larger than unity (AGMA, 2004).

The load distribution factor, $K_H$, is a combination of the face load distribution factor, $K_{H\beta}$, and the transverse load distribution factor, $K_{H\alpha}$. The expression for the load distribution factor can be simplified according to eq 10 since no standard procedures for evaluating the impact from the transverse load distribution are known to exist (AGMA, 2004). The nomenclature for the included factors is given in Table 2.

$$K_H \approx K_{H\beta} = 1 + K_{Hmc}\left(K_{Hpf}K_{Hpm} + K_{Hma}K_{He}\right) \quad (10)$$

**Table 22: Presentation of the different factors which are used for deriving the load distribution factor**

| Factor: | Definition: |
|---|---|
| $K_{Hmc}$ | Lead correction factor |
| $K_{Hpf}$ | Driving wheel proportion factor |
| $K_{Hpm}$ | Driving wheel proportion modifier |
| $K_{Hma}$ | Mesh alignment factor |
| $K_{He}$ | Mesh alignment correction factor |

The lead modification factor, $K_{Hmc}$, takes into consideration whether the gear has lead modification, e.g. crowning, or not (AGMA, 2004). Values of the lead modification factor are shown in eq 11.

$$K_{Hmc} = \begin{cases} 1.0 \ \ for\ an\ unmodified\ gear \\ 0.8 \ \ for\ a\ lead\ modified\ gear \end{cases} \quad (11)$$

The driving wheel proportion factor, $K_{Hpf}$, is defined by the conditions given in eq 12 to 15. The purpose of this factor is to take deflections due to loading into consideration (AGMA, 2004).

$$b \leq 25: \ \ K_{Hpf} = \frac{b}{10d_{W1}} - 0.025 \quad (12)$$

$$25 < b \leq 432: \ \ K_{Hpf} = \frac{b}{10d_{W1}} - 0.0375 + 0.000492b \quad (13)$$

$$432 < b \leq 1020: \ \ K_{Hpf} = \frac{b}{10d_{W1}} - 0.1109 + 0.000815b - 0.0000003534b^2 \quad (14)$$

$$if \ \ \frac{b}{10d_{W1}} < 0.05 \ \ \Longrightarrow \ \ \frac{b}{10d_{W1}} = 0.05 \quad (15)$$

The value of the factor $K_{Hpm}$ for a straddle-mounted driving wheel, i.e. a driving wheel mounted between two bearings, is given by eq 16 and 17 .The parameter *S* that occurs in the expression is the bearing span, i.e. the distance between two bearings located on the same shaft, and $S_1$ is defined as the driving wheel offset from the center span, i.e. the distance from the midpoint of the bearing span (Budynas and Nisbett, 2008).

$$K_{Hpm} = 1 \ for\ a\ straddle\ mounted\ pinion\ with \frac{S_1}{S} < 0.175 \quad (16)$$

$$K_{Hpm} = 1.1 \ for\ a\ straddle\ mounted\ pinion\ with \ \frac{S_1}{S} \geq 0.175 \quad (17)$$

The mesh alignment factor, $K_{Hma}$, is given by eq 18. Values on the included coefficients are given in Table 3 and varies for different applications, e.g. from open gearing to extra precision enclosed gear units (AGMA, 2004).

$$K_{Hma} = A + Bb + Cb^2 \quad (18)$$

**Table 23: The mesh alignment coefficients given for different applications**

| System: | A x 1e-1 | B x 1e-3 | C x 1e-7 |
|---|---|---|---|
| *Open gearing* | 2.47 | 0.657 | -1.186 |
| *Commercial enclosed gear units* | 1.27 | 0.622 | -1.69 |
| *Precision enclosed gear units* | 0.675 | 0.504 | -1.44 |
| *Extra precision enclosed gear units* | 0.380 | 0.402 | -1.27 |

In order to compensate for adjustments the AGMA standard uses the mesh alignment correction factor, $K_{He}$ (AGMA, 2004). Values on the correction factor are given in eq 19.

$$K_{He} = \begin{cases} 0.8 \ if \ adjusted \ at \ assembly \ or \ improved \ by \ lapping \\ 1.0 \ for \ all \ other \ conditions \end{cases} \quad (19)$$

The surface condition factor, $Z_R$, takes surface finish, residual stresses and plasticity into consideration. According to the AGMA standard there exists no standard procedure for determining the surface condition factor. Instead, it is recommended that a value larger than unity is used if any detrimental surface conditions are known to exist otherwise the factor should be set equal to unity (AGMA, 2004).

The shape factor, $Z_I$, can be found in the AGMA 908-B89 standard and is shown in eq 20 (AGMA, 1999). The nomenclatures of the included parameters are given in Table 4.

$$Z_I = \frac{\cos \Phi_r C_\psi^2}{\left(\frac{1}{\rho_1} + \frac{1}{\rho_2}\right) d_{W1} m_N} \quad (20)$$

**Table 24: Presentation of the parameters which are included in the shape factor equation**

| Factor: | Definition: |
|---|---|
| $\Phi_r$ | Operating pressure angle |
| $C_\psi$ | Helical overlap factor |
| $\rho_1$ | Radius of curvature of the driving wheel |
| $\rho_2$ | Radius of curvature of the gear |
| $d_{W1}$ | Operating pitch diameter |
| $m_N$ | Load sharing ratio |

For spur and conventional helical gears the helical overlap factor, $C_\psi$, is given as unity (AGMA, 1999). According to Shigley, Mischke and Brown (2004) the helical contact ratio compensates for the overlap which occurs when the face contact ratio is less than unity. In cases when the face contact ratio is larger than unity the value of the overlap factor is set equal to unity (Shigley, Mischke & Brown, 2004). Since only spur gears and conventional helical gears are refererred to in this study the value on the helical overlap factor defined the AGMA standard can be used, see eq 21 (AGMA, 1999).

$$C_\psi = 1 \quad (21)$$

The load sharing ratio, $m_N$, for spur gears with contact ratio less than 2.0, i.e. $m_p < 2.0$, the load sharing ratio is set equal to one. For helical gears it is given by eq 22. The transverse contact ratio is given by eq 23 (AGMA, 1999).

$$m_N = \frac{F}{L_{min}} \quad (22)$$

$$m_p = \frac{z}{p_b} \quad (23)$$

The parameters *F* and $L_{min}$ which occur in eq 22 are the effective face width and minimum length of the line of contact. For spur gears with contact ratio less than 2.0 the minimum length is given according to eq 24 (AGMA, 1999).

$$L_{min} = F \quad (24)$$

For helical gears two different cases need to be used in order to derive the line of contact (AGMA, 1999). The cases are given in eq 25 and 26 respectively.

$$L_{min} = \frac{m_p F - n_a n_r p_x}{\cos\psi_b}, \quad if\ n_a \leq 1 - n_r \quad (25)$$

$$L_{min} = \frac{m_p F - (1 - n_a)(1 - n_r)p_x}{\cos\psi_b}, \quad if\ n_a > 1 - n_r \quad (26)$$

The parameters $n_r$ and $n_a$ are defined as fractional parts of the transverse contact ratio, $m_p$, and the face contact ratio, $m_F$. For example, if $m_F$ is equal to 1.5 then $n_a$ becomes 0.5 (AGMA, 1999).

The parameter, $p_x$, which is used in eq 25 and 26, is the axial pitch and is given by eq 27. Another parameter, which is also used in the equations, is the base helix angle which is given in eq 28 (AGMA, 1999).

$$p_x = \frac{\pi}{\sin\psi} \quad (27)$$

$$\psi_b = cos^{-1}\left(\frac{n_1 cos\phi_n}{2R_{b1}}\right) \quad (28)$$

The driving wheel's radius of curvature for a spur gear is given by eq 29. For a conventional helical gear it is defined according to eq 30 (AGMA, 1999).

$$\rho_{1,spur} = \sqrt{R_{a1}^2 - R_{a2}^2} - p_b \quad (29)$$

$$\rho_{1,helix} = \sqrt{R_{m1}^2 - R_{b1}^2} \quad (30)$$

The parameter $R_{m1}$ which occurs in eq 30 is the mean radius of the driving wheel. This is used for conventional helical gears in order to obtain the radius of curvature at

the location where the stress occurs (AGMA, 1999). The mean radius of the driving wheel is shown in eq 31.

$$R_{m1} = \frac{1}{2}\left[R_{a1} + (a - R_{a2})\right] \quad (31)$$

The gear's radius of curvature is then given by eq 32. This expression is used for both spur and helical gears in order to obtain the radius of curvature of the gear (AGMA, 1999).

$$\rho_2 = a \sin \alpha_{wt} - \rho_1 \quad (32)$$

Values on the different parameters which have been used for determining the contact stress are shown in Table 5. Comments regarding assumptions that have been made and references are given in addition to the shown parameters.

**Table 25: Assumed values of factors which are included in the AGMA equations**

| **Parameter:** | **Nomenclature:** | **Value:** | **Comments:** |
|---|---|---|---|
| *Overload factor* | $K_0$ | 1 | Based on Childs (2005) |
| *Transmission accuracy number* | $A_v$ | 6 | Based on Budynas and Nisbett (2008) |
| *Size factor* | $K_s$ | 1 | Assumed no detrimental size effects |
| *Lead modification factor* | $K_{hmc}$ | 1 | Assumed no modification since this calculation is performed before the micro geometry has been defined |
| *Driving wheel proportion modifier* | $K_{hpm}$ | 1 | Assumed center mounted driving wheel |
| *Coefficients for calculating the mesh alignment factor,* $K_{hma}$, | *A* | 6.75*1e-2 | Assumed precision enclosed gear units |
| | *B* | 5.04*1e-4 | |
| | *C* | -1.44*1e-7 | |
| *Mesh alignment correction factor* | $K_{he}$ | 1 | Assumed that no adjustments or improvements have been done during manufacturing and assembly |
| *Transverse contact ratio* | $C_\psi$ | 1 | Delimitation to only spur and conventional helical gears |
| *Surface condition factor* | $Z_r$ | 1 | Assumed no detrimental surface conditions |

When the contact stress has been calculated it should be compared with the allowable contact stress number, $\sigma_{HP}$, which is shown in eq 33. Values of the allowable contact stress number for different materials can be found in the ANSI/AGMA 2101-D04 standard (AGMA, 2004). The other parameters which are used in the equation are defined in Table 6.

$$\sigma_{HP} \leq \frac{\sigma_{HP}}{S_H}\frac{Z_N}{Y_\theta}\frac{Z_W}{Y_z} \quad (33)$$

**Table 6: The factors used in the allowable contact stress equation**

| Factor: | Definition: |
|---|---|
| $S_H$ | Safety factor for pitting |
| $Z_N$ | Stress cycle factor for pitting resistance |
| $Z_W$ | Hardness ratio factor for pitting resistance |
| $Y_\theta$ | Temperature factor |
| $Y_z$ | Reliability factor |

According to Budynas and Nisbett (2008) the equation above is used when the allowable contact stress number, $\sigma_{HP}$, is given for a specific load case and a certain number of cycles and with a specific percentage of reliability. The other parameters are then used for modifying the allowable contact stress such that it will represent other scenarios, e.g. using the stress cycle factor in order to calculate for other number of lives such that a stress rating curve can be established. The factors can be derived by consulting the ANSI/AGMA 2101-D04 standard (AGMA, 2004).

*References:*

American Gear Manufacturers Association (1999). AGMA 908-B89 Geometry Factors for Determining the Pitting Resistance and Bending Strength of Spur, Helical and Herringbone Gear Teeth. Alexandria VA: AGMA

American Gear Manufacturers Association (2004). ANSI/AGMA 2101-D04 Fundamental Rating Factors and Calculation Methods for Involute Spur and Helical Gear Teeth. Alexandria VA: AGMA

Budynas, R. & Nisbett, K. (2008). Shigley's Mechanical Engineering Design. New York: McGraw-Hill

Childs, P. (2004). Mechanical Design. Oxford: Elsevier Butterworth-Heinemann

Shigley, J., Mischke, C. & Browne, T. (2004). Standard Handbook of Machine Design. New York: McGraw-Hill

## Appendix B: Validation Report

# Validation Report

**Marcus Slogén**

# Abstract

The intention of this report was to show how a model simulated in Transmission3D, a finite element based program, could be used for analyzing the contact mechanics in gears. The outcome from the analysis was then compared with another computational program and with a gear standard in order to investigate the credibility of the results. The results show that Transmission3D is a valid tool for analyzing contact mechanics, by showing the same trends in the results as the other methods. On the other hand, the other computational software yields faster results than Transmission3D due to the fact that it uses a different analytical approach in order to perform the calculations. One critical aspect regarding Transmission3D is that the software shows maximum stresses at sharp corners in the model which need to be modified in future simulations. Finally, the results obtained from the simulations indicate that there is a need for practical testing in order to completely verify that the software yields realistic results.

# Table of Contents

# 1. Introduction

Determining the contact stresses which a gear is subjected to can sometimes be time consuming and difficult, if it is performed by hand. Instead, computational methods like Finite Element Analysis (FEA) may be less cumbersome when a gear's contact durability should be analyzed. Ansol (2012) has shown that the contact stresses in a spur gear pair which are obtained from the commercial FEA software Transmission3D yield the same result as the theoretical Hertz stresses (Childs, 2005) calculated for the same gear.

The purpose of this report is to show how Transmission3D can be used in order to calculate the contact stresses on the surface of a gear tooth and to validate the results from the simulations. The simulation procedure can either be performed by using the interactive user interface that comes with the FEA package or by using a script, which contains commands to run the software, and then run the simulation as a batch job. The main advantage of using such a script is reduced time, especially if several similar simulations are to be done.

# 2. Method

This section includes a short introduction to the software that has been used for the FE simulations, i.e. Transmission3D. It also contains a description of the simulation procedure, e.g. how the model that has been used for the analysis has been generated in Transmission3D, the simulation set up and the post processing procedure.

## 2.1. Transmission3D

The computational software Transmission3D was used in order to analyze the contact mechanics of a gear pair, e.g. determining the contact stresses and subsurface stresses of the gear tooth. This program offered the possibility to generate a FE model based on gear parameters instead of reading the model from an external file, e.g. a step or iges file, generated from a CAD program.

The software Transmission3D is developed by the American company Ansol and is a computational program that uses a semi-analytical FE approach (Ansol, 2003). Transmission3D offers the possibility to model different kinds of three-dimensional transmissions, e.g. planetary systems and differentials.

The advantage of the semi-analytical finite element approach is that it does not require any mesh of high precision in the contact zone, which a conventional FE software would do, which in its turn reduces the calculation time significantly (Ansol, 2003). In a conventional finite element program a very fine mesh in the contact zone of the gears would have been required in order to properly reflect the contact conditions. If a coarse mesh then is used for the rest of the body the gears need to be re-meshed for every time step of the calculation due to the rotation of the gears, i.e. the contact point moves when the gears are rotating. Another approach is to use a very fine mesh over the entire gear. According to Ansol (2003) both these approaches result in long computational times.

Ansol's method, on the other hand, solves the contact issue by using finite element models in order to calculate relative deformations and stresses which are located far away from the contact zone. A semi-analytical approach is then used in order to calculate the relative deformations and stresses which are located within the contact zone (Ansol, 2003).

Each rigid body in Transmission3D, e.g. a gear or a shaft, is treated separately and given its own reference frame where the finite element calculations are carried out. This leads to a number of degrees of freedom which are constrained only by the contacts (Ansol, 2003) The contacts between the different bodies are calculated by using the revised simplex method, which is a method for solving linear programming problems in order to obtain convergence (Ansol, 2003), and by that avoiding singular stiffness matrices which will lead to the fact that no unique solution is obtained (Gavin, 2012). The revised simplex method is an updated version of the simplex method which is a mathematical procedure used in linear programming for finding an optimal solution to a problem. The method iterates between nearby extreme points until an optimal solution is found, which is achieved after a finite number of steps (Råde & Westergren, 2004).

### 2.1.1. Running Transmission3D

Transmission3D offers the possibility to either work in a graphical user interface, GUI, or to run the program from the command prompt, CMD, with a script that

contains the input to the software. The second alternative can be somewhat faster than the first when several similar simulations are to be done, while the first alternative gives the possibility to interactively generate a model which at sometimes can be desired when a new model has to be generated.

The Transmission3D GUI is shown in Figure 1. The program contains different menus which enable options for generating the model, setting up the analysis and post processing the results. The interaction with the user is made by letting the user input different parameters manually, which are then used in order to generate the model and setting up the analysis, etc.

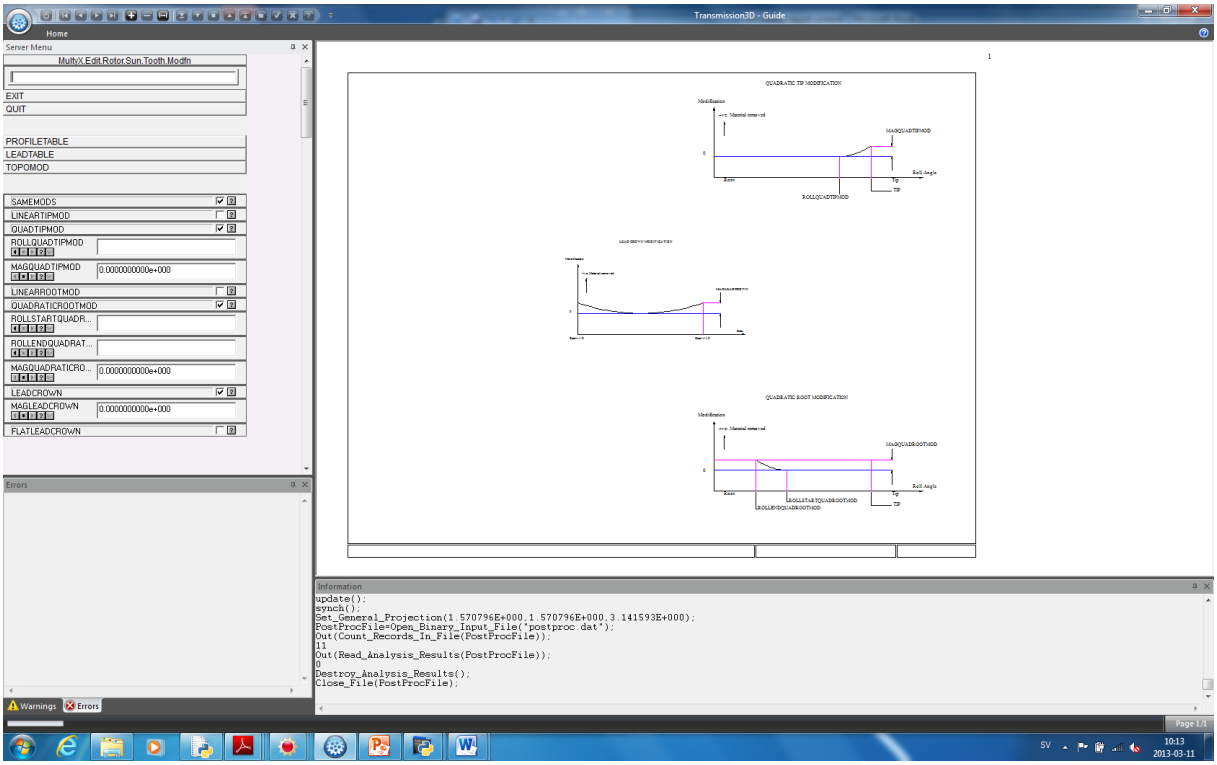


**Figure 1: The Transmission3D graphical user interface**

The second alternative, i.e. running Transmission3D from CMD, is made by defining all the input commands which define the model and the simulation, i.e. the same parameters which were defined manually in the GUI, in a text file and then send it to Transmission3D that reads and executes the commands. The process of running Transmission3D from CMD with a script is shown schematically in Figure 2.


**Figure 2: Schematic picture of how Transmission3D is executed from CMD**

## 2.2. The Model

The gears which were analyzed in this study were based on data taken from a study on gears which are used under high power and high temperature conditions (Leque, 2011). The data given for the gears was decided to be sufficient in order to create a model in Transmission3D that reflected the actual conditions. Leque (2011) also made a contact analysis in LDP (GearLab, 2009) which showed the contact pattern and the

highest stress for different load stages. The data obtained from that analysis was used as a reference in order to evaluate the outcome from Transmission3D.

The test gears which Leque (2011) used constituted of spur gears made of different steel materials, i.e. one steel that is used in aerospace applications and one for high speed automotive gears. Leque (2011) then divided the test gears into three different batches, i.e. two for the aerospace material and one for the automotive material, which shared the same base geometry of the gear but different micro geometry. The model that was chosen to be the reference in this study was the automotive gear pair made of SAE4118 steel. Data describing the base geometry and the micro geometry of the gears are shown in Table 1 and Table 2 respectively. The material data used for the model in Transmission3D is shown in Table 3.

**Table 1: Gear data defined in mm and degrees (Leque, 2011)**

| | **Driving wheel** | **Driven Wheel** |
|---|---|---|
| *Module, Mn* | 4.23 | |
| *Center Distance, CD* | 91.5 | |
| *Number of Teeth* | 17 | 26 |
| *Pressure Angle, An* | 22.5 | |
| *Face Width, W* | 14 | 20.29 |
| *Tip Radius, Da* | 80.02 | 117.11 |
| *Root Radius, Df* | 62.87 | 99.95 |
| *Circular Tooth Thickness, St* | 7.81 | 5.65 |

**Table 2: Micro geometry defined in µm and degrees (Leque, 2011)**

| | | **Driving wheel** | **Driven Wheel** |
|---|---|---|---|
| *Tip relief:* | Magnitude | 36 | 36 |
| | Start roll angle | 34 | 30 |
| *Root relief:* | Magnitude | 5 | 5 |
| | Start roll angle | 12 | 15.6 |
| | End roll angle | 34 | 30 |
| *Lead crown:* | Magnitude | 5 | 8 |

**Table 3: Material data**

| | **SAE4118 at 25°C (SteelSS, 2011)** | **Used in Transmission3D** | **Unit** |
|---|---|---|---|
| *Young's modulus of elasticity, E* | 190 – 210 | 210 | GPa |
| *Poisson's coefficient, ν* | 0.27 - 0.3 | 0.3 | |
| *Density, ρ* | 7700 – 7900 | 7900 | $kg/m^3$ |

One parameter that was required as input by Transmission3D was the tip radius of the hob, i.e. the tool that is used for generating the gear tooth. This was thus given by performing an initial calculation in LDP (GearLab, 2009) which gave the maximum tip radius of the hob as 1.29 mm and 2.60 mm for the driving wheel and gear respectively.

For the contact analysis Leque (2011) used two different load stages. The speed was kept constant at 13500 rpm at both stages but the torque varied. At the first load stage the torque was chosen to be 250 Nm, while for the other load stage a torque of 340 Nm was used.

Transmission3D does not use the torque of the driving wheel as input instead it uses the torque of the gear. The torque of the gear was then obtained by using the speed ratio equation, which can be seen in eq 1, which resulted in the torques 382.35 Nm and 520 Nm for the different load stages.

$$i = \frac{T_2}{T_1} = \frac{z_2}{z_1} \quad (1)$$

Based on the data given by Leque (2011) a model was created in Transmission3D. A picture of the model is shown in Figure 3.

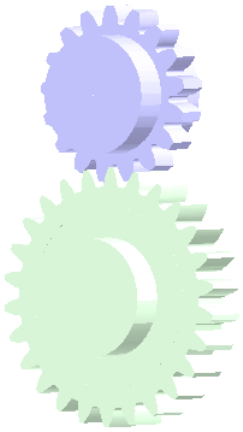

**Figure 3: Model generated in Transmission3D**

The shafts and rims of the gears were roughly modeled due to the fact that only the durability of the gear teeth was of interest in the study. This fact was also valid for the mesh and therefore was a coarser mesh used for the rims and shafts of the gears whilst a finer mesh was used for the teeth, which is shown in Figure 4.

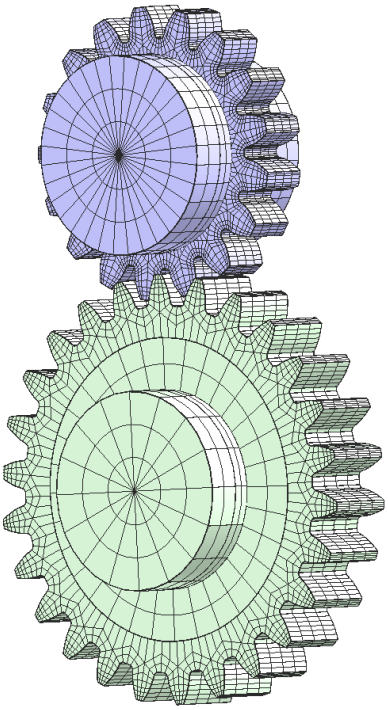

**Figure 4: Meshed gears**

As can be seen in Figure 4 a somewhat finer mesh was used for the driving wheel. This choice was based on a fact presented by Dudley (1994) regarding that the worst load position in a spur gear pair can be found at the lowest point of the driving wheel tooth where the entire load is carried by one pair of teeth, i.e. when the contact ratio of the gears is, at most, equal to one.

## 2.3. Simulation

The simulation procedure in Transmission3D can be carried out for different ranges, e.g. if a duty cycle is to be simulated then speed and torque intervals may be defined for a specific range. This option was not used in this study since only two different load stages were of interest with a constant speed at 13500 RPM. Instead two separate simulations were made, one for the load of 250 Nm and one for the load of 340 Nm.

The analysis set up parameters were mainly based on default values given by Transmission3D, except from the delta time which is the gear mesh cycle time divided by the number of simulation steps minus one. Since this parameter varies for different gears, i.e. due to number of teeth and speed, it has to be calculated for every simulation. An example on how the delta time is calculated is given in eq 2.

$$\Delta t = \frac{2\pi}{\omega_{pinion}\, z_{pinion}} \frac{1}{(n_{steps} - 1)} \quad (2)$$

The number of simulation steps was chosen as 11. This value was decided to be sufficient in order to obtain good results. If a lower value had been used then the simulation time would have been faster but to the cost of the accuracy of the results. A higher value would yield more accurate results but would have resulted in longer calculation times.

## 2.4. Post Processing

The post processing work began after a simulation had finished. Transmission3D offers possibilities to plot contact pattern, load diagram and sub-surface stresses which may be of interest when contact failures are to be investigated. These pictures and diagrams were sent to a pdf file which could be read after the simulation had finished, but they could also be illustrated immediately in the GUI.

Beside the inbuilt post processing options Transmission3D uses an external application, i.e. Iglassviewer, for three-dimensional visualization of the results. The viewer can also be used for displaying the model before a simulation is started. An example of a model shown in Iglassviewer is given in Figure 5.

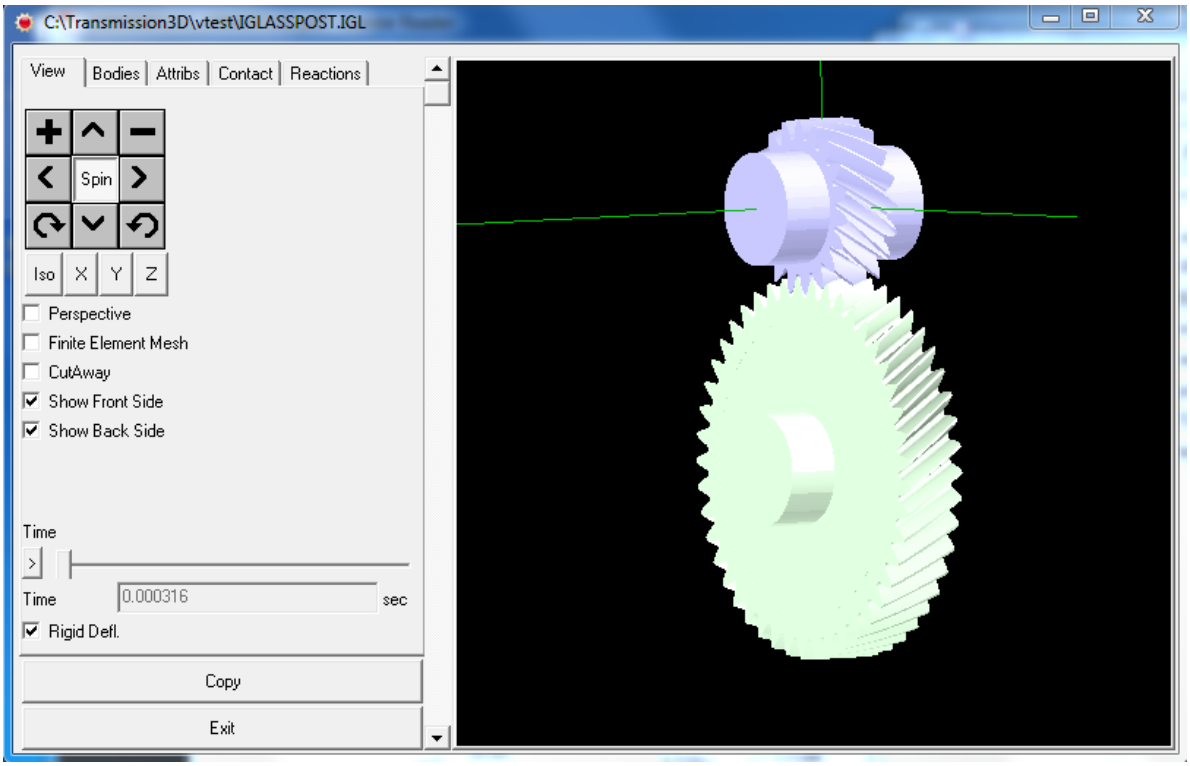


**Figure 5: Example of a model shown in Iglassviewer**

## 2.5. Validation

The results from the simulations in Transmission3D were compared with the results obtained by Leque (2011). The results were also compared with results from LDP and from a gear standard, e.g. AGMA, in order to verify the accuracy of the results which were obtained from Transmission3D. The maximum contact stress calculated from the gear standard was performed for an ideal spur gear with no profile modification.

LDP, Load Distribution Program, is a program that is developed by GearLab at Ohio State University and is used for analyzing the load distribution in a gear pair (Harianto and Houser, 2002). LDP uses a simplex technique for solving the contacts but in combination with theoretical models for calculating deformations, etc. which enable fast calculation times (Harianto and Houser, 2002). The reason for why LDP was used in this study was to obtain contact stress patterns which could be compared with the output from Transmission3D. It was also used in order to verify that the data presented by Leque (2011) were complete such that the results obtained from LDP were in compliance with Leque's results from LDP.

A gear standard, i.e. ANSI/AGMA 2001-D04 (AGMA, 2004), was also used in the Validation process. The calculations were performed for an unmodified gear that was assumed to operate under ideal conditions, due to the fact that many of the parameters which are used for modifying the load case require experience within the field of application (Budynas and Nisbett, 2008). The aspiration with the calculations was therefore not to obtain definite values that could be compared with the results from Transmission3D. The theoretical calculations were, instead, performed in order to see if the values which were obtained from the standard and from Transmission3D followed the same trend, e.g. showed values which were in the same region for the two load cases and also showed a similar increase in the contact stresses from the first load stage to the second.

# 3. Results

In this section follows a presentation of the results which were obtained from Transmission3D and LDP. The section is divided into two parts one for the gears which have a modified tooth profile and one for the gears which are unmodified.

Transmission3D shows maximum stresses in the root and tip section due to bad geometries, e.g. sharp transitions in the tooth flank geometry, in these areas. LDP, on the other hand, plots the contact pattern along the active face width and the line of action. LDP will, in this way, obtain its maximum contact stresses at the positions where only one gear pair carries the entire load, i.e. at the positions located between the root and the tip of the tooth. Due to the risk of fictitious stresses which may occur in the tip and root sections and at the edges of the tooth flank the maximum stresses which are located in these regions will be neglected in the following text.

Leque (2011) only showed values on the contact stresses for gears with lead and profile modification, i.e. 1695 MPa and 1921 MPa respectively. In this study were also gears with only lead modification and without any modification tested in order to compare the results obtained from the two programs.

## 3.1. Gears with Profile Modification and Lead Modification

In this section follows a presentation of the results for the gears which have both lead and profile modification, i.e. gears that have a similar design as the test gears used by Leque (2011).

The highest contact stress was obtained as 1682 MPa from Transmission3D for the 250 Nm load stage and was found slightly below the pitch diameter. A picture of the contact pattern, which was obtained from Iglassviewer, is shown in Figure 6.

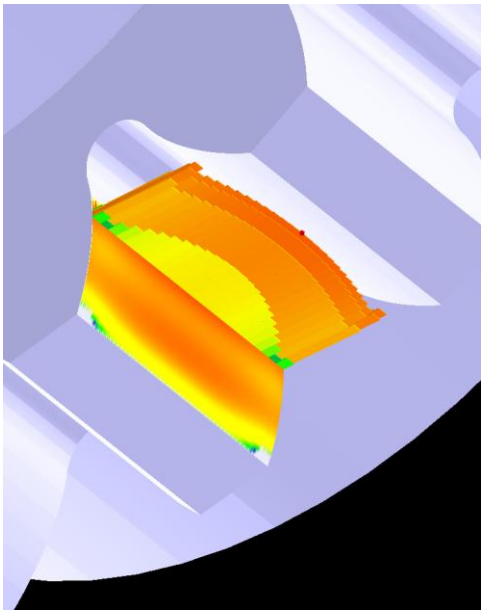

**Figure 6: Contact pattern for the 250 Nm load simulated in Transmission3D**

The corresponding case simulated in LDP resulted in a maximum contact stress of 1692MPa and was also located at a small distance below the pitch diameter. The contact pattern for the active face width plotted against the line of action is shown in Figure 7.

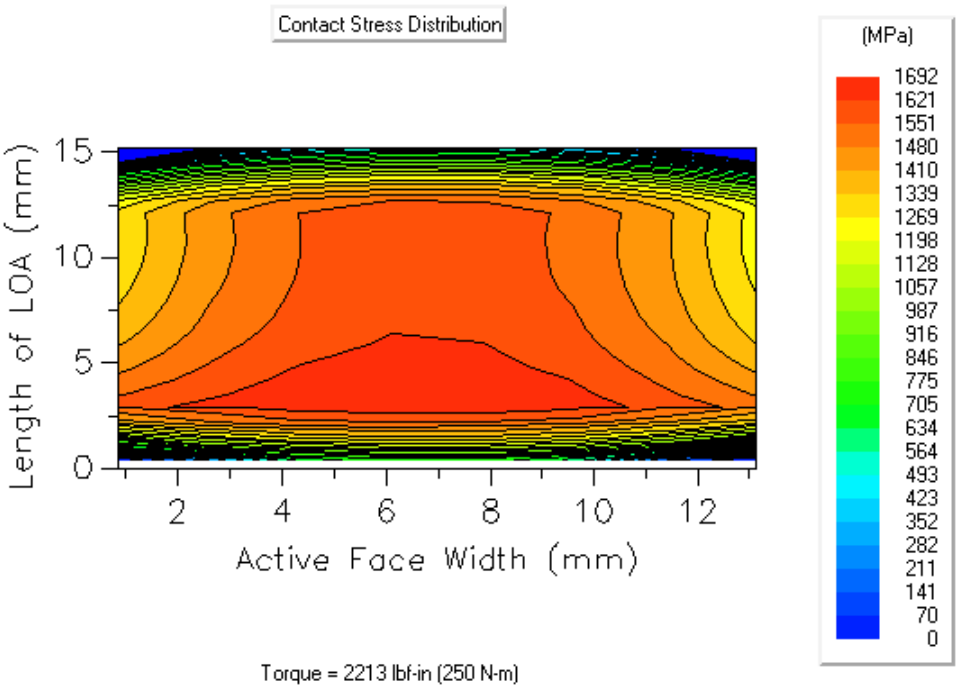


**Figure 7: Contact pattern, for the 250 Nm load, obtained from LDP**

For the load case of 340 Nm the maximum contact stress was obtained as 1912 MPa and was found at the same location as for the 250 Nm load case. A picture displaying the contact pattern is shown in Figure 8.

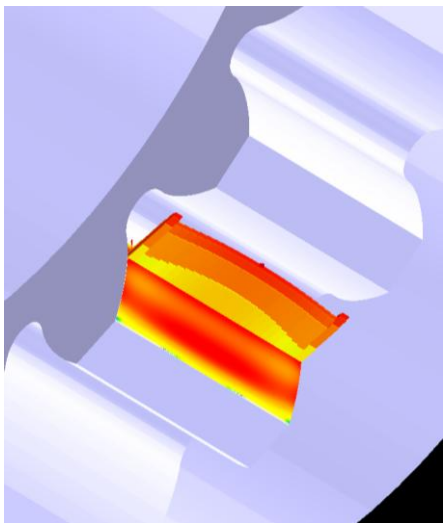

**Figure 8: Contact pattern, for the 340 Nm load, obtained from Transmission3D**

The 340 Nm load case simulated in LDP showed a maximum contact stress of 1924 MPa. The contact pattern is shown in Figure 9.

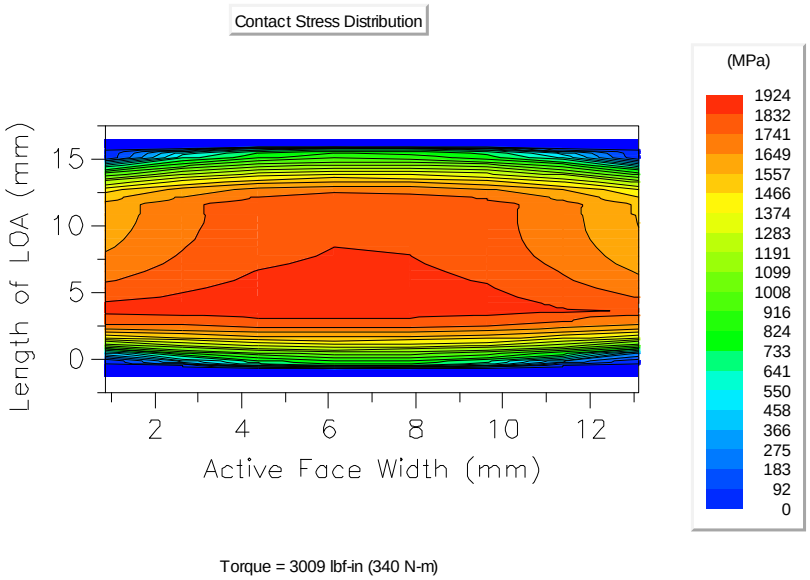


**Figure 9: Contact pattern, for the 340 Nm load, obtained from LDP**

## 3.2. Gears with Only Lead Modification

This section shows results for gears that only have lead modification, i.e. crowning.

The simulation for the 250 Nm load case with crowning gave a maximum contact stress of 1652 MPa. The contact pattern is shown in Figure 10.

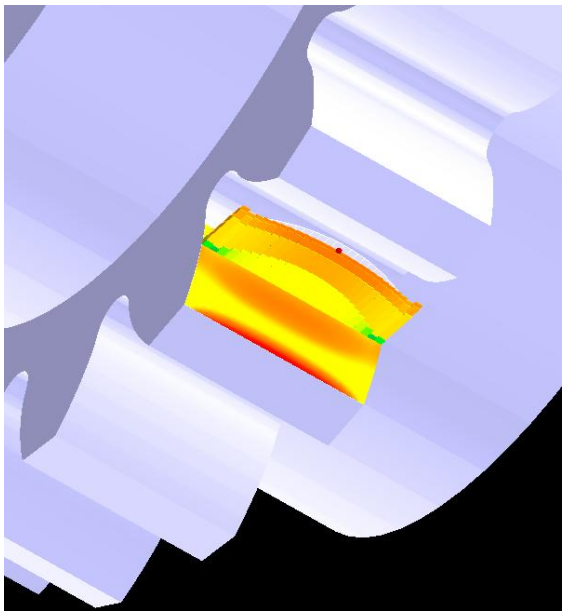

**Figure 10: Contact pattern, for the 250 Nm load, obtained from Transmission3D**

The corresponding case analyzed in LDP gave a maximum contact stress of 1687 MPa. The contact stress distribution is shown in Figure 11.

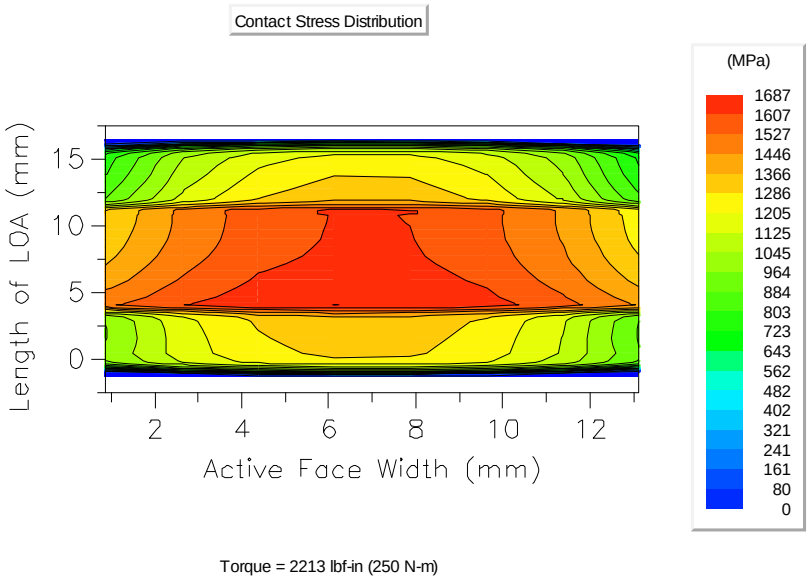


**Figure 11: Contact pattern, for the 250 Nm load, obtained from LDP**

The maximum contact stress for the 340 Nm load case was obtained as 1878 Nm. The contact pattern is shown in Figure 12:

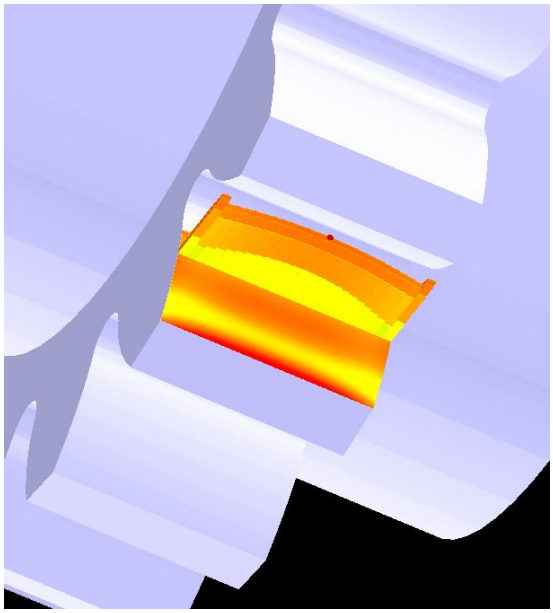

**Figure 12: Contact pattern, for the 340 Nm load, obtained from Transmission3D**

The corresponding case simulated in LDP resulted in a maximum contact stress of 1894 MPa. The contact stress distribution is shown in Figure 13.

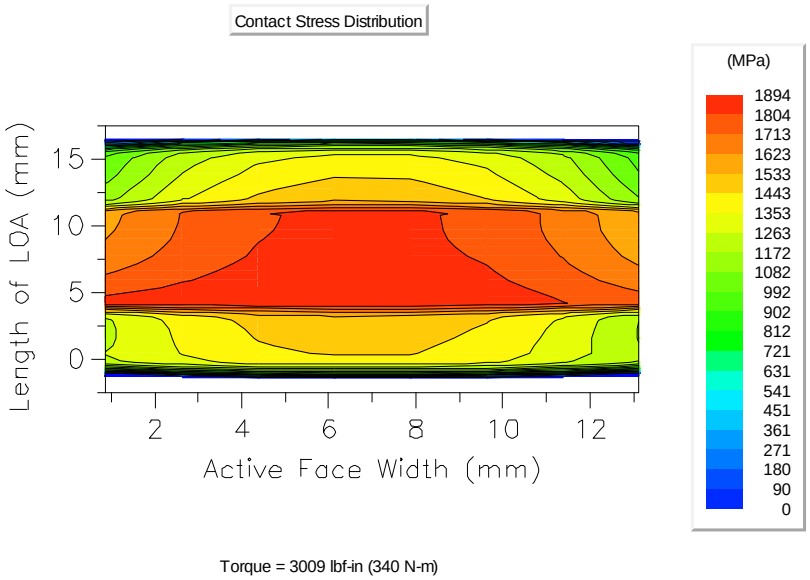


**Figure 13: Contact pattern, for the 340 Nm load, obtained from LDP**

## 3.3. Gears without Any Modification of the Micro Geometry

This section contains the results for gears without any tooth modification, i.e. profile or lead modification.

The maximum contact stress was obtained as 1944 MPa for the non-modified gear. The contact pattern is shown in Figure 14.

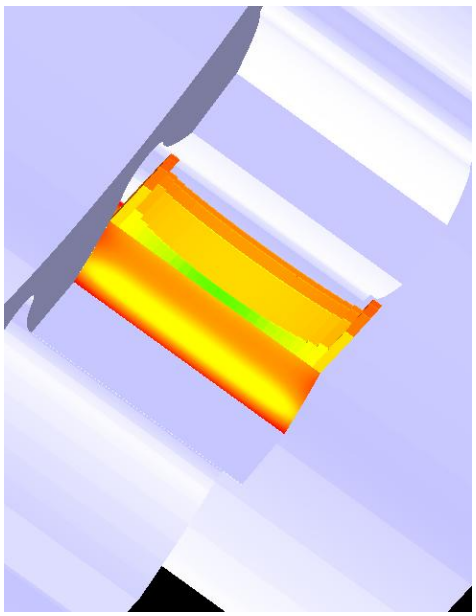

**Figure 14: Contact pattern, for the 250 Nm load, obtained from Transmission3D**

The corresponding case simulated in LDP resulted in a maximum contact stress of 1805 MPa. The stress distribution is shown in Figure 15.

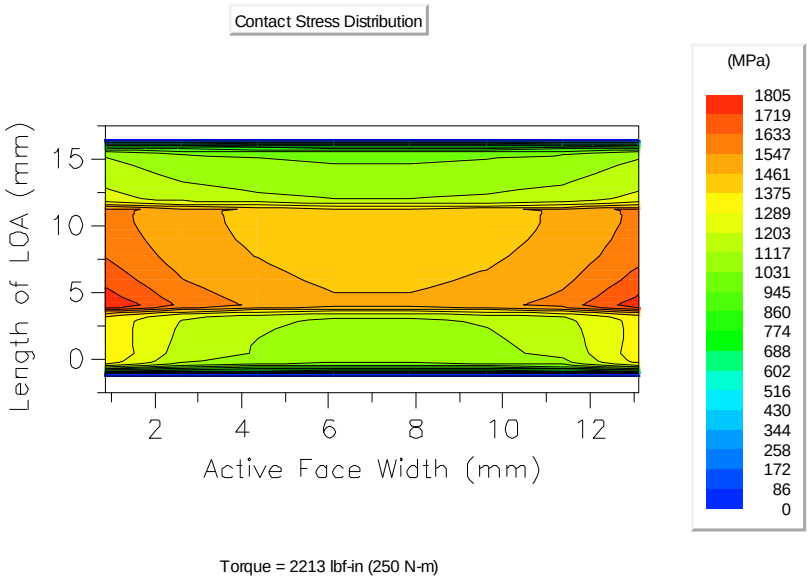


**Figure 15: Contact pattern, for the 250 Nm load, obtained from LDP**

The highest contact stress for the 340 Nm load stage was obtained as 2314 MPa. The contact pattern is shown in Figure 16.

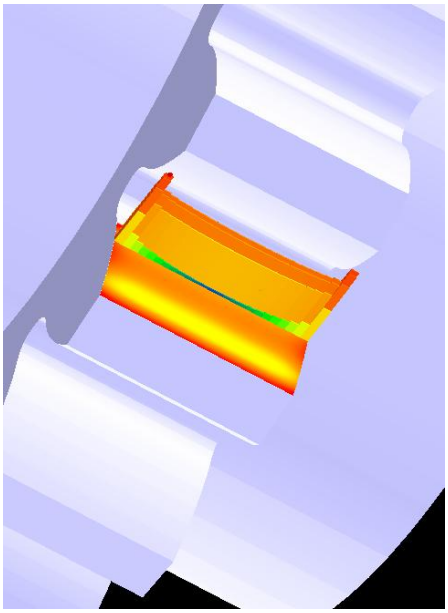

**Figure 16: Contact pattern, for the 340 Nm load, obtained from Transmission3D**

The 340 Nm load stage simulated in LDP resulted in a maximum stress of 2115 MPa. The contact stress distribution is shown in Figure 17 below.

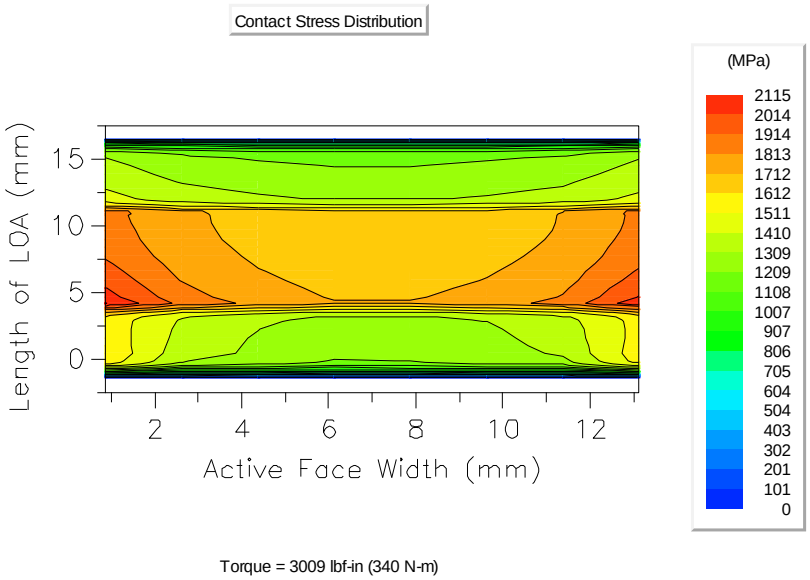


**Figure 17: Contact pattern, for the 340 Nm load, obtained from LDP**

## 3.4. Stresses at the Root and Tip Sections

From the simulations, made in Transmission3D, it could clearly be noticed that the maximum stresses were located in the tip and root areas of the gear tooth. The same phenomenon did not appear in LDP.

For an unmodified gear, i.e. without any lead or profile modification, the maximum stresses were identified at the tip of the tooth and at the start of active profile (SAP). The latter position defines the location where the transition from the root section to the involute profile takes place. The stress distribution over the tooth flank is shown in Figure 18.

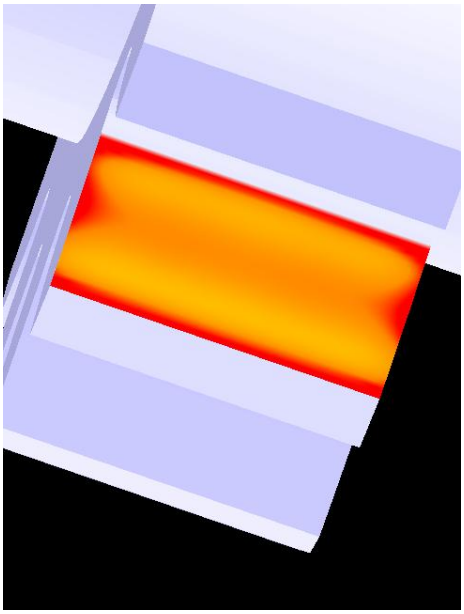

**Figure 18: Stress distribution over an unmodified tooth flank**

The maximum stresses for a gear with only lead modification were noticed at the locations as for an unmodified gear but with a stress peak located at the center of the tip and the root sections. The stress distribution for the gear with lead modification is shown in Figure 19.

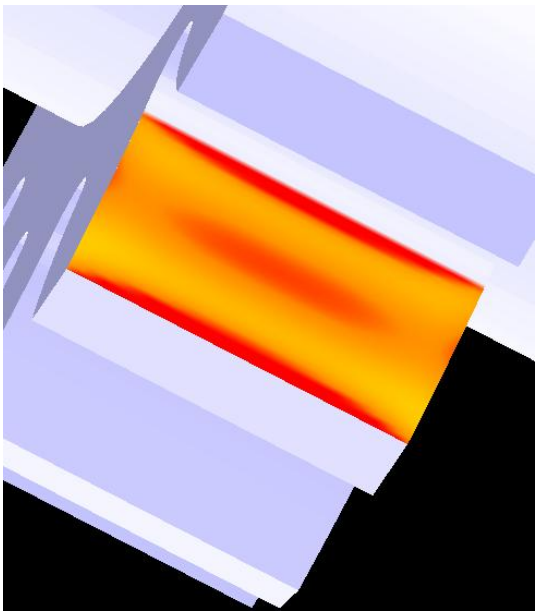

**Figure 19: Stress distribution over a lead crowned tooth flank**

For the gear which had both lead and profile modification the maximum stresses on the tooth flank were displace towards the center of the tooth flank, due to the profile modification. The stress distribution is shown in Figure 20. What can be noticed in the picture is that the maximum stresses have a lighter red color compared to the cases with the unmodified and the lead crowned gears. This indicates that the maximum stress is not as high as for the gear with lead and profile modification.

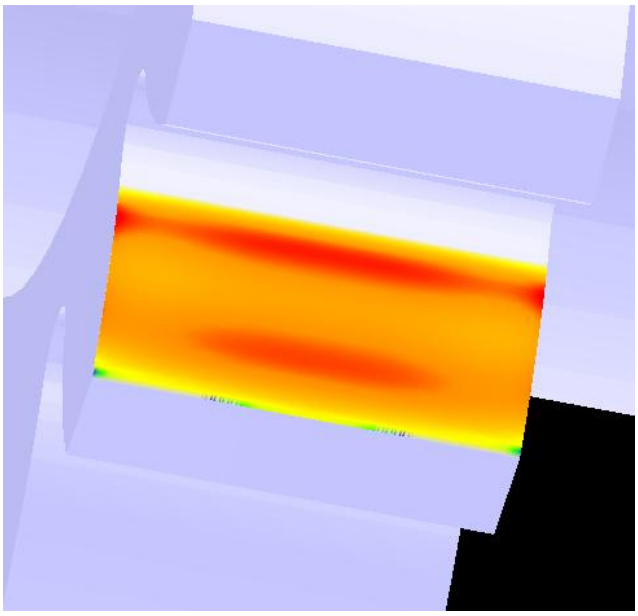

**Figure 20: Stress distribution over a gear tooth with both lead and profile modification**

## 3.5. Standard Results

The following section shows the results obtained from ANSI/AGMA 2001-D04 standard (AGMA, 2004). The results should only be viewed as estimations of the maximum contact stresses that may occur in the gears, since the equations used in the standards involve a lot of parameters which are based on experience within the field of application (Budynas and Nisbett, 2008).

The maximum stresses are shown displayed in S-N diagrams based on data obtained from Radzevich (2012). The maximum contact stress for the 250 Nm load is shown in Figure 21 and the corresponding stress for the 340 Nm load is shown in Figure 22.

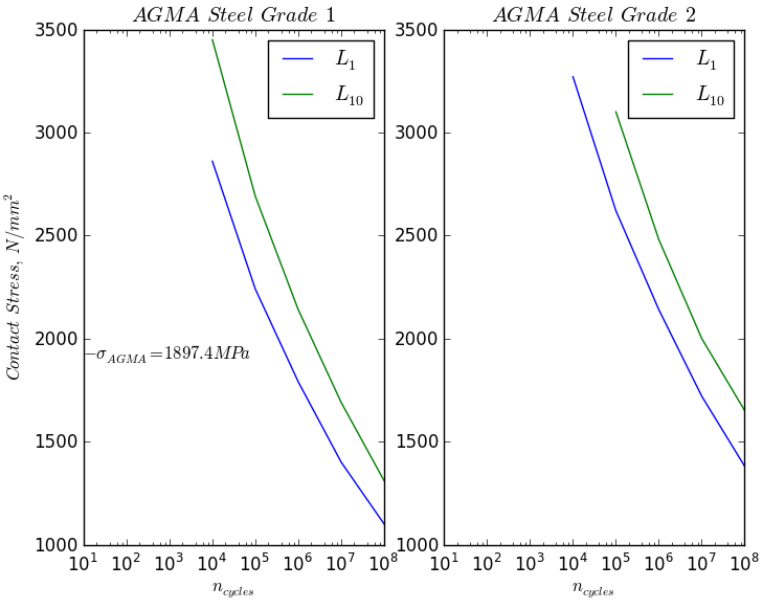


**Figure 21: Contact stress, for the 250 Nm load, according to AGMA**

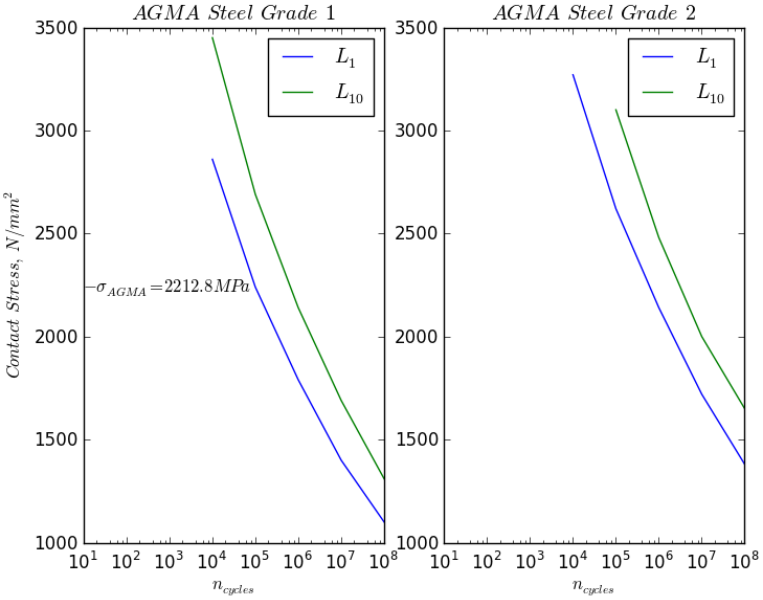


**Figure 22: Contact stress, for the 340 Nm load, according to AGMA**

## 3.6. Summary of the Results

The results from the simulations are summarized in Table 4 in order to highlight eventual differences and similarities between them.

**Table 4: Summary of results**

| **Modification:** | **Method:** | **250 Nm** | **340 Nm** | **Unit:** |
|---|---|---|---|---|
| *Lead and profile modification* | T3D | 1682 | 1912 | MPa |
| | LDP | 1692 | 1924 | MPa |
| | Leque (2011) | 1695 | 1921 | MPa |
| *Lead modification* | T3D | 1652 | 1878 | MPa |
| | LDP | 1687 | 1894 | MPa |
| *No modification* | T3D | 1944 | 2314 | MPa |
| | LDP | 1805 | 2115 | MPa |
| | AGMA standard | 1897 | 2212 | MPa |

# 4. Conclusion and Discussion

The obtained results from the simulations showed that the model used in Transmission3D yielded similar values of the contact stresses, especially at the lower torque stages for the modified gears. At higher torque stages the differences in the results obtained from LDP and Transmission3D got larger but were still considered to be within reasonable limits, e.g. it differed with approximately 9 percent for the worst case which took place at the 340 Nm load stage for an unmodified gear pair.

The standard showed values of the contact stresses which were located between the values which were obtained from LDP and Transmission3D. The difference in contact stresses between the lower and the higher torque stage was, on the other hand, almost equal to the increase noticed in LDP. Anyhow, it should be kept in mind that the equations which are used in the AGMA standard involve parameters which are based on experience and knowledge about the system where the gears are to be used.

The difference in the results obtained from LDP and the results shown by Leque (2011) were minor at both load stages. This implies that the model used for the simulations in LDP is valid. The minor differences in the results may be due to changes in geometry as well as material properties since Leque (2011) did not show any absolute data on the material properties or the type of profile modification, i.e. linear or quadratic, which had been used in the simulations.

The accuracy of the results, obtained from LDP and Transmission3D, mainly depends on the precision of the model. For example, a rough model will yield less accurate contact stresses but which are still within reasonable limits. The primary differences, which were noticed during the simulations, between Transmission3D and LDP are the time it takes to perform a simulation and the influence of the model geometry.

The time difference is due to the fact that the two programs use different techniques for calculating the contact mechanics. LDP combines gear standard calculations with semi analytical techniques (GearLab, 2009) in order to calculate the load distribution in mating gears which results in fast calculation times. Transmission3D is an FE based program that uses semi analytical techniques for solving the contact problems. This implies that Transmission3D will be faster than conventional FE solvers but slower than LDP since it still uses traditional FE techniques for the other parts located far away from the contact zone. On the other hand, this will give a more detailed view of the gear behavior since the entire gear, including rim and shaft, is taken into consideration.

From the simulations it was shown that the gear geometry had an impact on the simulation results. Transmission3D showed clear stress concentrations at the transition from the involute section to the root section and at the transition from the involute section to the tip section. This phenomenon did not appear in the results from LDP. In fact, the results obtained from LDP showed very small influences from changes in the root and tip sections. Thus, this can probably also be related to the fact that edge contact was used in the Transmission3D simulations, which may result in fictitious stresses due to bad mesh quality at these locations. Another contributor to this issue might be the use of linear reliefs, for the root and the tip, instead of parabolic reliefs. This would probably have resulted in smoother transitions from the root to the involute section and from the involute section to the tip region.

The complexity of the model was also proved to have an impact on the outcome from the simulations. In Transmission3D it is required that the entire gear is defined in order be able to perform a simulation. This means that not only the gear teeth need to be defined but also shafts, rims, etc. and the connections between them. In LDP, on the other hand, the minimal requirement for running a simulation is that the parameters which define the tooth geometry are included which in its turn reduces the complexity of the input. The drawback of not taking other parts of the gear into consideration is that the results will only show the performance of the gear tooth and neglecting the influence from other parts. For a simple gear model it might be less cumbersome to use this approach but for more advanced geometries, e.g. complex rim geometries and the impact of bearings, the method used in Transmission3D may be more appropriate.

Finally, since Leque (2011) did not show any absolute values on the contact stresses from the practical tests it is hard to determine whether Transmission3D or LDP yields the most realistic values. Of that reason, follows a future recommendation of making a practical test and report the results in an S-N diagram which then can be used in order to evaluate the outcome from the computational program.

# References

American Gear Manufacturers Association (2004). ANSI/AGMA 2101-D04 Fundamental Rating Factors and Calculation Methods for Involute Spur and Helical Gear Teeth. Alexandria VA: AGMA

Ansol (2003). Transmission3D User's Manual. Hillard OH: Advanced Numerical Solutions

Ansol (2012). Transmission3D Validation Manual. Hillard OH: Advanced Numerical Solutions

Childs, P. (2004). Mechanical Design. Oxford: Elsevier Butterworth-Heinemann

Dudley, D. W. (1994). Handbook of Practical Gear Design. Lancaster: Technomic Publishing Company

Gavin, H. (2012). Mathematical Properties of Stiffness Matrices. Available: http://people.duke.edu/~hpgavin/cee421/matrix.pdf [2013-04-05]

Gear and Power Transmission Research Laboratory (GearLab) at The Ohio State University. (2009). Software. http://gearlab.org/ [2013-04-05]

Harianto, J. & Houser, D. (2002). Load Distribution Program. Columbus OH: The Ohio State University

Leque, N. (2011). Development of an Experimental Methodology for Evaluation of Gear Contact Fatigue under High-Power and High-Temperature Conditions. Columbus OH: The Ohio State University. Available: OhioLink ETD Center [2013-04-05]

Radzevich S. P. (2012). Dudley's Handbook of Practical Gear Design and Manufacture. Boca Raton FL: CRC Press

Special Steel Co. (2011). Data Table for: Carbon Steel: SAE 4118RH. http://www.steelss.com/Carbon-steel/sae-4118rh.html [2013-04-05]